J. Chem. Thermodynamics 151 (2020) 106176

Contents lists available at ScienceDirect

J. Chem. Thermodynamics

journal homepage: www.elsevier.com/locate/jct

# Carbon dioxide solubility in mixtures of methyldiethanolamine with monoethylene glycol, monoethylene glycol–water, water and triethylene glycol

Eirini Skylogianni [a], Cristina Perinu [a,b], Blanca Y. Cervantes Gameros [a], Hanna K. Knuutila [a]

[a] Department of Chemical Engineering, Norwegian University of Science and Technology (NTNU), NO-7491 Trondheim, Norway
[b] Department of Process, Energy and Environmental Technology, University of Southeast Norway, NO-3603 Kongsberg, Norway

ARTICLE INFO

*Article history:*
Received 3 February 2020
Received in revised form 18 May 2020
Accepted 19 May 2020
Available online 26 May 2020

*Keywords:*
Absorption
Vapor-liquid equilibrium
MDEA
Glycol
Highly concentrated MDEA
NMR
Alkyl carbonate

ABSTRACT

Carbon dioxide solubility in non-aqueous and aqueous mixtures of methyldiethanolamine (MDEA) with monoethylene glycol (MEG) was studied due to the relevance of these solvents for the combined acid gas removal and hydrate control in natural gas treatment. Vapor-liquid equilibrium (VLE) measurements were conducted at temperatures from 303 K to 393 K and pressures up to 600 kPa. In the aqueous solvents, the effect of water content in carbon dioxide solubility was investigated. The absorption capacity of the aqueous solvents decreased with increasing glycol content and decreasing water content, at constant amine concentration. A comparison of the studied systems with concentrated aqueous MDEA was also performed. The non-aqueous solvents were studied in the whole composition range, from pure MDEA to pure MEG. The solubility of carbon dioxide increased with increasing amine content only up to 30–50 wt% MDEA-MEG, upon which it decreased. Water content determination and Nuclear Magnetic Resonance (NMR) analysis were used for the chemical characterization of the systems and explanation of the results. It was found that in the presence of MDEA, a chemical reaction occurs between carbon dioxide and MEG. A theory based on MEG autoprotolysis is proposed which is further supported by supplementary VLE data obtained in blends of MDEA and triethylene glycol.


## 1. Introduction

### 1.1. Literature review

Primary downstream processes in natural gas production are the removal of acid gases, namely carbon dioxide ($CO_2$) and hydrogen sulfide ($H_2S$), and the removal of water in order to meet pipeline transportation specifications, gas quality specifications and environmental requirements. Acid gases in the presence of water are highly corrosive and can jeopardize the safety of operations, both in terms of the personnel's wellbeing as well as equipment failure. The same applies in the event of hydrate formation if excess of water is present, which can lead to pipeline clogging and, in extreme cases, production shut-down [1].

In offshore gas and oil wells, non-regenerative chemicals, called scavengers, are commonly used to control hydrogen sulfide content in natural gas. However, they are not ideal since their use imposes space, weight and disposal requirements which are not friendly for offshore/subsea application [2], and they cannot treat high $H_2S$ concentrations. A typical example is triazine, which is injected directly into the gas stream and is able to treat hydrogen sulfide at concentrations not higher than $200 \times 10^{-6}$ ppmv [3]. As a result, fields are abandoned or not even produced due to high $H_2S$ content. In addition, oil and gas fields experience reservoir souring, *i.e.* increase in sulfur content, due to EOR (Enhanced Oil Recovery) activities such as water injection [4]. Maintaining production and safe operation in increasingly sour fields is an important industrial challenge.

A solution to the problematic high $H_2S$ concentrations in production wells is the development of a regenerative process where hydrogen sulfide and water content can be removed simultaneously. Despite the fact that the employment of a regenerative solvent requires additional equipment for its regeneration, it could enable trouble-free operations and extend the life of the field. Aqueous methyldiethanolamine (MDEA) and aqueous monoethylene glycol (MEG) are regenerative solutions traditionally used today for the selective removal of $H_2S$ over $CO_2$ and for hydrate control, respectively. MDEA is a tertiary amine whose aqueous solutions have significantly higher reaction rates with $H_2S$ than with $CO_2$. Therefore, mixtures of MDEA-MEG as well as highly concentrated

*E-mail address:* hanna.knuutila@ntnu.no (H.K. Knuutila)

https://doi.org/10.1016/j.jct.2020.106176
0021-9614/

MDEA are promising candidates for the combined removal of $H_2S$ and water vapor.

The concept of a gas treating process for combined acid gas and water vapor removal from natural gas was conceived already in 1930s and was first patented in 1939 by Hutchinson [5]. Process improvements were suggested in the following years [6–8] and the amine-glycol process found wide acceptance in the gas processing industry. An aqueous mixture of monoethanolamine (MEA) and either diethylene (DEG) or triethylene glycol (TEG) was used for the simultaneous absorption of acid gas and water from natural gas [9]. In spite of many advantages, severe corrosion was encountered and the process was eventually abandoned. However, MEA is known for its corrosivity issues, thus its substitution with another amine and/or the decrease in water content can potentially eliminate this problem. The years that followed until today, many researchers have studied blended aqueous and non-aqueous amine-glycol solvents, mainly in the framework of water-lean solvents, which can potentially have increased absorption capacity and reduced regeneration heating duties [10–20]. The majority of the literature studies concerns MEA and diethanolamine (DEA) and few sources were found for MDEA-glycol systems [16,17,19].

Wanderley and co-workers [20] studied vapor-liquid equilibrium and mass transfer in MDEA – MEG – $H_2O$ among other solvents, promising for $CO_2$ capture in biogas upgrading. They observed that the solubility of $CO_2$ decreased compared to aqueous MDEA, and they underlined the fact that higher $CO_2$ partial pressure than in aqueous MDEA was also accompanied by faster reaction rates for the same $CO_2$ pressure. Eimer [19] and Xu et al. [16] focused on the selectivity of $H_2S$ over $CO_2$ with non-aqueous or water-lean MDEA-containing solvents. Eimer [19] investigated the performance of a mixture composed of MDEA and TEG aiming for the combined selective removal of $H_2S$ over $CO_2$ and dehydration. It was found that the reaction rate of $H_2S$ in the combined solvent decreases with increasing glycol content. High viscosity promotes low absorption rate and this is one of the main reasons why, in this study, we consider the far less viscous MEG as a more suitable glycol than TEG for this multifunctional solvent. Moreover, following a first screening of potential diluents which showed increased $H_2S$ selectivity in MDEA – MEG compared to aqueous MDEA, Xu et al. [16] measured the solubility of $CO_2$ and $H_2S$ in aqueous and non-aqueous MDEA – MEG blends. They concluded that the carbon dioxide solubility significantly decreases in MDEA – MEG than MDEA – $H_2O$, while the solubility of $H_2S$ is only slightly lower.

### 1.2. Aim of this work

Successful process development relies on accurate data and/or models to describe the physical properties, thermodynamic behavior and system kinetics. The first step for the evaluation of a complex multicomponent system, such as the combined hydrogen sulfide and hydrate control process, is the study of its subsystems. The aim of this work is to describe and understand the thermodynamic behavior of the subsystems $CO_2$ – MDEA – MEG and $CO_2$ – MDEA – MEG – $H_2O$. Since carbon dioxide is generally present in natural gas with hydrogen sulfide, investigating this system is of equal importance as the absorption of $H_2S$ in the proposed solvent.

This work includes two main studies: a) an extensive study of the vapor-liquid equilibrium (VLE) behavior of $CO_2$ – MDEA – MEG systems in the whole composition range from pure MEG to pure MDEA, and b) a study of $CO_2$ – MDEA – MEG – $H_2O$ systems with focus on the effect of water content in the system and a comparison with highly concentrated amine solutions, *i.e.* 70 wt% and 90 wt% MDEA – $H_2O$. The measurements were performed at $CO_2$ pressures up to 600 kPa and temperatures from 303 to 393 K. We further investigated our VLE results through Karl-Fischer titration (for the non-aqueous systems), Nuclear Magnetic Resonance (NMR) spectroscopy, and comparison with MDEA – TEG systems in order to understand the underlying phenomena and identify possible chemical reactions undergone during the absorption of $CO_2$ into aqueous and non-aqueous MDEA-glycol blends. Density measurements were also performed as part of the VLE data processing.

## 2. Materials and methods

### 2.1. Materials

Table 1 contains information for the chemicals used in this work. They were used as received from the supplier without further purification. Deionized water was used for preparation of the aqueous mixtures. The solutions were prepared gravimetrically in a METTLER PM1200 scale with an accuracy of $1 \times 10^{-6}$ kg, they were sealed and let under magnetic stirring for at least 8 h to ensure homogeneous solutions. Amine analysis by means of acid-base titration was performed in order to verify the MDEA concentration in the studied systems.

### 2.2. Experimental methods

#### 2.2.1. Vapor-liquid equilibrium measurements

Two similar setups were used to conduct the vapor-liquid equilibrium (VLE) measurements, named VLE-1 and VLE-2. The main components of the setups are a glass reactor and a storage cylinder for $CO_2$ of ca. $1 \times 10^{-3}$ $m^3$ volume each, whose pressure and temperature are monitored. Measurements can be conducted at temperature range of (303 – 393) K (accuracy ± 0.1 K) and pressures (0 – 600) kPa (accuracy ± 0.9 kPa). The setups' description and instrumentation are provided in detail by Hartono et al. [21] Experiments were performed in two different ways, either at multiple temperatures with one $CO_2$ loading or at one temperature and multiple loadings.

Each experiment started by evacuating the reactor. The solvent was introduced and the reactor was set again to vacuum to eliminate possible air introduced with the solvent. The exact amount of solvent introduced was known by weighing the solvent holder, before and after charging the reactor. For measurements performed at multiple temperatures with one $CO_2$ loading, the temperature was set to automatically increase from 303 to 393 K with a step of 10 K. At 393 K, $CO_2$ was injected to the maximum pressure of the reactor and the temperature was decreased in reversed steps until 303 K. For the measurements performed under isothermal conditions and multiple loadings, once equilibrium was reached at the desired temperature, $CO_2$ was added. After each system equilibration, more $CO_2$ was added manually until the pressure inside the reactor was close to 600 kPa. Equilibrium in every temperature level, both for the vapor pressure of the solution and the $CO_2$-solvent equilibrium, required approximately (4–8) hours. The system was under constant stirring (ca. 500 rpm) and equilibrium was assumed when the temperature and pressure of the reactor were constant for 5 min.

The pressure and temperature were recorded every 5 s during the experiment, which lasted (3–4) days. The calculations are based on mass balances; the solvent is added from a beaker whose weight before and after the reactor filling is measured. The temperature, volume and pressure of the $CO_2$ storage vessel are known, and thus the amount of gas before and after the $CO_2$ loading of the solvent can be calculated. The amount of carbon dioxide in the vessel was calculated using Peng-Robinson equation of state [22]. The equilibrium pressure was calculated according to Eq. (1):

**Table 1**
Chemical Sample Table.

| Component | UIPAC name | CAS | Supplier | Mass fraction purity as stated by supplier |
|---|---|---|---|---|
| N-methyldiethanolamine (MDEA) | 2-[2-hydroxyethyl(methyl) amino] ethanol) | 105-59-9 | Sigma-Aldrich | ≥0.99 |
| monoethylene glycol (MEG) | ethane-1,2-diol | 107-21-1 | Sigma-Aldrich | 0.998 |
| triethylene glycol (TEG) | 2-[2-(2-hydroxyethoxy) ethoxy]ethanol | 112-27-6 | Sigma-Aldrich | ≥0.985 |
| carbon dioxide | carbon dioxide | 124-38-9 | AGA | 0.99999 |
| water | oxidane | – | – | – |

$$P_{CO_2} = P_{tot} - P_{res} \quad (1)$$

where $P_{CO_2}$: partial pressure of $CO_2$, $P_{tot}$: total pressure inside the reactor and $P_{res}$: residual pressure inside the reactor before $CO_2$ addition. Amine analysis was performed in the end of every experiment to verify that the amine concentration remained the same (within 2% error). $CO_2$ analysis was also performed in most of the experiments to confirm our mass balance-based calculations. The average absolute relative deviation (AARD), calculated according to Eq. (2), is 4% for all the experiments, excluding those in pure $H_2O$, MEG and TEG where the very low values of carbon dioxide absorbed leads to large relative deviations. However, the results from those experiments are compared to and found in agreement with values reported in the literature in Section 3.

$$AARD[\%] = \frac{100}{NP}\sum_{i=1}^{NP}\left|\frac{x_i^{calc} - x_i^{exp}}{x_i^{exp}}\right| \quad (2)$$

where $x$ stands for any property whose relative deviations were calculated in this work, and NP stands for number of points.

For the non-aqueous systems, the Henry's constant was calculated according to Eq. (3). $c_{CO_2}$ denotes the concentration of $CO_2$ in the solvent and the Henry's constant $H$ is expressed in kPa·m$^3$·kmol$^{-1}$. For the aqueous systems, the loading $\alpha$, expressed in mol $CO_2$ per mol MDEA, was calculated and reported.

$$H = \frac{P_{CO_2}}{c_{CO_2}} \quad (3)$$

The experimental apparatuses and procedure were validated by measuring the solubility of carbon dioxide in pure water and comparing our results to the correlation provided by Carroll et al. [23], as formulated by Penttilä et al. [24] (Fig. 1). The experiments were repeated two times and conducted both before and during the experimental campaigns to ensure good quality data. The validation measurements are presented in Table A.1. The AARD between measured and literature values was always lower than 3% for both VLE-1 and VLE-2, and the repeatability was found to be within 3% as well.

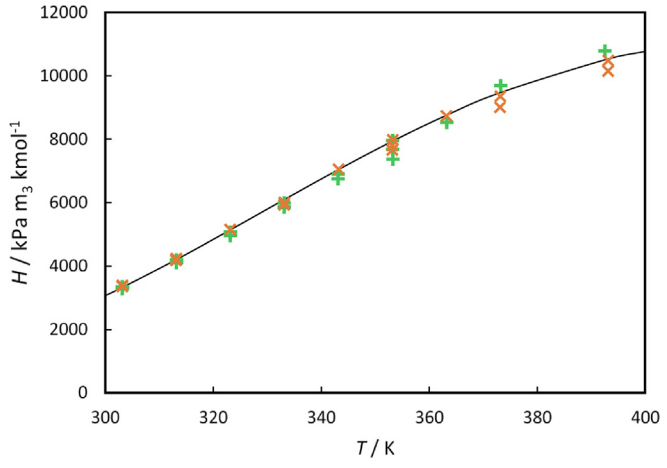


**Fig. 1.** Henry's constant for $CO_2$ in water as a function of temperature. (+) Measurements in VLE-1, (×) Measurements in VLE-2, (—) Correlation by Penttilä et al. [24].

*2.2.2. Density measurements*

An Anton Paar Density Meter DMA 4500 M was used to measure the density of the solutions used in this work, when not reported in the literature. The knowledge of the density as a function of temperature was necessary in order to calculate the volume of the solution inside the reactor, assuming that pressure effect is negligible. Calibration and validation of the apparatus was performed according to Hartono et al. [25] and Skylogianni et al. [26] An average absolute relative deviation of 0.01% was found for two repeated measurements.

*2.2.3. Karl-Fischer titration*

The presence of water in the MDEA-glycol systems was studied through Karl-Fischer titration measurements using a METHROM 831 KF coulometer. Coulometric Karl-Fischer titration is an established method for water content determination as low as a few ppm. The AARD in this work is 11%.

*2.2.4. NMR experiments*

NMR is a powerful non-invasive analytical technique for chemical analyses. Interpretation of the NMR spectra leads to the identification of the chemical structures of the molecules, including unknown products and/or side-products, and in proper performed NMR experiments the species can also be quantified [27].

In this study, qualitative $^1$H, $^{13}$C and 2D NMR experiments were performed on selected liquid samples after $CO_2$ absorption to identify reaction products formed upon the addition of carbon dioxide. In particular, $^{13}$C NMR spectra show the signals belonging to all the $CO_2$-derivatives formed upon the addition of $CO_2$, like e.g. amine carbonate, alkyl carbonate, bicarbonate and carbonate which all contain carbon (-C) nuclei in their structure [28].

Each sample was inserted in an NMR tube, together with a coaxial insert containing deuterated benzene ($C_6D_6$) for locking and referencing. The NMR experiments were performed at 300 K on a Bruker 600 MHz Avance III HD equipped with a 5-mm cryogenic CP-TCI z-gradient probe. The qualitative $^{13}$C NMR spectra shown in this work were all obtained with a standard decoupling acquisition sequence with 30-degree pulse angle and Nuclear Overhauser Effect (NOE) growth (zgpg30), using a recycle delay time of 2 s and 1024 scans.

*2.3. Modeling methods*

Vapor-liquid equilibrium of $CO_2$ with aqueous MDEA and aqueous MDEA-MEG was modeled employing the so-called "soft model", proposed by Brúder et al. [29]. It is a purely empirical correlation which is described by Eqs. (4)–(7).

$$ln(P_{CO_2}) = Aln\alpha + k_1 + \frac{B}{(1 + k_2 exp(-k_3))} \quad (4)$$

where A, B are parameters and $k_1$, $k_2$ and $k_3$ are temperature-dependent coefficients:

$$k_1 = k_{1,a} ln\left(\frac{1}{T}\right) + k_{1,b} \quad (5)$$

$$k_2 = exp(\frac{k_{2,a}}{T} + k_{2,b}) \quad (6)$$

$$k_3 = \frac{k_{3,a}}{T} + k_{3,b} \quad (7)$$

$P_{CO_2}$ is expressed in kPa, $\alpha$ in mol $CO_2$/mol MDEA and $T$ in K in the fitted model.

The model can predict the $CO_2$ partial pressures based only on temperature and loading and it has been employed in the past to successfully describe amine-containing reactive systems [29–31]. The VLE data were fitted to the correlation by minimizing the sum of the relative least square error and for each system, a different set of parameters is proposed. The binary systems, for which one or two points are obtained per temperature, were not possible to be described with the model due to the limited number of data.

## 3. Results and discussion

### 3.1. Analysis of the water content

As we investigate several non-aqueous blends, it was decided to use Karl-Fischer titration for the quantification of the water present. Analysis was performed both before and after the VLE experiments for selected non-aqueous systems studied in this work. For all the systems titrated, low water amount was found before the experiment equal or lower than 0.1 wt% $H_2O$. The detailed water concentrations and corresponding uncertainties are given in Supporting Information (Section C). It is important to note here that water was also detected in pure MEG samples even though we purchased anhydrous ethylene glycol. This signifies that some humidity was absorbed through the solution's contact with the atmosphere during solution preparation and experiment preparation.

Higher water contents were detected after the experiment was concluded. The increased water content after the experiment indicates that humidity must have remained in the reactors or in the condenser on the top of the reactor even after their thorough cleaning and drying. The observed water content was typically below 0.2 wt% while the maximum water content was observed for pure MDEA (0.5 wt%) in the end of the experiment. The impact of the detected water is discussed on the following sections.

### 3.2. MDEA – MEG mixtures

Carbon dioxide absorption in pure MEG, pure MDEA and their blends was investigated and the data obtained are presented in the Appendix (Table A.2). The measurements are reported with their respective uncertainties, calculated using the Law of propagation of uncertainty, according to the uncertainty analysis provided in Supporting Information (Section E). As explained in the experimental procedure, the solubility of a fixed $CO_2$ amount was measured at temperatures from 303 K to 393 K. The densities of the MDEA – MEG blends, required for the data processing, were calculated using the model proposed by Skylogianni et al. [26]. Density measurements of indicative systems, which were conducted to verify the model results, demonstrated maximum ARD of 1% (Section B of Supporting Information).

Several authors have reported *P-T-x* data for the binary system $CO_2$ – MEG. Fig. 2 and Fig. 3 show the mole fraction of $CO_2$ in the liquid phase against pressure at 323 K and 373 K, respectively. Literature data are also available at the studied temperatures 303 K, 333 K and 343 K and a graphical comparison can be found at Supporting Information (Figs. S.1–S.3). It is observed that the data obtained in this work are in line with those reported in the literature. The Henry's constant values are plotted as a function of temperature in Fig. 4 for all studied blends, from pure MEG to pure MDEA.

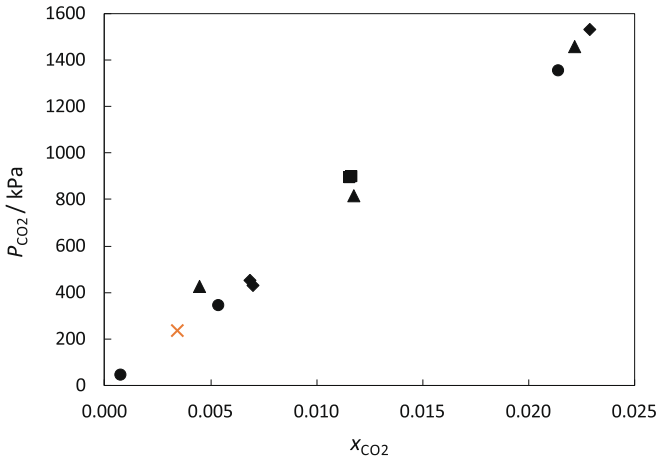


**Fig. 2.** Carbon dioxide solubility in MEG expressed in mole fraction ($x_{CO2}$) as a function of pressure at 323 K. (■) Zheng et al. (1999) [32], (▲) Galvao and Franscesconi (2010) [33], (●) Jou et al. (1990) [34], (◆) Wise and Chapoy (2017) [35], (×) This work.

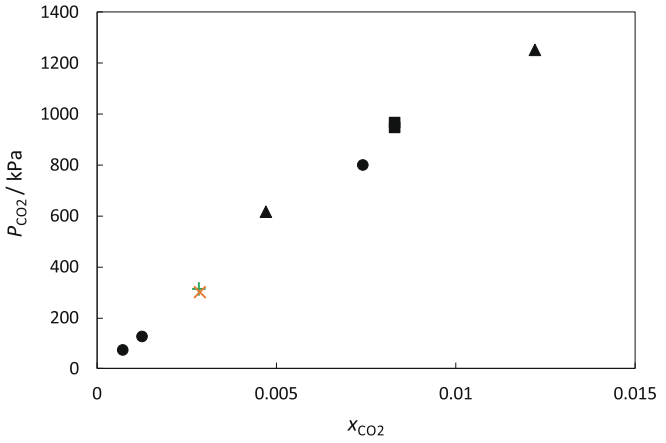


**Fig. 3.** Carbon dioxide solubility in MEG expressed in mole fraction ($x_{CO2}$) as a function of pressure at 373 K. (■) Zheng et al. (1999) [32], (▲) Galvao and Franscesconi (2010) [33], (●) Jou et al. (1990) [34], (×) This work (A), (+) This work (B).

As illustrated in Fig. 4, Henry's constant increases with temperature, thus the solubility of $CO_2$ into the solvent decreases, for both unitary and binary solvents studied in this work. This is explained by the higher kinetic energy with temperature resulting to the escape of gas molecules from the liquid and in the gas phase. Moreover, it is shown that the Henry's constant of $CO_2$ in MEG is higher than the Henry's constant of $CO_2$ in MDEA. The uncertainties calculated have an average deviation from their corresponding properties of 7%. It was found that Henry's constant has higher sensitivity to the amount of $CO_2$ absorbed in the solvent, due to the propagation of errors in its calculation (Eq. S.24 in Supporting Information). Therefore, the experiments with low $CO_2$ uptake are expected to have the highest uncertainty in Henry's constant. These experiments include mainly those experiments performed with a single loading.

An unexpected behavior was observed for the mixtures of the glycol with the amine: the solubility of carbon dioxide in mixtures

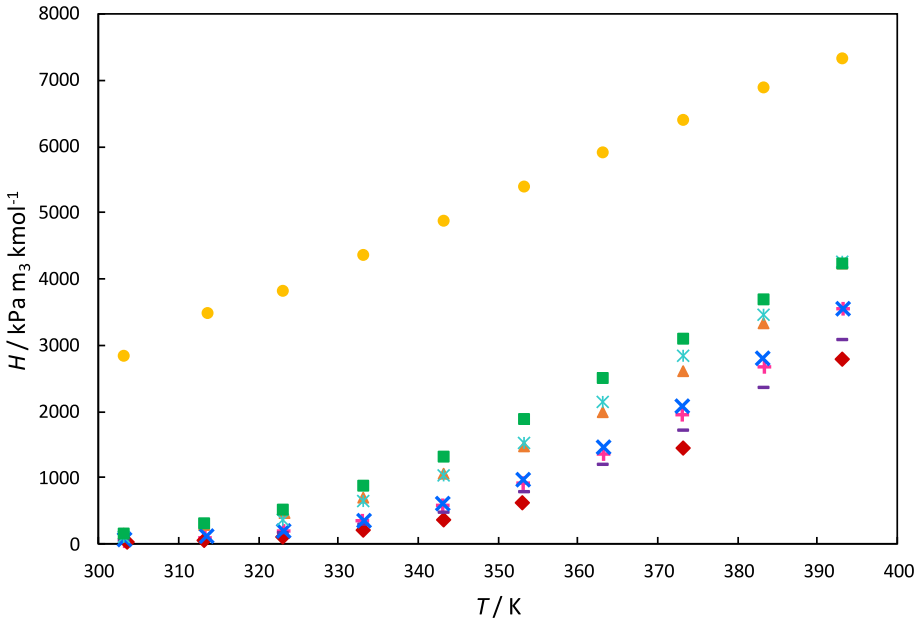


**Fig. 4.** Henry's constant as a function of temperature for pure MEG, pure MDEA and their blends as measured in this work. (●) Pure MEG, (▲) 5 wt% MDEA – 95 wt% MEG, (+) 10 wt% MDEA – 90 wt% MEG, (◆) 30 wt% MDEA – 70 wt% MEG, (—) 50 wt% MDEA – 50 wt% MEG, (×) 70 wt% MDEA – 30 wt% MEG, (✳) 90 wt% MDEA – 10 wt% MEG, (■) Pure MDEA.

of MDEA – MEG is higher than it is in its individual components. The measurements for selected blends of MDEA – MEG were repeated in order to confirm the observed trends. To be specific, the $CO_2$ solubility measurements were conducted twice in the blends of 5 wt% MDEA – 95 wt% MEG, 10 wt% MDEA – 90 wt% MEG, 30 wt% MDEA – 70 wt% MEG and 50 wt% MDEA – 50 wt% MEG as well as in pure MEG. Good repeatability was found with AARD equal to 4%. The repeated measurements are given in the Appendix (Table A.4).

In addition, we can observe that as amine is added in MEG, initially the solubility of carbon dioxide increases. Between 30 and 50 wt% MDEA content, a transition occurs, after which addition of amine leads to lower $CO_2$ solubility. As a result, the Henry's constant of $CO_2$ is similar in a rich-amine system and a lean-amine system, for example in 70 wt% MDEA – 30 wt% MEG system and 10 wt% MDEA – 90 wt% MEG system. This behavior indicates the presence of chemical effects for $CO_2$ – MDEA – MEG systems. Therefore, the solubility of $CO_2$ in MDEA – MEG may not be only physical as initially assumed.

No chemical reactions are indeed expected between $CO_2$ and neither pure MEG nor pure MDEA. MDEA is a tertiary amine which cannot react with carbon dioxide in the absence of water [9,36]. In order to gain an understanding of the phenomena observed, we conducted isothermal VLE experiments at 313 K and 343 K for the systems $CO_2$ – MEG and $CO_2$ – MDEA. $CO_2$ solubility in 50 wt % MDEA – 50 wt% MEG was also measured at constant temperature in order to provide more insights. The results of this study are reported in Table A.3. The data obtained at 313 K are plotted in Fig. 5 while a similar plot of the data at 343 K can be found in Supporting Information (Fig. S.4).

A linear relation between the partial pressure of a gas and its solubility in a solvent denotes that only physical absorption occurs, according to the simplified form of Henry's Law for ideal systems. In that case, the $H_{gas,solvent}$, *i.e.* the slope, is constant and a strong function of temperature. The linearity is assessed using the coefficient of determination, $R^2$. It is clear that the *P-x* relation is linear for pure MEG with $R^2$ equal to almost unity, *i.e.* 0.9995 and 0.9998 for 313 K and 373 K, respectively. This indicates that there

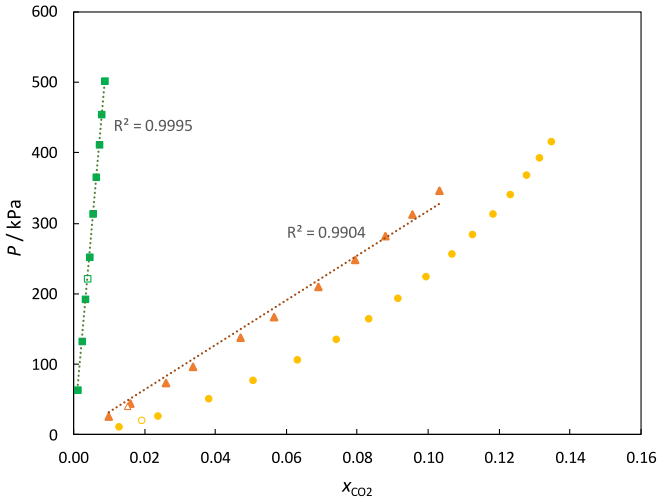


**Fig. 5.** Partial pressure of $CO_2$ as a function of $CO_2$ solubility in pure MEG, pure MDEA and their 50 – 50 wt% blend at 313 K. Filled symbols denote isothermal experiment (Table A.3) and hollow symbols denote previous experiment (Table A.2); (■) MEG, (▲) MDEA, (●) 50 wt% MDEA – 50 wt% MEG. Dotted lines are linear trend lines; the linearity between *P* and *x* for pure MEG and pure MDEA is assessed through the coefficient of determination, $R^2$.

are no chemicals effects. For pure MDEA, a linear relation can be also seen at the studied conditions with a coefficient of determination 0.9904 and 0.9982 for 313 K and 373 K, respectively. One could, however, argue that some chemical effects might be present since the coefficient of determination for MDEA data is lower and also some curvature can be observed with a naked eye, particularly at 313 K (Fig. 5). A non-linear relationship between the partial pressure of carbon dioxide and its solubility in a 50 wt% MDEA – 50 wt% MEG blend is also pronounced in the same figure.

Chemical absorption of carbon dioxide into pure MDEA or blends of MDEA-MEG could take place if water is present in the system. Some amounts of water were detected by Karl-Fischer titration in our samples, as presented in Section 3.1. Although

the presence of small amount of water can explain the noticed chemical effects in pure MDEA, it does not explain the interesting behavior of increased $CO_2$ solubility up to (30 – 50) wt% MDEA-MEG and decreased solubility as the amine content further rises. For this reason, we also conducted NMR experiments to identify the species present in our loaded systems and further understand the system chemistry. The NMR results follow the VLE results for the aqueous systems.

### 3.3. MDEA – MEG – $H_2O$ mixtures

Solubility measurements of carbon dioxide into aqueous solutions of MDEA – MEG were performed with MDEA concentration in the solution kept constant at 30 wt% while the water content varied from 10 wt% to 50 wt% (Table A.6). Similar to the MDEA – MEG study, the densities, which are necessary for the data treatment, were found in the literature [26]. Comparison between experimental and literature values at selected temperatures revealed 0.3% maximum absolute relative deviation (Section B of Supporting Information).

The partial pressure of $CO_2$ as a function of $CO_2$ loading at 313 K and 343 K is shown in Fig. 6 for the 30 wt% MDEA – 60 wt% MEG – 10 wt% $H_2O$ studied mixture. The increase in loading as temperature decreases, at constant pressure, is justified by the exothermic nature of the reaction of $CO_2$ with aqueous MDEA. One can also observe the good repeatability between two experiments, one with multiple pressurizations under isothermal conditions and one with single $CO_2$ pressurization and temperature variation, which was performed for repeatability checks and to provide data points in several temperatures (Table A.5). These remarks are also valid for the additional aqueous mixtures studied in this work, as shown in Supporting Information (Figs. S.5 and S.6).

The effect of water content is illustrated in Fig. 7 and Fig. 8 for 313 K and 343 K, respectively. At 313 K, our measurements are compared with the data points reported by Shen and Li [37] and Xu et al. [16] for a 30 wt% MDEA – $H_2O$ system, for non-aqueous and aqueous MDEA – MEG blends. Although the data produced in this work for the ternary systems cover partial pressures up to 500 kPa, the y axis of Fig. 7 extends up to 140 kPa, in order for the data points at low partial pressures and loadings to be shown distinctly. The same figure covering pressures in the whole range

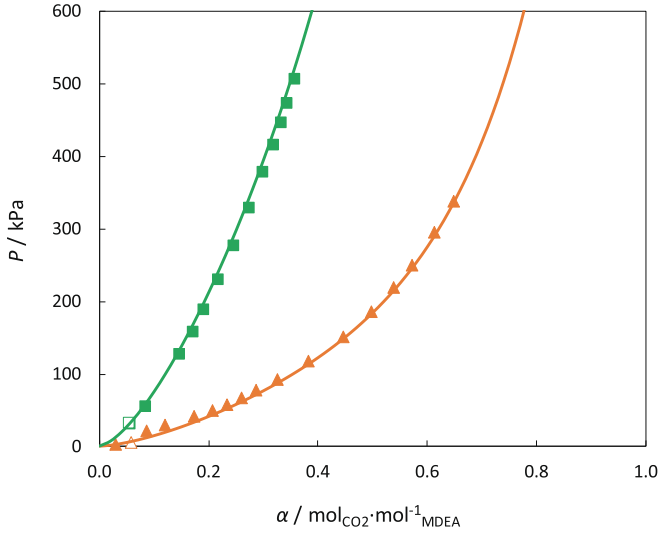


**Fig. 6.** Partial pressure of $CO_2$ as a function of $CO_2$ loading in a solution of 30 wt% MDEA – 60 wt% MEG – 10 wt% $H_2O$. Filled symbols denote isothermal experiment (Table A.6) and hollow symbols denote repeated experiment with a single loading (Table A.5). (▲) 313.2 K, (■) 343.2 K.

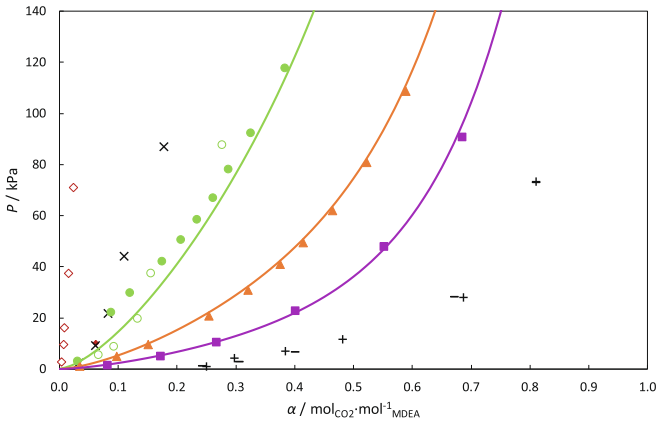


**Fig. 7.** Partial pressure of $CO_2$ as a function of $CO_2$ loading in MDEA (1) – MEG (2) – $H_2O$ (3) blends at 313 K. 30 wt% MDEA – 70 wt% MEG: (◆) This work and (◇) data from Xu et al. [16], 30 wt% MDEA – 65 wt% MEG – 5 wt% $H_2O$: (×) Xu et al. [16], 30 wt% MDEA – 60 wt% MEG – 10 wt% $H_2O$: (●) This work and (○) Xu et al. [16], 30 wt% MDEA – 40 wt% MEG – 30 wt% $H_2O$: (▲) This work, 30 wt% MDEA – 20 wt% MEG – 50 wt% $H_2O$: (■) This work, 30 wt% MDEA – 70 wt% $H_2O$: *(+)* Xu et al. [16] and (−) Shen and Li [37]. The lines represent model estimations.

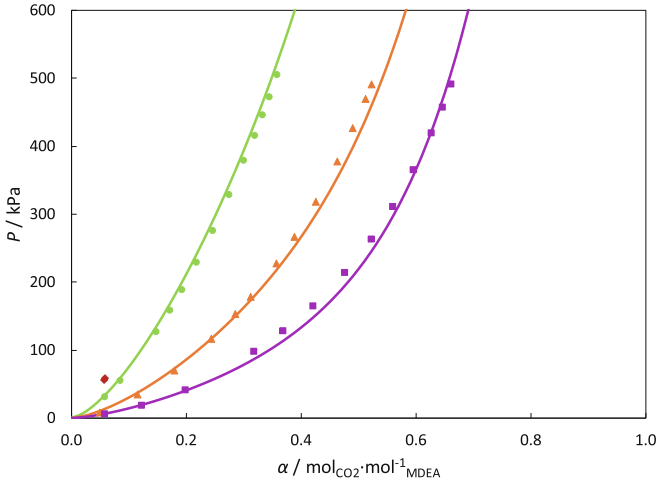


**Fig. 8.** Partial pressure of $CO_2$ as a function of $CO_2$ loading in MDEA (1) – MEG (2) – $H_2O$ (3) blends at 343 K as measured in this work. (◆) 30 wt% MDEA – 70 wt% MEG, (●) 30 wt% MDEA – 60 wt% MEG – 10 wt% $H_2O$, (▲) 30 wt% MDEA – 40 wt% MEG – 30 wt% $H_2O$, (■) 30 wt% MDEA – 20 wt% MEG – 50 wt% $H_2O$. The lines represent model estimations.

of this study can be found in Supporting Information (Fig. S.7). We notice that the $CO_2$ solubility in aqueous blends of MDEA – MEG is lower than the one in aqueous MDEA. The higher the water content, the higher loading at constant pressure, as shown for both 313 K and 343 K. For example, at pressure ca. 50 kPa and 313 K, the loading is approximately 0.20, 0.41 and 0.55 at water compositions 10 wt%, 30 wt% and 50 wt% respectively and constant amine content (30 wt%).

The presence of glycol and its substitution with water therefore leads to lower solution loadings. On the one hand, the physical solubility of $CO_2$ into pure MEG is higher than the one in water. For example, at 323 K, $H_{CO2,water}$ = 5000 kPa·m$^3$·kmol$^{-1}$ while $H_{CO2,MEG}$ = 3800 kPa·m$^3$·kmol$^{-1}$ approximately. On the other hand, the carbon dioxide uptake from MDEA due to the reaction in the presence of water is much larger than the one due to dissolution in the solvent. We can confidently say that this behavior of decreasing solution loading with increasing glycol content is true as the water content decreases down to 10 wt%. Interestingly, the data point

obtained for the 30 wt% MDEA – 70 wt% MEG system at 313 K in the first experimental campaign coincides with the measurements performed in the presence of 10 wt% water (30 wt% MDEA – 60 wt % MEG – 10 wt% $H_2O$). At 343 K and Fig. 8 though, employment of 30 wt% MDEA – 70 wt% MEG solution yields indeed lower amine loadings. NMR analysis was therefore decided to be performed also for the aqueous systems.

As far as the comparison with literature data on MDEA – MEG – $H_2O$ and 30 wt% MDEA – 70 wt% is concerned, some disagreements can be observed. For the non-aqueous system, a significant deviation can be seen between the measured solubility and the literature one. Xu et al. [16] state that they performed Karl-Fischer titration but they do not inform the amount of detected water in their systems. Lower water content in Xu et al.'s samples than in ours, could explain the observed deviations. Moreover, at amine loadings lower than 0.15 mol $CO_2$/mol MDEA, our data for a 30 wt% MDEA – 60 wt% MEG – 10 wt% $H_2O$ system fall together with literature data for a 30 wt% MDEA – 65 wt% MEG – 5 wt% $H_2O$ system. Our measurements were performed twice demonstrating a maximum ARD of 6% at 303 K and the uncertainties of the data obtained in this study are low and cannot explain the deviations from the literature.

The solid lines in Figs. 6–8 are model estimations using the so-called "soft model", as described in Section 2.3. In the aforementioned figures, it can be seen that the model yields accurate predictions of the VLE data. The AARD is 9% for the systems 30 wt% MDEA – 60 wt% MEG – 10 wt% $H_2O$ and 30 wt% MDEA – 20 wt% MEG – 50 wt% $H_2O$ while for the system 30 wt% MDEA – 40 wt% MEG – 30 wt% $H_2O$, whose number of data points is higher than the other two systems, the AARD is 4%. The AARDs for the 70 wt% aqueous MDEA and for the 90 wt% aqueous MDEA investigated in the next section, are 3% and 5%, respectively. The model parameters are presented in Appendix B.

### 3.4. Comparison with highly concentrated MDEA solutions

After investigating the effect of water and after observing the effect of MEG concentration in $CO_2$ loading of the non-aqueous solvent, as described in Section 3.2, we decided to investigate the outcome of substituting glycol with amine. In this framework, $CO_2$ solubility measurements were conducted in 70 wt% MDEA – 30 wt% $H_2O$ and in 90 wt% MDEA – 10 wt% $H_2O$. Similar to the experiments with aqueous MDEA – MEG, the experiments were performed at 313 K and 343 K. The obtained data are reported in Appendix A (Table A.7). At constant pressure, higher $CO_2$ loadings are achieved with 70 wt% aqueous MDEA than with 90 wt% aqueous MDEA. Thus, increasing amine concentrations in the solvent leads to lower absorption capacities and the $CO_2$ capture by the aqueous MDEA seems to be limited by water availability.

A comparison was performed between the amine and amine-glycol systems with constant water content, *i.e.* 10 wt% and 30 wt% water. Fig. 9 shows the results of the comparison between 30 wt% MDEA – 60 wt% MEG – 10 wt% $H_2O$ and 90 wt% MDEA – 10 wt% $H_2O$ in terms of $CO_2$ absorbed per kg of solution in order to give a more perceptible sense of the capacity of the solvent. One can observe that at constant pressure, the glycol-containing system demonstrates similar or better performance than the MDEA-$H_2O$ system in terms of $CO_2$ removed per kg of solution. Although $CO_2$ solubility in MDEA is higher than in MEG, some additional reactivity is observed in the aqueous MDEA – MEG system, at same water content, in line with previous observations. At 313 K, this behavior is shown for pressures lower than 200 kPa. For the systems with 30 wt% water however, aqueous MDEA outperforms the glycol-containing system (Fig. S.8 in Supporting Information). It is worth mentioning that non-aqueous systems, *i.e.* 90 wt% MDEA – 10 wt% MEG and 70 wt% MDEA – 30 wt% MEG, yield lower $CO_2$ concentrations than their aqueous counterparts.

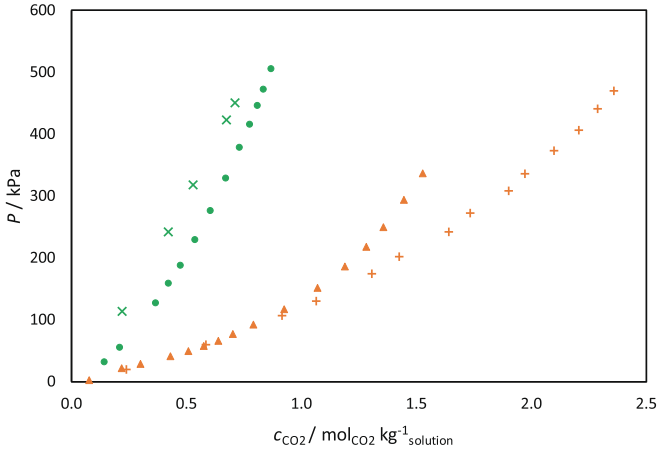


**Fig. 9.** Partial pressure of $CO_2$ as a function of $CO_2$ liquid phase concentration in 30 wt% MDEA – 60 wt% MEG – 10 wt% $H_2O$ and 90 wt% MDEA – 10 wt% $H_2O$. (▲) denotes data obtained at 313 K with MDEA – MEG – $H_2O$ system, (+) 313 K with MDEA – $H_2O$ system; (●) 343 K with MDEA – MEG – $H_2O$ system and (×) 343 K with MDEA – $H_2O$ system.

### 3.5. Chemical characterization by NMR spectroscopy

Small amounts of water were detected in our non-aqueous systems signifying a possible reaction with carbon dioxide, due to the amine protonation by the water which is present. The reactions taking place in $CO_2$ – MDEA – $H_2O$ systems are listed below. Reactions R. 1 to R. 4 are usually considered in the description of chemical equilibrium, however, there are several studies in literature showing that aqueous tertiary amines can react with $CO_2$ to form alkyl carbonate [38,39]. Behrens et al. [40] showed by means of NMR analysis that, in $CO_2$ – MDEA – $H_2O$ system, more than 10 mol% of the absorbed $CO_2$ is in the form of MDEA carbonate ($MDEACOO^-$) (Reactions R. 5 and R. 6).

$$CO_2 + OH^- \leftrightarrows HCO_3^- \quad (R1)$$

$$HCO_3^- + OH^- \leftrightarrows CO_3^{2-} + H_2O \quad (R2)$$

$$CO_2 + H_2O \leftrightarrows H_2CO_3 \leftrightarrows HCO_3^- + H^+ \quad (R3)$$

$$MDEA + H_2O \leftrightarrows MDEAH^+ + OH^- \quad (R4)$$

$$MDEA + HCO_3^- \leftrightarrows MDEACOO^- + H_2O \quad (R5)$$

$$MDEAH^+ + HCO_3^- \leftrightarrows MDEAH^+COO^- + H_2O \quad (R6)$$

With the aim of identifying possible chemical products deriving from the addition of $CO_2$ in the VLE measurements of pure MEG, pure MDEA, non-aqueous MDEA – MEG blends (5 wt% MDEA – 95 wt% MEG and 50 wt% MDEA – 50 wt% MEG) and aqueous MDEA – MEG blends (30 wt% MDEA – 60 wt% MEG – 10 wt% $H_2O$ and 30 wt% MDEA – 20 wt% MEG – 50 wt% $H_2O$), $^1H$ and $^{13}C$ NMR experiments were performed, together with 2D NMR experiments. The interpretation of the spectra and their comparison allowed the structural characterization of the species in the solutions.

Fig. 10 shows the $^{13}C$ NMR spectra and the signal assignment of the species at equilibrium in pure MEG, pure MDEA and 50 wt% MDEA – 50 wt% MEG in the presence of $CO_2$. In the up field region of the $^{13}C$ NMR spectra, which here spans from ca. (40 to 70) × $10^{-6}$, the signals belonging to carbons nuclei –$CH_2$ and $CH_3$

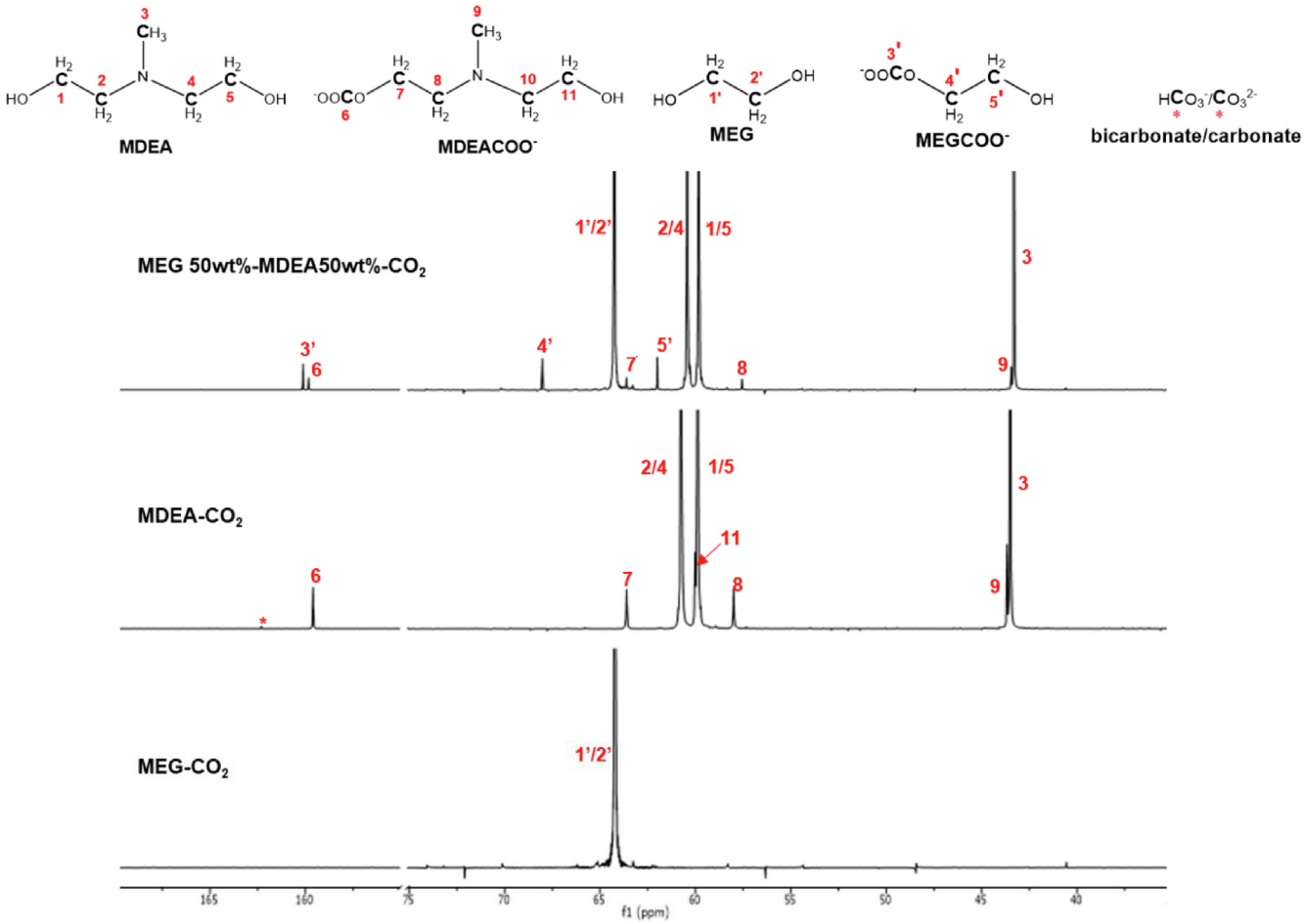


**Fig. 10.** $^{13}C$ NMR spectra of $CO_2$ loaded pure MEG, pure MDEA, and 50 wt% MDEA – 50 wt% MEG.

of MDEA, MEG and their derivatives are resonating. In the downfield region, here spanning from ca. (155 to 170) $\times 10^{-6}$, the nuclei of the carbonyl carbons in the alkyl carbonates (R-O-$COO^-$) and bicarbonate/carbonate ($HCO_3^-/CO_3^{2-}$) are found. The downfield region is therefore very representative of the formation of $CO_2$-derivatives in the samples under study. It is worth mentioning that, in the $^{13}C$ NMR spectra, the carbons of $HCO_3^-$ and $CO_3^{2-}$ appear with a common signal at an averaged chemical shift. This is due to the fact that they are two species in equilibrium, and the proton exchange between them (R. 2) is faster than the NMR time scale. The same is true for the amine and its protonated form (such as shown in R. 4 and R. 6) [41].

Looking at the species content, we observe that in $CO_2$-MDEA system, in addition to MDEA itself, MDEA carbonate ($MDEACOO^-$) is formed, together with negligible traces of $HCO_3^-/CO_3^{2-}$. These reaction products may be the result of the presence of water traces which start a series of reactions (R. 1 to R. 6). On the contrary, in $CO_2$-MEG system, neither MEG is chemically reacting with carbon dioxide nor $HCO_3^-/CO_3^{2-}$ is formed. Interestingly, in the presence of MDEA, MEG is reacting to $CO_2$, giving MEG carbonate ($MEGCOO^-$). This is even formed in the presence of only 5 wt% MDEA (Fig. S.11 in the Supporting Information). With regard to the electroneutrality, it would be expected that the protonated form of MDEA ($MDEAH^+$) would act as counterion of the alkyl carbonates and $HCO_3^-/CO_3^{2-}$.

In Fig. 11, the comparison of the downfield region in the $^{13}C$ NMR spectra of the MEG – MDEA blends in water are reported (Full spectra are available in Fig. S.12 of the Supporting Information). In

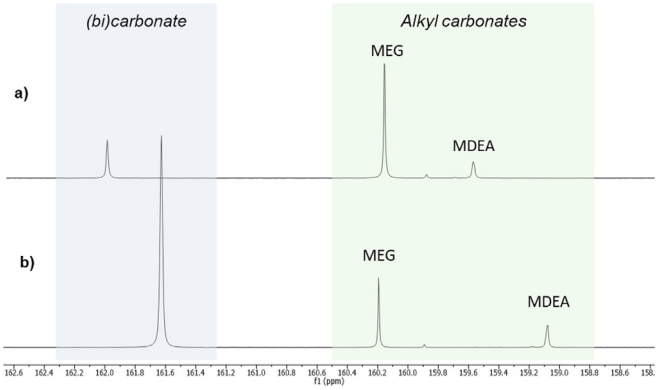


**Fig. 11.** Downfield region of the $^{13}C$ NMR spectra of $CO_2$ loaded a) 30 wt% MDEA – 60 wt% MEG – 10 wt% $H_2O$ and b) 30 wt% MDEA – 20 wt% MEG – 50 wt% $H_2O$; (bi)carbonate stands for $HCO_3^-/CO_3^{2-}$.

the presence of water, consistent amounts of bicarbonate/carbonate are formed, and the intensity of the peak is proportional to the amount of water in the sample. In the alkyl carbonates region, the carbonyl carbon belonging to MEG and MDEA carbonates are found, and the presence of additional weak signals may suggest the formation of additional MEG-$CO_2$ and MDEA-$CO_2$ derivatives, like e.g. MEG dicarbonate ($MEG(COO^-)_2$) and/or MDEA dicarbonate ($MDEA(COO^-)_2$). However, due to weakness and/or overlapping of these signals in the spectra, these compounds were not identified.

### 3.6. Hypothesis on reaction mechanisms of MEG with $CO_2$ in the presence of MDEA and comparison with TEG

The NMR results can explain the behavior of $CO_2$ – MDEA – MEG system as illustrated in Fig. 4. The solubility of carbon dioxide into MDEA – MEG is higher than in pure MEG or pure MDEA because of the chemical reaction taking place between $CO_2$ and MEG in the presence of MDEA. This may be the result of autoprotolysis of MEG in the alkaline environment created by the amine [42]. The absence of $MEGCOO^-$ in MEG-$CO_2$ system indicates that, in the presence of MDEA, the hydroxyl group (–OH) of MEG is more prone to lose its proton, and it is then available to chemically bind carbon dioxide. As a result, in MDEA – MEG blends, both MDEA carbonate and MEG carbonate are formed. The chemical absorption of carbon dioxide into monoethylene glycol is a trade-off between the amount of amine available to offer the basicity required for MEG to autoprotolyze and the amount of MEG available for autoprotolysis.

The solvent composition between 30 and 50 wt% MDEA where we observed the reduced $CO_2$ solubility upon addition of amine, is probably the limits of this trade-off. From that point towards leaner-in-glycol systems, smaller amount of MEG autoprotolyzes and therefore the Henry's constant increases, for a given temperature. Moreover, the overlapping data for 30 wt% MDEA – 60 wt% MEG – 10 wt% $H_2O$ and 30 wt% MDEA – 70 wt% MEG discussed earlier can be attributed to the $CO_2$ – MEG reaction and MEG carbonate formation in the MDEA – MEG system which is probably in the same extent as the combined MEG carbonate and MDEA carbonate formation in the aqueous system.

Barzagli et al. [43] have also reported the presence of the glycol carbonate in their studies of $CO_2$ solubility into non-aqueous MDEA – MEG – propanol systems and discussed the ability of alcohols to absorb carbon dioxide when in the presence of a base. For these phenomena to take place, only tertiary amines should serve as a base. If a primary or a secondary amine was used, the glycol carbonate formation would be hindered by the stable carbamate formation. On the contrary, tertiary amines cannot form carbamates, making them ideal for selective removal of hydrogen sulfide over carbon dioxide, since $H_2S$ can react directly with the amine. The increased reactivity of MDEA – MEG blends for the selective removal of $H_2S$ over $CO_2$ is also discussed by Dag Eimer [42].

The degree of autoprotolysis of a compound is informed by its dissociation constant (autoprotolysis constant, $K_{ap}$). The higher the $K_{ap}$ (the lower the $pK_{ap} = -\log_{10}(K_{ap})$), the higher the tendency of releasing a proton from the –OH group. As suggested by Eimer [42], amine-MEG mixtures should have higher reactivity than amine-TEG blends, due to the lower $pK_{ap}$ value of MEG. The $pK_{ap}$ values for MEG and TEG are approximately 16 and 18.5, respectively [42]. Thus, the degree of autoprotolysis in TEG is lower than that in MEG and, it would be expected that the solubility of $CO_2$ in MDEA – TEG mixtures would be lower than in MDEA – MEG mixtures at the same concentrations.

To confirm this theory, we performed an additional VLE experimental campaign for the system $CO_2$ – MDEA – TEG. The VLE data for the TEG-containing systems are presented in Table A.8 in the Appendix and the required for the data processing measured densities can be found in Table S.1 in the Supporting Information. Available literature data for the density of pure TEG were compared with our measurements (Fig. 12). The obtained experimental points follow the behavior of the literature data, except for the data of Sagdeev et al. [44] and Tawfik and Teja [45], which are consistently higher than the rest of the data. The uncertainties reported by the different authors in most cases are higher than the deviations observed. These deviations can be attributed to the different chemical purity as well as to possible unwanted humidity absorption from the air due to the high hygroscopicity of TEG. However,

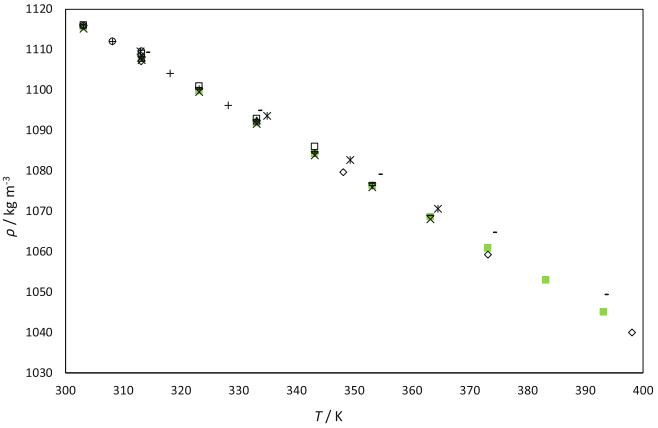


**Fig. 12.** Density of pure TEG as a function of temperature at atmospheric pressure. (×) Pereira et al. (2019) [46], (—) Crespo et al. (2017) [47], (✱) Sagdeev et al. (2011) [44], (□) Tsai et al. (2009) [48],(○) Sastry et al. (2008) [49], (+) Valtz et al. (2004) [50], (◇) Steele et al. (2002) [51], (Δ) Kumagai et al. (1993) [52], (-) Tawfik and Teja (1989) [45], (■) This work.

the calculated absolute relative deviations (ARD) are low, ranging from 0.01% to 0.15%.

In this study of TEG-containing systems, we first measured the carbon dioxide solubility in pure TEG and compared our results with literature values [53,54] (Fig. 13). It is observed that the obtained data are in good agreement with the literature. Moreover, Tan et al. [18] reported Henry's constant of $CO_2$ in pure TEG. Their data agree with the measured Henry's constants in this work, and any small deviations observed are well within experimental uncertainty. A graphical comparison is provided in Supporting Information (Fig. S.10).

Moreover, we studied MDEA – TEG blends in two different compositions, 30 wt% MDEA – 70 wt% TEG and 50 wt% MDEA – 50 wt% TEG. These compositions were selected in order to allow for a direct comparison with MDEA – MEG mixtures at same amine weight fraction.

The following figure (Fig. 14) depicts Henry's constant as a function of temperature and composition in MDEA – MEG and

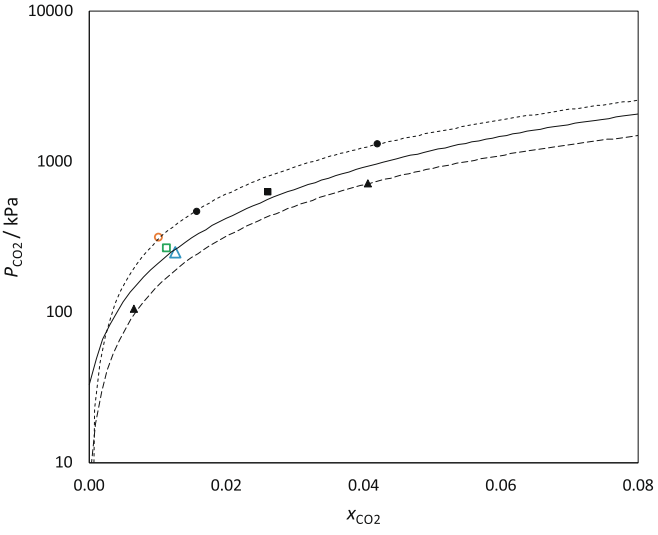


**Fig. 13.** Partial pressure of $CO_2$ as a function of $CO_2$ solubility and temperature in pure TEG. Triangles denote 323 K, squares denote 343 K and circles denote 373 K. Filled symbols are literature values; (●), (▲) from Jou et al. [53] and (■) from Wise and Chapoy [54]. Hollow symbols are data obtained in this work. Tendency curves are drawn: dashed line (—) for 323 K, solid line (––) for 343 K and dotted line (••••) for 373 K.

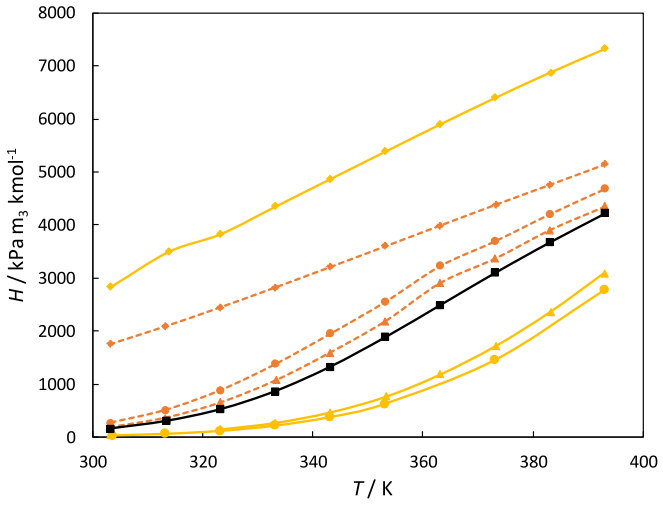


**Fig. 14.** Henry's constants as a function of temperature for MDEA – MEG and MDEA – TEG systems. Tendency curves are drawn: (—•—, dashed dot line) MEG-containing systems, (.....,dotted line) TEG-containing systems. (◆) Pure glycol, (●) 30 wt% MDEA – 70 wt% glycol, (▲) 50 wt% MDEA – 50 wt% glycol, (■) Pure MDEA.

MDEA – TEG systems. Henry's constant is higher in MDEA – TEG blends than MDEA – MEG blends, while it is lower in pure TEG than in pure MEG. These results are therefore in agreement with the theory, since the degree of autoprotolysis of TEG is lower than that of MEG, leading to lower $CO_2$ solubility. In addition to this, the Henry's constant values in MDEA – TEG blends lie between the Henry's constants in pure TEG and pure MDEA suggesting that $CO_2$ is absorbed mainly physically in the solvent. However, some chemical effects are also present as indicated by the results of an isothermal experiment at 313 K for the 50 wt% MDEA – 50 wt% TEG system where a non-linear relation between *P-x* is pronounced (Fig. S.9). Based on the NMR data obtained in this study, there is no formation of TEG carbonate ($TEGCOO^-$) in $CO_2$ – TEG system, as it was also observed in $CO_2$ – MEG. In $CO_2$ – MDEA – TEG systems, $MDEACOO^-$ was found, but the presence of $TEGCOO^-$ was not clear. Due to overlapping signals and crowded-signals spectra, some low-intensity signals were not assigned, but it is expected that the correspondent molecules would be in negligible amounts. Therefore, the chemical effects observed in MDEA – TEG systems are mainly due to the reaction of $CO_2$ with MDEA in the presence of water traces. All relevant spectra are available in Supporting Information (Fig. S.13).

The findings of this work are important for the industrial application of an MDEA – MEG mixture for the combined hydrogen sulfide removal and hydrate control. For a successful design and trouble-free operations, the knowledge of the amount of co-absorbed carbon dioxide into the solvent through the known aqueous amine mechanism as well as through its reaction with MEG is necessary. The importance of this work lies in the need to account for the $CO_2$ absorbed in the glycol as well in the amine during solvent regeneration. As proven from the data presented for $CO_2$ – MDEA – TEG systems, these implications are in a significantly lesser extent in the systems using TEG.

## 4. Conclusions

Aqueous and non-aqueous solvents composed by MDEA and MEG are promising for the simultaneous $H_2S$ removal and hydrate control in natural gas. Since $CO_2$ co-exists with $H_2S$ in natural gas streams, the solubility of carbon dioxide in non-aqueous and aqueous MDEA – MEG systems was investigated in this work.

VLE data were obtained at temperatures from 303 K to 393 K and pressures up to 600 kPa. It was found that the absorption capacity of the aqueous solvents decreases with increasing glycol content and substitution of water, at constant amine concentration. Increasing amine content up to 90 wt% in aqueous MDEA systems, also leads to lower solvent $CO_2$ loadings.

In the non-aqueous solvents, a transition phase was observed at compositions between 30 and 50 wt% MDEA – MEG. $CO_2$ solubility increases with amine concentration up to this transition area, after which the solubility starts decreasing. This behavior is attributed to the $CO_2$ capture through chemical reaction of $CO_2$ with MEG in the presence of MDEA, as a result of MEG autoprotolysis in the alkaline environment of the amine. This theory is supported by supplementary VLE data obtained for MDEA – TEG systems.

NMR experiments proved the formation of glycol carbonate, both in non-aqueous and aqueous MDEA – MEG blends. MDEA carbonate was also identified both in single and blended MDEA, which is probably due to the small amounts of water found in our non-aqueous solvents. The $CO_2$ solubility in aqueous blends of MDEA – MEG is generally higher than the one in their non-aqueous counterparts. However, similar absorption capacities can be observed for aqueous systems containing less than 10 wt% water and non-aqueous systems.

The $CO_2$ uptake by the glycol demonstrated in this work is important knowledge for the application of aqueous or non-aqueous MDEA – MEG mixtures for the combined removal of $H_2S$ and hydrate control, and specifically for the solvent regeneration.

## CRediT authorship contribution statement

**Eirini Skylogianni:** Conceptualization, Investigation, Validation, Writing - original draft, Writing - review & editing. **Cristina Perinu:** Investigation, Writing - review & editing. **Blanca Y. Cervantes Gameros:** Investigation. **Hanna K. Knuutila:** Conceptualization, Investigation, Writing - review & editing, Supervision, Project administration, Funding acquisition.

## Declaration of Competing Interest

The authors declare that they have no known competing financial interests or personal relationships that could have appeared to influence the work reported in this paper.

## Acknowledgement

This work was carried out as a part of SUBPRO (Subsea Production and Processing), a Research-based Innovation Centre within Subsea Production and Processing. It is funded by major industry partners, the Norwegian University of Science and Technology (NTNU) and the Research Council of Norway (RCN) [project number 237893]. Karen Karolina Høisæter is acknowledged for running some 2D NMR experiments on MDEA-TEG systems.

## Appendix A

All VLE data obtained in this work are presented in this section.

**Table A.1**
Measured mole fraction solubility $x_{CO2}$ and Henry's constant $H$ for $CO_2$ in water as a function of temperature $T$ and pressure (total pressure $P_{tot}$, residual pressure $P_{res}$ and their difference, $CO_2$ partial pressure $P_{CO2}$).[a]

| T | $P_{tot}$ | $P_{res}$ | $P_{CO2}$ | $x_{CO2}$ | $u(x_{CO2})$ | H | u(H) | T | $P_{tot}$ | $P_{res}$ | $P_{CO2}$ | $x_{CO2}$ | $u(x_{CO2})$ | H | u(H) |
|---|---|---|---|---|---|---|---|---|---|---|---|---|---|---|---|
| K | kPa | kPa | kPa | $\cdot 10^2$ | | kPa $m^3$ $kmol^{-1}$ | | K | kPa | kPa | kPa | $\cdot 10^2$ | | kPa $m^3$ $kmol^{-1}$ | |
| | | | | VLE 1 | | | | | | | | VLE 2 | | | |
| 303.1 | 200.3 | 4.6 | 195.7 | 0.108 | 0.015 | 3281 | 454 | 303.1 | 168.2 | 5.3 | 162.9 | 0.087 | 0.006 | 3389 | 512 |
| 313.2 | 224.0 | 7.6 | 216.4 | 0.096 | 0.015 | 4108 | 648 | 313.2 | 188.6 | 8.7 | 180.0 | 0.077 | 0.006 | 4234 | 727 |
| 323.2 | 247.0 | 12.4 | 234.6 | 0.086 | 0.015 | 4952 | 873 | 323.2 | 209.3 | 13.6 | 195.6 | 0.069 | 0.006 | 5145 | 992 |
| 333.2 | 271.4 | 19.5 | 251.8 | 0.079 | 0.015 | 5854 | 1141 | 343.2 | 255.8 | 32.3 | 223.5 | 0.058 | 0.006 | 7046 | 1645 |
| 343.1 | 298.1 | 30.5 | 267.7 | 0.073 | 0.015 | 6748 | 1435 | 353.2 | 284.5 | 48.5 | 236.0 | 0.055 | 0.006 | 7981 | 2013 |
| 353.2 | 329.6 | 46.6 | 283.0 | 0.068 | 0.015 | 7679 | 1770 | 363.2 | 318.8 | 71.9 | 246.9 | 0.053 | 0.006 | 8733 | 2328 |
| 363.2 | 366.4 | 69.4 | 297.1 | 0.065 | 0.015 | 8527 | 2100 | 313.2 | 167.2 | 8.0 | 159.2 | 0.069 | 0.013 | 4203 | 798 |
| 303.1 | 230.5 | 4.6 | 225.9 | 0.122 | 0.016 | 3345 | 442 | 333.2 | 206.4 | 20.6 | 185.8 | 0.057 | 0.013 | 6001 | 1401 |
| 313.2 | 256.5 | 7.8 | 248.6 | 0.108 | 0.016 | 4196 | 637 | 353.1 | 256.4 | 47.8 | 208.6 | 0.050 | 0.013 | 7802 | 2129 |
| 323.2 | 281.6 | 12.8 | 268.8 | 0.097 | 0.016 | 5074 | 866 | 373.1 | 330.3 | 101.7 | 228.5 | 0.046 | 0.014 | 9359 | 2860 |
| 333.2 | 307.9 | 20.4 | 287.5 | 0.088 | 0.016 | 5988 | 1135 | 393.2 | 445.7 | 199.7 | 246.0 | 0.045 | 0.015 | 10481 | 3496 |
| 343.2 | 336.2 | 31.4 | 304.8 | 0.081 | 0.017 | 6904 | 1432 | 303.2 | 143.9 | 5.3 | 138.6 | 0.075 | 0.014 | 3362 | 640 |
| 353.2 | 369.4 | 46.9 | 322.5 | 0.075 | 0.017 | 7956 | 1813 | 313.1 | 160.6 | 8.6 | 152.0 | 0.066 | 0.014 | 4183 | 905 |
| 364.7 | 414.1 | 69.4 | 344.7 | 0.067 | 0.016 | 9618 | 2514 | 333.2 | 196.8 | 21.3 | 175.5 | 0.054 | 0.014 | 5935 | 1584 |
| 303.2 | 138.9 | 4.3 | 134.6 | 0.073 | 0.016 | 3325 | 722 | 353.1 | 244.1 | 48.5 | 195.6 | 0.047 | 0.015 | 7656 | 2383 |
| 313.2 | 155.2 | 7.5 | 147.7 | 0.065 | 0.016 | 4153 | 1027 | 373.1 | 315.5 | 102.9 | 212.6 | 0.044 | 0.015 | 9011 | 3099 |
| 333.2 | 190.2 | 20.2 | 170.0 | 0.053 | 0.016 | 5868 | 1784 | 393.1 | 429.8 | 201.1 | 228.7 | 0.043 | 0.016 | 10154 | 3829 |
| 353.3 | 235.8 | 47.6 | 188.2 | 0.047 | 0.016 | 7374 | 2554 | – | | | – | – | – | – | – |
| 373.2 | 308.9 | 100.1 | 208.8 | 0.041 | 0.017 | 9689 | 4035 | – | | | – | – | – | – | – |
| 392.5 | 411.6 | 188.1 | 223.5 | 0.040 | 0.018 | 10783 | 4814 | – | | | – | – | – | – | – |

[a] Standard uncertainties are reported (level of confidence 0.68). Standard uncertainty for temperature is $u(T)$ = 0.1 K, for total and residual pressure is $u(P_{tot})$ = $u(P_{res})$ = 0.9 kPa and for $CO_2$ pressure is $u(P_{CO2})$ = 1.3 kPa.

**Table A.2**
Measured mole fraction solubility $x_{CO2}$, loading $\alpha$ and Henry's constant $H$ for $CO_2$ in MDEA (1) – MEG (2) blends as a function of weight fraction $w$ of unloaded solvent, temperature $T$ and pressure (total pressure $P_{tot}$, residual pressure $P_{res}$ and their difference, $CO_2$ partial pressure $P_{CO2}$).[a]

| $w_1$ | $u(w_1)$ | $T$ | $P_{tot}$ | $P_{res}$ | $P_{CO2}$ | $x_{CO2}$ | $u(x_{CO2})$ | $\alpha$ | $u(\alpha)$ | $H$ | $u(H)$ |
|---|---|---|---|---|---|---|---|---|---|---|---|
| | | K | kPa | kPa | kPa | | | $mol_{CO2}$ $mol^{-1}_{MDEA}$ | | kPa $m^3$ $kmol^{-1}$ | |
| 0.000 | 0.000 | 303.2 | 200.5 | 2.3 | 198.2 | 0.0039 | 0.0004 | – | – | 2835 | 284 |
| | | 313.7 | 223.8 | 2.5 | 221.3 | 0.0036 | 0.0004 | – | – | 3498 | 389 |
| | | 323.2 | 236.8 | 2.8 | 234.0 | 0.0035 | 0.0004 | – | – | 3833 | 440 |
| | | 333.2 | 253.9 | 3.1 | 250.8 | 0.0033 | 0.0004 | – | – | 4355 | 530 |
| | | 343.2 | 270.4 | 3.5 | 266.9 | 0.0031 | 0.0004 | – | – | 4875 | 624 |
| | | 353.2 | 286.3 | 3.9 | 282.4 | 0.0030 | 0.0004 | – | – | 5393 | 720 |
| | | 363.2 | 301.7 | 4.5 | 297.2 | 0.0029 | 0.0004 | – | – | 5907 | 820 |
| | | 373.1 | 317.2 | 5.5 | 311.7 | 0.0028 | 0.0004 | – | – | 6406 | 918 |
| | | 383.2 | 332.8 | 7.1 | 325.7 | 0.0028 | 0.0004 | – | – | 6886 | 1013 |
| | | 393.2 | 348.7 | 9.6 | 339.1 | 0.0027 | 0.0004 | – | – | 7333 | 1100 |
| 0.050 | 0.001 | 303.2 | 42.9 | 1.8 | 41.1 | 0.0141 | 0.0005 | 0.535 | 0.024 | 166 | 8 |
| | | 313.1 | 66.2 | 1.9 | 64.3 | 0.0132 | 0.0005 | 0.501 | 0.024 | 279 | 13 |
| | | 323.2 | 97.6 | 2.0 | 95.6 | 0.0121 | 0.0005 | 0.458 | 0.024 | 457 | 22 |
| | | 333.1 | 134.0 | 2.2 | 131.8 | 0.0108 | 0.0005 | 0.411 | 0.023 | 709 | 38 |
| | | 343.2 | 173.2 | 2.4 | 170.8 | 0.0096 | 0.0005 | 0.363 | 0.023 | 1048 | 63 |
| | | 353.2 | 212.5 | 2.8 | 209.7 | 0.0084 | 0.0006 | 0.318 | 0.023 | 1479 | 103 |
| | | 363.2 | 250.1 | 3.4 | 246.7 | 0.0074 | 0.0006 | 0.279 | 0.023 | 2001 | 161 |
| | | 373.1 | 285.4 | 4.4 | 281.0 | 0.0065 | 0.0006 | 0.246 | 0.023 | 2610 | 241 |
| | | 383.1 | 319.2 | 5.8 | 313.4 | 0.0058 | 0.0006 | 0.217 | 0.023 | 3321 | 352 |
| | | 393.2 | 354.4 | 8.1 | 346.4 | 0.0050 | 0.0006 | 0.190 | 0.024 | 4239 | 521 |
| 0.100 | 0.001 | 303.2 | 10.7 | 1.9 | 8.8 | 0.0096 | 0.0004 | 0.178 | 0.008 | 53 | 6 |
| | | 313.2 | 18.8 | 2.2 | 16.5 | 0.0094 | 0.0004 | 0.174 | 0.008 | 103 | 7 |
| | | 323.2 | 32.1 | 2.5 | 29.7 | 0.0091 | 0.0004 | 0.168 | 0.008 | 193 | 11 |
| | | 333.1 | 52.3 | 2.8 | 49.5 | 0.0086 | 0.0004 | 0.159 | 0.008 | 342 | 19 |
| | | 343.2 | 79.9 | 3.5 | 76.4 | 0.0080 | 0.0004 | 0.147 | 0.008 | 575 | 33 |
| | | 353.1 | 113.6 | 4.6 | 109.0 | 0.0073 | 0.0004 | 0.134 | 0.009 | 909 | 58 |
| | | 363.1 | 151.3 | 5.9 | 145.4 | 0.0065 | 0.0004 | 0.120 | 0.009 | 1365 | 97 |
| | | 373.1 | 190.6 | 8.0 | 182.6 | 0.0058 | 0.0004 | 0.106 | 0.009 | 1948 | 158 |
| | | 383.3 | 230.1 | 10.8 | 219.3 | 0.0051 | 0.0005 | 0.094 | 0.009 | 2667 | 248 |
| | | 393.2 | 266.9 | 15.2 | 251.7 | 0.0044 | 0.0005 | 0.081 | 0.009 | 3557 | 386 |
| 0.300 | 0.001 | 303.5 | 7.8 | 2.3 | 5.5 | 0.0114 | 0.0004 | 0.063 | 0.003 | 32 | 5 |
| | | 313.1 | 12.6 | 2.5 | 10.1 | 0.0112 | 0.0004 | 0.062 | 0.003 | 60 | 6 |
| | | 323.1 | 21.7 | 2.7 | 19.0 | 0.0110 | 0.0005 | 0.061 | 0.003 | 115 | 7 |
| | | 333.2 | 36.8 | 2.9 | 33.9 | 0.0106 | 0.0005 | 0.059 | 0.003 | 214 | 11 |
| | | 343.1 | 59.3 | 3.2 | 56.1 | 0.0101 | 0.0005 | 0.056 | 0.003 | 376 | 19 |
| | | 353.1 | 90.0 | 3.7 | 86.4 | 0.0094 | 0.0005 | 0.052 | 0.003 | 627 | 33 |
| | | 373.2 | 169.2 | 6.0 | 163.3 | 0.0078 | 0.0005 | 0.043 | 0.003 | 1454 | 92 |

(*continued on next page*)

**Table A.2** (*continued*)

| $w_1$ | $u(w_1)$ | $T$ | $P_{tot}$ | $P_{res}$ | $P_{CO2}$ | $x_{CO2}$ | $u(x_{CO2})$ | $\alpha$ | $u(\alpha)$ | $H$ | $u(H)$ |
|---|---|---|---|---|---|---|---|---|---|---|---|
| | | K | kPa | kPa | kPa | | | $mol_{CO2}\ mol^{-1}_{MDEA}$ | | kPa $m^3$ $kmol^{-1}$ | |
| | | 393.2 | 257.4 | 11.1 | 246.3 | 0.0063 | 0.0005 | 0.035 | 0.003 | 2780 | 226 |
| 0.500 | 0.002 | 303.1 | 13.0 | 2.1 | 11.0 | 0.0200 | 0.0006 | 0.060 | 0.002 | 41 | 4 |
| | | 323.2 | 39.9 | 2.3 | 37.5 | 0.0188 | 0.0007 | 0.056 | 0.002 | 151 | 6 |
| | | 333.2 | 65.9 | 2.5 | 63.4 | 0.0177 | 0.0006 | 0.053 | 0.002 | 274 | 11 |
| | | 343.2 | 101.5 | 2.7 | 98.9 | 0.0162 | 0.0006 | 0.048 | 0.002 | 471 | 20 |
| | | 353.3 | 145.0 | 2.9 | 142.1 | 0.0144 | 0.0006 | 0.043 | 0.002 | 767 | 36 |
| | | 363.1 | 192.3 | 3.3 | 189.0 | 0.0126 | 0.0006 | 0.037 | 0.002 | 1178 | 64 |
| | | 373.2 | 239.7 | 4.0 | 235.7 | 0.0109 | 0.0006 | 0.032 | 0.002 | 1713 | 109 |
| | | 383.2 | 283.9 | 5.3 | 278.6 | 0.0095 | 0.0007 | 0.028 | 0.002 | 2353 | 176 |
| | | 393.1 | 324.3 | 7.3 | 317.0 | 0.0083 | 0.0007 | 0.024 | 0.002 | 3084 | 268 |
| 0.700 | 0.003 | 303.2 | 10.9 | 2.4 | 8.6 | 0.0132 | 0.0006 | 0.024 | 0.001 | 56 | 6 |
| | | 313.6 | 21.1 | 2.6 | 18.5 | 0.0129 | 0.0006 | 0.024 | 0.001 | 126 | 9 |
| | | 323.2 | 30.9 | 3.0 | 28.0 | 0.0125 | 0.0006 | 0.023 | 0.001 | 198 | 11 |
| | | 333.2 | 50.4 | 3.2 | 47.2 | 0.0119 | 0.0006 | 0.022 | 0.001 | 355 | 19 |
| | | 343.2 | 77.4 | 3.6 | 73.8 | 0.0110 | 0.0006 | 0.020 | 0.001 | 605 | 34 |
| | | 353.2 | 110.7 | 4.0 | 106.8 | 0.0099 | 0.0006 | 0.018 | 0.001 | 975 | 61 |
| | | 363.2 | 147.2 | 4.6 | 142.5 | 0.0089 | 0.0006 | 0.016 | 0.001 | 1472 | 103 |
| | | 373.1 | 183.8 | 5.6 | 178.2 | 0.0079 | 0.0006 | 0.014 | 0.001 | 2090 | 166 |
| | | 383.2 | 218.2 | 7.2 | 211.0 | 0.0070 | 0.0006 | 0.013 | 0.001 | 2796 | 252 |
| | | 393.1 | 249.8 | 9.6 | 240.2 | 0.0063 | 0.0006 | 0.012 | 0.001 | 3549 | 358 |
| 0.900 | 0.005 | 303.1 | 18.5 | 1.6 | 16.8 | 0.0162 | 0.0006 | 0.0200 | 0.001 | 107 | 7 |
| | | 323.2 | 53.9 | 2.0 | 51.9 | 0.0147 | 0.0007 | 0.0181 | 0.001 | 370 | 19 |
| | | 333.2 | 83.4 | 2.1 | 81.2 | 0.0135 | 0.0007 | 0.0166 | 0.001 | 635 | 35 |
| | | 343.2 | 119.0 | 2.3 | 116.7 | 0.0122 | 0.0007 | 0.0149 | 0.001 | 1024 | 62 |
| | | 353.2 | 156.7 | 2.6 | 154.1 | 0.0108 | 0.0007 | 0.0132 | 0.001 | 1535 | 105 |
| | | 363.2 | 192.5 | 3.1 | 189.5 | 0.0096 | 0.0007 | 0.0118 | 0.001 | 2139 | 166 |
| | | 373.2 | 224.9 | 3.7 | 221.1 | 0.0085 | 0.0007 | 0.0104 | 0.001 | 2840 | 251 |
| | | 383.2 | 253.3 | 4.8 | 248.5 | 0.0079 | 0.0007 | 0.0097 | 0.001 | 3465 | 333 |
| | | 393.1 | 278.1 | 6.4 | 271.7 | 0.0071 | 0.0007 | 0.0087 | 0.001 | 4260 | 460 |
| 1.000 | 0.006 | 303.1 | 25.0 | 2.6 | 22.4 | 0.0160 | 0.0007 | 0.016 | 0.001 | 159 | 10 |
| | | 313.3 | 42.9 | 2.8 | 40.1 | 0.0152 | 0.0007 | 0.015 | 0.001 | 302 | 17 |
| | | 323.2 | 67.2 | 3.0 | 64.2 | 0.0141 | 0.0007 | 0.014 | 0.001 | 525 | 30 |
| | | 333.2 | 98.4 | 3.2 | 95.2 | 0.0128 | 0.0007 | 0.013 | 0.001 | 868 | 54 |
| | | 343.2 | 132.5 | 3.4 | 129.2 | 0.0114 | 0.0007 | 0.012 | 0.001 | 1331 | 93 |
| | | 353.2 | 165.6 | 3.5 | 162.1 | 0.0102 | 0.0008 | 0.010 | 0.001 | 1888 | 149 |
| | | 363.2 | 195.2 | 3.8 | 191.4 | 0.0092 | 0.0008 | 0.009 | 0.001 | 2494 | 219 |
| | | 373.2 | 221.0 | 4.3 | 216.7 | 0.0085 | 0.0008 | 0.009 | 0.001 | 3103 | 300 |
| | | 383.2 | 243.3 | 5.0 | 238.3 | 0.0079 | 0.0008 | 0.008 | 0.001 | 3681 | 383 |
| | | 393.1 | 263.2 | 6.1 | 257.2 | 0.0075 | 0.0007 | 0.008 | 0.001 | 4224 | 466 |

[a] Standard uncertainties are reported (level of confidence 0.68). Standard uncertainty for temperature is $u(T)$ = 0.1 K, for total and residual pressure is $u(P_{tot})$ = $u(P_{res})$ = 0.9 kPa and for $CO_2$ pressure is $u(P_{CO2})$ = 1.3 kPa.

**Table A.3**
Measured mole fraction solubility $x_{CO2}$, loading $\alpha$ and Henry's constant $H$ for $CO_2$ in MDEA (1) – MEG (2) blends as a function of weight fraction $w$ of unloaded solvent and pressure (total pressure $P_{tot}$, residual pressure $P_{res}$ and their difference, $CO_2$ partial pressure $P_{CO2}$) at temperatures of 313 K and 343 K.[a]

| $w_1$ | $u(w_1)$ | $T$ | $P_{tot}$ | $P_{res}$ | $P_{CO2}$ | $x_{CO2}$ | $u(x_{CO2})$ | $\alpha$ | $u(\alpha)$ | $H$ | $u(H)$ |
|---|---|---|---|---|---|---|---|---|---|---|---|
| | | K | kPa | kPa | kPa | | | $mol_{CO2}\ mol^{-1}_{MDEA}$ | | kPa $m^3$ $kmol^{-1}$ | |
| 0.000 | 0.000 | 313.1 | 66.0 | 2.2 | 63.8 | 0.0011 | 0.0005 | – | – | 3188 | 1560 |
| | | 313.2 | 133.9 | 2.2 | 131.7 | 0.0023 | 0.0008 | – | – | 3187 | 1074 |
| | | 313.1 | 194.3 | 2.2 | 192.1 | 0.0034 | 0.0008 | – | – | 3158 | 737 |
| | | 313.2 | 254.4 | 2.2 | 252.1 | 0.0045 | 0.0008 | – | – | 3145 | 572 |
| | | 313.2 | 315.8 | 2.2 | 313.5 | 0.0056 | 0.0008 | – | – | 3157 | 480 |
| | | 313.2 | 367.8 | 2.2 | 365.6 | 0.0065 | 0.0009 | – | – | 3173 | 436 |
| | | 313.1 | 413.6 | 2.2 | 411.4 | 0.0072 | 0.0009 | – | – | 3186 | 407 |
| | | 313.1 | 456.6 | 2.2 | 454.4 | 0.0079 | 0.0009 | – | – | 3209 | 387 |
| | | 313.1 | 503.9 | 2.2 | 501.7 | 0.0087 | 0.0009 | – | – | 3219 | 366 |
| | | 343.2 | 61.9 | 2.9 | 59.1 | 0.0007 | 0.0005 | – | – | 4663 | 3299 |
| | | 343.1 | 113.3 | 2.9 | 110.4 | 0.0014 | 0.0007 | – | – | 4663 | 2502 |
| | | 343.2 | 152.4 | 2.9 | 149.5 | 0.0018 | 0.0007 | – | – | 4667 | 1865 |
| | | 343.2 | 200.0 | 2.9 | 197.1 | 0.0024 | 0.0007 | – | – | 4676 | 1437 |
| | | 343.2 | 251.5 | 2.9 | 248.7 | 0.0030 | 0.0007 | – | – | 4691 | 1169 |
| | | 343.2 | 305.1 | 2.9 | 302.3 | 0.0037 | 0.0008 | – | – | 4721 | 999 |
| | | 343.2 | 348.7 | 2.9 | 345.9 | 0.0042 | 0.0008 | – | – | 4704 | 897 |
| | | 343.1 | 400.2 | 2.9 | 397.4 | 0.0048 | 0.0008 | – | – | 4701 | 809 |
| | | 343.1 | 455.3 | 2.9 | 452.5 | 0.0055 | 0.0008 | – | – | 4739 | 750 |
| | | 343.2 | 505.3 | 2.9 | 502.4 | 0.0061 | 0.0009 | – | – | 4742 | 703 |
| | | 343.1 | 548.2 | 2.9 | 545.4 | 0.0066 | 0.0009 | – | – | 4738 | 669 |

**Table A.3** (*continued*)

| $w_1$ | $u(w_1)$ | $T$ | $P_{tot}$ | $P_{res}$ | $P_{CO2}$ | $x_{CO2}$ | $u(x_{CO2})$ | $\alpha$ | $u(\alpha)$ | $H$ | $u(H)$ |
|---|---|---|---|---|---|---|---|---|---|---|---|
| | | K | kPa | kPa | kPa | | | $mol_{CO2}\ mol^{-1}_{MDEA}$ | | kPa $m^3$ $kmol^{-1}$ | |
| 0.500 | 0.002 | 313.1 | 14.1 | 2.1 | 11.9 | 0.0129 | 0.0006 | 0.038 | 0.002 | 70 | 6 |
| | | 313.1 | 29.4 | 2.1 | 27.2 | 0.0238 | 0.0008 | 0.071 | 0.003 | 86 | 4 |
| | | 313.1 | 53.4 | 2.1 | 51.2 | 0.0380 | 0.0009 | 0.115 | 0.003 | 99 | 4 |
| | | 313.1 | 78.7 | 2.1 | 76.5 | 0.0505 | 0.0009 | 0.155 | 0.004 | 110 | 3 |
| | | 313.2 | 108.2 | 2.1 | 106.0 | 0.0631 | 0.0010 | 0.197 | 0.005 | 121 | 3 |
| | | 313.2 | 137.8 | 2.1 | 135.6 | 0.0739 | 0.0010 | 0.233 | 0.005 | 130 | 3 |
| | | 313.2 | 167.1 | 2.1 | 164.9 | 0.0833 | 0.0010 | 0.265 | 0.006 | 139 | 3 |
| | | 313.2 | 196.0 | 2.1 | 193.9 | 0.0916 | 0.0011 | 0.294 | 0.006 | 147 | 3 |
| | | 313.2 | 226.6 | 2.1 | 224.5 | 0.0994 | 0.0011 | 0.322 | 0.007 | 156 | 4 |
| | | 313.2 | 258.6 | 2.1 | 256.4 | 0.1066 | 0.0012 | 0.349 | 0.007 | 164 | 4 |
| | | 313.1 | 286.7 | 2.1 | 284.6 | 0.1126 | 0.0012 | 0.371 | 0.007 | 172 | 4 |
| | | 313.2 | 314.8 | 2.1 | 312.6 | 0.1182 | 0.0013 | 0.391 | 0.008 | 179 | 4 |
| | | 313.2 | 342.3 | 2.1 | 340.2 | 0.1231 | 0.0014 | 0.410 | 0.008 | 186 | 4 |
| | | 313.2 | 370.0 | 2.1 | 367.9 | 0.1276 | 0.0014 | 0.427 | 0.008 | 193 | 4 |
| | | 313.2 | 395.0 | 2.1 | 392.8 | 0.1315 | 0.0015 | 0.442 | 0.009 | 199 | 4 |
| | | 313.2 | 417.4 | 2.1 | 415.2 | 0.1348 | 0.0015 | 0.455 | 0.009 | 204 | 5 |
| 1.000 | 0.006 | 313.1 | 27.9 | 2.3 | 25.6 | 0.0099 | 0.0010 | 0.010 | 0.001 | 296 | 34 |
| | | 313.1 | 45.8 | 2.3 | 43.6 | 0.0161 | 0.0014 | 0.016 | 0.002 | 309 | 30 |
| | | 313.1 | 75.1 | 2.3 | 72.8 | 0.0259 | 0.0017 | 0.027 | 0.002 | 318 | 23 |
| | | 313.1 | 98.3 | 2.3 | 96.0 | 0.0337 | 0.0019 | 0.035 | 0.002 | 320 | 20 |
| | | 313.2 | 139.8 | 2.3 | 137.5 | 0.0472 | 0.0020 | 0.050 | 0.002 | 323 | 16 |
| | | 313.2 | 169.4 | 2.3 | 167.1 | 0.0565 | 0.0021 | 0.060 | 0.003 | 324 | 15 |
| | | 313.1 | 211.6 | 2.3 | 209.3 | 0.0689 | 0.0021 | 0.074 | 0.003 | 329 | 13 |
| | | 313.1 | 250.4 | 2.3 | 248.2 | 0.0796 | 0.0021 | 0.086 | 0.003 | 334 | 13 |
| | | 313.2 | 284.1 | 2.3 | 281.8 | 0.0881 | 0.0022 | 0.097 | 0.003 | 339 | 12 |
| | | 313.2 | 315.3 | 2.3 | 313.0 | 0.0956 | 0.0022 | 0.106 | 0.004 | 344 | 12 |
| | | 313.1 | 349.2 | 2.3 | 346.9 | 0.1031 | 0.0023 | 0.115 | 0.004 | 351 | 12 |
| | | 343.1 | 58.2 | 4.3 | 54.0 | 0.0059 | 0.0011 | 0.006 | 0.001 | 1078 | 198 |
| | | 343.2 | 101.7 | 4.3 | 97.4 | 0.0103 | 0.0015 | 0.010 | 0.002 | 1110 | 164 |
| | | 343.1 | 130.2 | 4.3 | 125.9 | 0.0132 | 0.0018 | 0.013 | 0.002 | 1120 | 159 |
| | | 343.2 | 173.2 | 4.3 | 169.0 | 0.0174 | 0.0020 | 0.018 | 0.002 | 1132 | 140 |
| | | 343.2 | 222.9 | 4.3 | 218.6 | 0.0222 | 0.0022 | 0.023 | 0.002 | 1144 | 124 |
| | | 343.1 | 247.8 | 4.3 | 243.6 | 0.0248 | 0.0024 | 0.025 | 0.003 | 1138 | 122 |
| | | 343.2 | 301.9 | 4.3 | 297.6 | 0.0298 | 0.0026 | 0.031 | 0.003 | 1150 | 111 |
| | | 343.2 | 351.0 | 4.3 | 346.8 | 0.0344 | 0.0027 | 0.036 | 0.003 | 1159 | 105 |
| | | 343.2 | 372.5 | 4.3 | 368.3 | 0.0364 | 0.0029 | 0.038 | 0.003 | 1160 | 106 |

[a] Standard uncertainties are reported (level of confidence 0.68). Standard uncertainty for temperature is $u(T)$ = 0.1 K, for total and residual pressure is $u(P_{tot})$ = $u(P_{res})$ = 0.9 kPa and for $CO_2$ pressure is $u(P_{CO2})$ = 1.3 kPa.

**Table A.4**
Measured mole fraction solubility $x_{CO2}$, loading $\alpha$ and Henry's constant $H$ for $CO_2$ in MDEA (1) – MEG (2) – $H_2O$ (3) blends in two repeated experiments as a function of weight fraction $w$ of unloaded solvent, temperature $T$ and pressure (total pressure $P_{tot}$, residual pressure $P_{res}$ and their difference, $CO_2$ partial pressure $P_{CO2}$).[a] Experiment A denotes the first experiment, also tabulated in Table A.2 for MDEA-MEG systems and in Table A.5 for MDEA-MEG-$H_2O$ system. Experiment B is the repeated experiment.

| $w_1$ | $u(w_1)$ | $w_2$ | $u(w_2)$ | $T$ | $P_{tot}$ | $P_{res}$ | $P_{CO2}$ | $x_{CO2}$ | $u(x_{CO2})$ | $\alpha$ | $u(\alpha)$ | $H$ | $u(H)$ |
|---|---|---|---|---|---|---|---|---|---|---|---|---|---|
| | | | | K | kPa | kPa | kPa | | | $mol_{CO2}{\cdot}mol^{-1}_{MDEA}$ | | kPa $m^3$ $kmol^{-1}$ | |
| 0.000 | 0.000 | 1.000 | 0.006 | | | | | Experiment A | | | | | |
| | | | | 303.2 | 200.5 | 2.3 | 198.2 | 0.0039 | 0.0004 | – | – | 2835 | 284 |
| | | | | 313.7 | 223.8 | 2.5 | 221.3 | 0.0036 | 0.0004 | – | – | 3498 | 389 |
| | | | | 323.2 | 236.8 | 2.8 | 234.0 | 0.0035 | 0.0004 | – | – | 3833 | 440 |
| | | | | 333.2 | 253.9 | 3.1 | 250.8 | 0.0033 | 0.0004 | – | – | 4355 | 530 |
| | | | | 343.2 | 270.4 | 3.5 | 266.9 | 0.0031 | 0.0004 | – | – | 4875 | 624 |
| | | | | 353.2 | 286.3 | 3.9 | 282.4 | 0.0030 | 0.0004 | – | – | 5393 | 720 |
| | | | | 363.2 | 301.7 | 4.5 | 297.2 | 0.0029 | 0.0004 | – | – | 5907 | 820 |
| | | | | 373.1 | 317.2 | 5.5 | 311.7 | 0.0028 | 0.0004 | – | – | 6406 | 918 |
| | | | | 383.2 | 332.8 | 7.1 | 325.7 | 0.0028 | 0.0004 | – | – | 6886 | 1013 |
| | | | | 393.2 | 348.7 | 9.6 | 339.1 | 0.0027 | 0.0004 | – | – | 7333 | 1100 |
| | | | | | | | | Experiment B | | | | | |
| | | | | 303.2 | 207.2 | 2.0 | 205.2 | 0.0042 | 0.0006 | – | – | 2749 | 376 |
| | | | | 313.2 | 223.1 | 2.2 | 220.9 | 0.0039 | 0.0006 | – | – | 3222 | 478 |
| | | | | 333.2 | 252.7 | 2.6 | 250.1 | 0.0034 | 0.0006 | – | – | 4217 | 720 |
| | | | | 353.2 | 280.0 | 3.7 | 276.3 | 0.0031 | 0.0006 | – | – | 5183 | 977 |
| | | | | 373.2 | 306.7 | 5.7 | 300.9 | 0.0029 | 0.0006 | – | – | 6139 | 1251 |
| | | | | 393.2 | 334.8 | 10.9 | 323.9 | 0.0027 | 0.0006 | – | – | 6991 | 1495 |
| 0.050 | 0.001 | 0.950 | 0.001 | | | | | Experiment A | | | | | |
| | | | | 303.2 | 42.9 | 1.8 | 41.1 | 0.0141 | 0.0005 | 0.535 | 0.024 | 166 | 8 |
| | | | | 313.1 | 66.2 | 1.9 | 64.3 | 0.0132 | 0.0005 | 0.501 | 0.024 | 279 | 13 |

(*continued on next page*)

**Table A.4** (*continued*)

| $w_1$ | $u(w_1)$ | $w_2$ | $u(w_2)$ | $T$ | $P_{tot}$ | $P_{res}$ | $P_{CO2}$ | $x_{CO2}$ | $u(x_{CO2})$ | α | $u(\alpha)$ | $H$ | $u(H)$ |
|---|---|---|---|---|---|---|---|---|---|---|---|---|---|
| | | | | K | kPa | kPa | kPa | | | $mol_{CO2} \cdot mol_{MDEA}^{-1}$ | | kPa $m^3$ $kmol^{-1}$ | |
| | | | | 323.2 | 97.6 | 2.0 | 95.6 | 0.0121 | 0.0005 | 0.458 | 0.024 | 457 | 22 |
| | | | | 333.1 | 134.0 | 2.2 | 131.8 | 0.0108 | 0.0005 | 0.411 | 0.023 | 709 | 38 |
| | | | | 343.2 | 173.2 | 2.4 | 170.8 | 0.0096 | 0.0005 | 0.363 | 0.023 | 1048 | 63 |
| | | | | 353.2 | 212.5 | 2.8 | 209.7 | 0.0084 | 0.0006 | 0.318 | 0.023 | 1479 | 103 |
| | | | | 363.2 | 250.1 | 3.4 | 246.7 | 0.0074 | 0.0006 | 0.279 | 0.023 | 2001 | 161 |
| | | | | 373.1 | 285.4 | 4.4 | 281.0 | 0.0065 | 0.0006 | 0.246 | 0.023 | 2610 | 241 |
| | | | | 383.1 | 319.2 | 5.8 | 313.4 | 0.0058 | 0.0006 | 0.217 | 0.023 | 3321 | 352 |
| | | | | 393.2 | 354.4 | 8.1 | 346.4 | 0.0050 | 0.0006 | 0.190 | 0.024 | 4239 | 521 |
| | | | | | | | | Experiment B | | | | | |
| | | | | 313.2 | 64.5 | 16.7 | 62.8 | 0.0128 | 0.0005 | 0.487 | 0.023 | 281 | 13 |
| | | | | 323.2 | 96.5 | 17.6 | 94.8 | 0.0117 | 0.0005 | 0.445 | 0.023 | 467 | 22 |
| | | | | 333.2 | 133.8 | 19.8 | 131.8 | 0.0105 | 0.0005 | 0.398 | 0.023 | 732 | 39 |
| | | | | 343.2 | 173.6 | 22.5 | 171.4 | 0.0093 | 0.0005 | 0.351 | 0.023 | 1088 | 66 |
| | | | | 353.2 | 214.0 | 27.6 | 211.2 | 0.0081 | 0.0005 | 0.307 | 0.023 | 1546 | 109 |
| | | | | 363.2 | 252.6 | 35.1 | 249.1 | 0.0071 | 0.0006 | 0.268 | 0.023 | 2104 | 172 |
| | | | | 373.2 | 288.4 | 45.3 | 283.9 | 0.0062 | 0.0006 | 0.236 | 0.023 | 2750 | 259 |
| | | | | 383.1 | 321.3 | 61.6 | 315.1 | 0.0056 | 0.0006 | 0.209 | 0.023 | 3463 | 371 |
| | | | | 393.1 | 352.4 | 84.9 | 343.9 | 0.0050 | 0.0006 | 0.188 | 0.023 | 4248 | 513 |
| 0.100 | 0.001 | 0.900 | 0.001 | | | | | Experiment A | | | | | |
| | | | | 303.2 | 10.7 | 1.9 | 8.8 | 0.0096 | 0.0004 | 0.178 | 0.008 | 53 | 6 |
| | | | | 313.2 | 18.8 | 2.2 | 16.5 | 0.0094 | 0.0004 | 0.174 | 0.008 | 103 | 7 |
| | | | | 323.2 | 32.1 | 2.5 | 29.7 | 0.0091 | 0.0004 | 0.168 | 0.008 | 193 | 11 |
| | | | | 333.1 | 52.3 | 2.8 | 49.5 | 0.0086 | 0.0004 | 0.159 | 0.008 | 342 | 19 |
| | | | | 343.2 | 79.9 | 3.5 | 76.4 | 0.0080 | 0.0004 | 0.147 | 0.008 | 575 | 33 |
| | | | | 353.1 | 113.6 | 4.6 | 109.0 | 0.0073 | 0.0004 | 0.134 | 0.009 | 909 | 58 |
| | | | | 363.1 | 151.3 | 5.9 | 145.4 | 0.0065 | 0.0004 | 0.120 | 0.009 | 1365 | 97 |
| | | | | 373.1 | 190.6 | 8.0 | 182.6 | 0.0058 | 0.0004 | 0.106 | 0.009 | 1948 | 158 |
| | | | | 383.3 | 230.1 | 10.8 | 219.3 | 0.0051 | 0.0005 | 0.094 | 0.009 | 2667 | 248 |
| | | | | 393.2 | 266.9 | 15.2 | 251.7 | 0.0044 | 0.0005 | 0.081 | 0.009 | 3557 | 386 |
| | | | | | | | | Experiment B | | | | | |
| | | | | 303.2 | 13.0 | 2.2 | 10.8 | 0.0108 | 0.0004 | 0.200 | 0.009 | 58 | 5 |
| | | | | 323.2 | 40.1 | 2.6 | 37.4 | 0.0102 | 0.0004 | 0.188 | 0.008 | 218 | 11 |
| | | | | 343.2 | 97.4 | 3.2 | 94.2 | 0.0088 | 0.0004 | 0.163 | 0.008 | 639 | 33 |
| | | | | 353.2 | 135.8 | 3.6 | 132.1 | 0.0080 | 0.0004 | 0.148 | 0.008 | 996 | 56 |
| 0.300 | 0.001 | 0.700 | 0.001 | | | | | Experiment A | | | | | |
| | | | | 303.5 | 7.8 | 2.3 | 5.5 | 0.0114 | 0.0004 | 0.063 | 0.003 | 32 | 5 |
| | | | | 313.1 | 12.6 | 2.5 | 10.1 | 0.0112 | 0.0004 | 0.062 | 0.003 | 60 | 6 |
| | | | | 323.1 | 21.7 | 2.7 | 19.0 | 0.0110 | 0.0005 | 0.061 | 0.003 | 115 | 7 |
| | | | | 333.2 | 36.8 | 2.9 | 33.9 | 0.0106 | 0.0005 | 0.059 | 0.003 | 214 | 11 |
| | | | | 343.1 | 59.3 | 3.2 | 56.1 | 0.0101 | 0.0005 | 0.056 | 0.003 | 376 | 19 |
| | | | | 353.1 | 90.0 | 3.7 | 86.4 | 0.0094 | 0.0005 | 0.052 | 0.003 | 627 | 33 |
| | | | | 373.2 | 169.2 | 6.0 | 163.3 | 0.0078 | 0.0005 | 0.043 | 0.003 | 1454 | 92 |
| | | | | 393.2 | 257.4 | 11.1 | 246.3 | 0.0063 | 0.0005 | 0.035 | 0.003 | 2780 | 226 |
| | | | | | | | | Experiment B | | | | | |
| | | | | 303.2 | 7.5 | 2.4 | 5.1 | 0.0120 | 0.0005 | 0.067 | 0.003 | 28 | 5 |
| | | | | 323.2 | 22.7 | 3.0 | 19.7 | 0.0116 | 0.0005 | 0.064 | 0.003 | 113 | 7 |
| | | | | 343.2 | 62.5 | 3.9 | 58.7 | 0.0106 | 0.0005 | 0.059 | 0.003 | 376 | 19 |
| | | | | 353.1 | 94.8 | 4.7 | 90.1 | 0.0098 | 0.0005 | 0.054 | 0.003 | 628 | 33 |
| 0.500 | 0.002 | 0.500 | 0.002 | | | | | Experiment A | | | | | |
| | | | | 303.1 | 13.0 | 2.1 | 11.0 | 0.0200 | 0.0006 | 0.060 | 0.002 | 41 | 4 |
| | | | | 323.2 | 39.87 | 2.3 | 37.5 | 0.0188 | 0.0007 | 0.056 | 0.002 | 151 | 6 |
| | | | | 333.2 | 65.9 | 2.5 | 63.4 | 0.0177 | 0.0006 | 0.053 | 0.002 | 274 | 11 |
| | | | | 343.2 | 101.5 | 2.7 | 98.9 | 0.0162 | 0.0006 | 0.048 | 0.002 | 471 | 20 |
| | | | | 353.3 | 145.0 | 2.9 | 142.1 | 0.0144 | 0.0006 | 0.043 | 0.002 | 767 | 36 |
| | | | | 363.1 | 192.3 | 3.3 | 189.0 | 0.0126 | 0.0006 | 0.037 | 0.002 | 1178 | 64 |
| | | | | 373.2 | 239.7 | 4.0 | 235.7 | 0.0109 | 0.0006 | 0.032 | 0.002 | 1713 | 109 |
| | | | | 383.2 | 283.9 | 5.3 | 278.6 | 0.0095 | 0.0007 | 0.028 | 0.002 | 2353 | 176 |
| | | | | 393.1 | 324.3 | 7.3 | 317.0 | 0.0083 | 0.0007 | 0.024 | 0.002 | 3084 | 268 |
| | | | | | | | | Experiment B | | | | | |
| | | | | 303.1 | 12.5 | 2.1 | 10.4 | 0.0197 | 0.0006 | 0.059 | 0.002 | 39 | 4 |
| | | | | 313.1 | 22.3 | 2.2 | 20.1 | 0.0192 | 0.0006 | 0.057 | 0.002 | 79 | 4 |
| | | | | 323.1 | 38.9 | 2.2 | 36.6 | 0.0185 | 0.0006 | 0.055 | 0.002 | 150 | 7 |
| | | | | 343.2 | 100.4 | 2.5 | 98.0 | 0.0160 | 0.0006 | 0.048 | 0.002 | 470 | 20 |
| | | | | 353.1 | 144.4 | 2.7 | 141.6 | 0.0144 | 0.0006 | 0.043 | 0.002 | 766 | 36 |
| | | | | 363.2 | 193.2 | 3.2 | 190.0 | 0.0126 | 0.0006 | 0.037 | 0.002 | 1182 | 63 |
| | | | | 373.2 | 242.9 | 4.1 | 238.8 | 0.0110 | 0.0006 | 0.032 | 0.002 | 1727 | 107 |
| | | | | 383.1 | 288.8 | 5.5 | 283.4 | 0.0096 | 0.0006 | 0.028 | 0.002 | 2372 | 171 |
| | | | | 393.1 | 330.9 | 7.7 | 323.2 | 0.0084 | 0.0007 | 0.025 | 0.002 | 3100 | 259 |

**Table A.4** (*continued*)

| $w_1$ | $u(w_1)$ | $w_2$ | $u(w_2)$ | $T$ | $P_{tot}$ | $P_{res}$ | $P_{CO2}$ | $x_{CO2}$ | $u(x_{CO2})$ | $\alpha$ | $u(\alpha)$ | $H$ | $u(H)$ |
|---|---|---|---|---|---|---|---|---|---|---|---|---|---|
| | | | | K | kPa | kPa | kPa | | | $mol_{CO2} \cdot mol_{MDEA}^{-1}$ | | kPa $m^3$ $kmol^{-1}$ | |
| 0.300 | 0.001 | 0.400 | 0.001 | | | | | Experiment A | | | | | |
| | | | | 303.1 | 5.3 | 3.3 | 2.0 | 0.0065 | 0.0002 | 0.066 | 0.003 | 11 | 5 |
| | | | | 313.1 | 8.5 | 5.4 | 3.0 | 0.0064 | 0.0002 | 0.066 | 0.003 | 17 | 5 |
| | | | | 323.2 | 13.8 | 8.6 | 5.1 | 0.0064 | 0.0002 | 0.066 | 0.003 | 29 | 5 |
| | | | | 343.2 | 36.5 | 21.1 | 15.4 | 0.0062 | 0.0003 | 0.064 | 0.003 | 92 | 7 |
| | | | | 353.2 | 57.9 | 31.9 | 26.0 | 0.0061 | 0.0002 | 0.062 | 0.003 | 162 | 9 |
| | | | | 363.1 | 89.1 | 46.7 | 42.4 | 0.0058 | 0.0002 | 0.059 | 0.003 | 277 | 15 |
| | | | | 373.2 | 133.0 | 66.4 | 66.5 | 0.0054 | 0.0002 | 0.056 | 0.003 | 467 | 25 |
| | | | | 383.2 | 190.6 | 94.2 | 96.5 | 0.0050 | 0.0002 | 0.051 | 0.003 | 740 | 42 |
| | | | | 393.1 | 262.1 | 131.6 | 130.5 | 0.0046 | 0.0002 | 0.047 | 0.003 | 1112 | 68 |
| | | | | | | | | Experiment B | | | | | |
| | | | | 313.4 | 7.9 | 5.3 | 2.6 | 0.0049 | 0.0002 | 0.050 | 0.002 | 19 | 7 |
| | | | | 323.1 | 12.4 | 8.7 | 3.7 | 0.0048 | 0.0002 | 0.050 | 0.002 | 28 | 7 |
| | | | | 333.1 | 19.8 | 13.7 | 6.0 | 0.0048 | 0.0002 | 0.049 | 0.002 | 46 | 7 |
| | | | | 343.2 | 31.5 | 21.2 | 10.4 | 0.0048 | 0.0002 | 0.049 | 0.002 | 81 | 8 |
| | | | | 353.1 | 49.6 | 32.0 | 17.6 | 0.0047 | 0.0002 | 0.048 | 0.002 | 142 | 10 |
| | | | | 363.1 | 75.9 | 47.2 | 28.7 | 0.0045 | 0.0002 | 0.046 | 0.002 | 240 | 15 |
| | | | | 373.2 | 113.7 | 67.3 | 46.4 | 0.0043 | 0.0002 | 0.044 | 0.002 | 409 | 24 |
| | | | | 383.2 | 164.7 | 94.3 | 70.4 | 0.0041 | 0.0002 | 0.042 | 0.002 | 667 | 7 |
| | | | | 393.2 | 230.9 | 131.7 | 99.2 | 0.0038 | 0.0002 | 0.038 | 0.002 | 1022 | 41 |

[a] Standard uncertainties are reported (level of confidence 0.68). Standard uncertainty for temperature is $u(T)$ = 0.1 K, for total and residual pressure is $u(P_{tot})$ = $u(P_{res})$ = 0.9 kPa and for $CO_2$ pressure is $u(P_{CO2})$ = 1.3 kPa.

**Table A.5**
Measured mole fraction solubility $x_{CO2}$, loading $\alpha$ and Henry's constant $H$ for $CO_2$ in MDEA (1) – MEG (2) – $H_2O$ (3) blends as a function of weight fraction $w$ of unloaded solvent, temperature $T$ and pressure (total pressure $P_{tot}$, residual pressure $P_{res}$ and their difference, $CO_2$ partial pressure $P_{CO2}$).[a]

| $w_1$ | $u(w_1)$ | $w_2$ | $u(w_2)$ | $T$ | $P_{tot}$ | $P_{res}$ | $P_{CO2}$ | $x_{CO2}$ | $u(x_{CO2})$ | $\alpha$ | $u(\alpha)$ | $H$ | $u(H)$ |
|---|---|---|---|---|---|---|---|---|---|---|---|---|---|
| | | | | K | kPa | kPa | /kPa | | | $mol_{CO2}$ $mol_{MDEA}^{-1}$ | | kPa $m^3$ $kmol^{-1}$ | |
| 0.300 | 0.001 | 0.599 | 0.001 | 303.2 | 5.5 | 2.4 | 3.1 | 0.0084 | 0.0003 | 0.059 | 0.002 | 19 | 6 |
| | | | | 313.0 | 9.0 | 3.5 | 5.5 | 0.0083 | 0.0003 | 0.059 | 0.002 | 35 | 6 |
| | | | | 323.1 | 15.3 | 5.1 | 10.2 | 0.0082 | 0.0003 | 0.058 | 0.002 | 65 | 6 |
| | | | | 333.2 | 26.0 | 7.5 | 18.5 | 0.0080 | 0.0003 | 0.057 | 0.002 | 121 | 8 |
| | | | | 343.2 | 43.1 | 11.1 | 32.0 | 0.0078 | 0.0003 | 0.055 | 0.002 | 219 | 12 |
| | | | | 353.2 | 68.7 | 16.3 | 52.4 | 0.0074 | 0.0003 | 0.052 | 0.002 | 380 | 19 |
| | | | | 363.2 | 103.2 | 23.7 | 79.5 | 0.0069 | 0.0003 | 0.049 | 0.003 | 622 | 33 |
| | | | | 373.2 | 147.5 | 33.9 | 113.7 | 0.0063 | 0.0003 | 0.045 | 0.003 | 979 | 56 |
| | | | | 383.2 | 199.9 | 47.7 | 152.2 | 0.0057 | 0.0003 | 0.040 | 0.003 | 1468 | 95 |
| | | | | 393.1 | 257.7 | 66.3 | 191.4 | 0.0051 | 0.0004 | 0.036 | 0.003 | 2080 | 153 |
| 0.300 | 0.001 | 0.400 | 0.001 | 303.1 | 5.3 | 3.3 | 2.0 | 0.0065 | 0.0002 | 0.066 | 0.002 | 11 | 5 |
| | | | | 313.1 | 8.5 | 5.4 | 3.0 | 0.0064 | 0.0002 | 0.066 | 0.002 | 17 | 5 |
| | | | | 323.2 | 13.8 | 8.6 | 5.1 | 0.0064 | 0.0002 | 0.066 | 0.002 | 29 | 5 |
| | | | | 343.2 | 36.5 | 21.1 | 15.4 | 0.0062 | 0.0002 | 0.064 | 0.002 | 92 | 7 |
| | | | | 353.2 | 57.9 | 31.9 | 26.0 | 0.0061 | 0.0002 | 0.062 | 0.002 | 162 | 9 |
| | | | | 363.1 | 89.1 | 46.7 | 42.4 | 0.0058 | 0.0002 | 0.059 | 0.002 | 277 | 15 |
| | | | | 373.2 | 133.0 | 66.4 | 66.5 | 0.0054 | 0.0002 | 0.056 | 0.002 | 467 | 25 |
| | | | | 383.2 | 190.6 | 94.2 | 96.5 | 0.0050 | 0.0002 | 0.051 | 0.002 | 740 | 42 |
| | | | | 393.1 | 262.1 | 131.6 | 130.5 | 0.0046 | 0.0002 | 0.047 | 0.002 | 1112 | 68 |
| 0.300 | 0.002 | 0.200 | 0.002 | 303.1 | 5.1 | 4.2 | 1.0 | 0.0067 | 0.0003 | 0.048 | 0.003 | 8 | 7 |
| | | | | 313.1 | 8.1 | 6.9 | 1.2 | 0.0067 | 0.0003 | 0.048 | 0.003 | 9 | 7 |
| | | | | 323.1 | 12.8 | 11.0 | 1.8 | 0.0067 | 0.0003 | 0.048 | 0.003 | 14 | 7 |
| | | | | 343.2 | 31.8 | 26.9 | 4.9 | 0.0067 | 0.0003 | 0.047 | 0.003 | 40 | 8 |
| | | | | 353.1 | 48.8 | 40.5 | 8.3 | 0.0066 | 0.0003 | 0.047 | 0.003 | 69 | 8 |
| | | | | 363.1 | 73.3 | 59.6 | 13.6 | 0.0065 | 0.0003 | 0.046 | 0.003 | 116 | 10 |
| | | | | 373.2 | 108.4 | 85.9 | 22.5 | 0.0063 | 0.0003 | 0.045 | 0.003 | 199 | 14 |
| | | | | 383.2 | 156.8 | 121.1 | 35.7 | 0.0061 | 0.0003 | 0.043 | 0.003 | 329 | 22 |
| | | | | 393.1 | 221.4 | 168.0 | 53.4 | 0.0058 | 0.0004 | 0.041 | 0.003 | 522 | 36 |

[a] Standard uncertainties are reported (level of confidence 0.68). Standard uncertainty for temperature is $u(T)$ = 0.1 K, for total and residual pressure is $u(P_{tot})$ = $u(P_{res})$ = 0.9 kPa and for $CO_2$ pressure is $u(P_{CO2})$ = 1.3 kPa.

**Table A.6**
Measured mole fraction solubility $x_{CO2}$, loading $\alpha$ and Henry's constant $H$ for $CO_2$ in MDEA (1) – MEG (2) – $H_2O$ (3) blends as a function of weight fraction $w$ of unloaded solvent and pressure (total pressure $P_{tot}$, residual pressure $P_{res}$ and their difference, $CO_2$ partial pressure $P_{CO2}$) at temperatures of 313 K and 343 K.[a]

| $w_1$ | $u(w_1)$ | $w_2$ | $u(w_2)$ | $T$ | $P_{tot}$ | $P_{res}$ | $P_{CO2}$ | $x_{CO2}$ | $u(x_{CO2})$ | $\alpha$ | $u(\alpha)$ | $H$ | $u(H)$ |
|---|---|---|---|---|---|---|---|---|---|---|---|---|---|
| | | | | K | kPa | kPa | kPa | – | | $mol_{CO2}\ mol^{-1}_{MDEA}$ | | kPa $m^3$ $kmol^{-1}$ | |
| 0.300 | 0.001 | 0.599 | 0.001 | 313.2 | 8.1 | 5.1 | 3.0 | 0.0044 | 0.0005 | 0.031 | 0.004 | 36 | 12 |
| | | | | 313.2 | 27.2 | 5.1 | 22.1 | 0.0123 | 0.0007 | 0.088 | 0.005 | 93 | 7 |
| | | | | 313.1 | 34.8 | 5.1 | 29.7 | 0.0168 | 0.0008 | 0.120 | 0.006 | 91 | 6 |
| | | | | 313.1 | 47.1 | 5.1 | 42.0 | 0.0242 | 0.0009 | 0.175 | 0.007 | 89 | 4 |
| | | | | 313.1 | 55.6 | 5.1 | 50.5 | 0.0285 | 0.0009 | 0.207 | 0.008 | 90 | 4 |
| | | | | 313.1 | 63.6 | 5.1 | 58.5 | 0.0322 | 0.0010 | 0.234 | 0.009 | 92 | 4 |
| | | | | 313.1 | 72.0 | 5.1 | 67.0 | 0.0357 | 0.0010 | 0.261 | 0.010 | 95 | 4 |
| | | | | 313.1 | 83.3 | 5.1 | 78.2 | 0.0392 | 0.0011 | 0.288 | 0.011 | 100 | 4 |
| | | | | 313.1 | 97.4 | 5.1 | 92.3 | 0.0442 | 0.0011 | 0.326 | 0.011 | 105 | 4 |
| | | | | 313.2 | 122.6 | 5.1 | 117.5 | 0.0516 | 0.0010 | 0.383 | 0.012 | 113 | 4 |
| | | | | 313.2 | 156.5 | 5.1 | 151.4 | 0.0596 | 0.0010 | 0.446 | 0.013 | 125 | 4 |
| | | | | 313.2 | 191.3 | 5.1 | 186.2 | 0.0661 | 0.0010 | 0.498 | 0.013 | 138 | 4 |
| | | | | 313.2 | 224.1 | 5.1 | 219.0 | 0.0711 | 0.0010 | 0.539 | 0.014 | 150 | 4 |
| | | | | 313.2 | 254.7 | 5.1 | 249.6 | 0.0751 | 0.0010 | 0.572 | 0.015 | 161 | 4 |
| | | | | 313.2 | 300.0 | 5.1 | 295.0 | 0.0801 | 0.0010 | 0.614 | 0.015 | 178 | 5 |
| | | | | 313.2 | 342.6 | 5.1 | 337.6 | 0.0844 | 0.0010 | 0.650 | 0.016 | 192 | 5 |
| | | | | 343.2 | 42.8 | 11.1 | 31.6 | 0.0081 | 0.0005 | 0.058 | 0.004 | 206 | 14 |
| | | | | 343.1 | 66.9 | 11.1 | 55.8 | 0.0119 | 0.0006 | 0.085 | 0.005 | 249 | 15 |
| | | | | 343.2 | 137.9 | 11.1 | 126.8 | 0.0205 | 0.0007 | 0.148 | 0.006 | 324 | 14 |
| | | | | 343.2 | 169.7 | 11.1 | 158.6 | 0.0238 | 0.0008 | 0.172 | 0.007 | 349 | 15 |
| | | | | 343.1 | 199.6 | 11.1 | 188.5 | 0.0266 | 0.0009 | 0.192 | 0.008 | 370 | 16 |
| | | | | 343.2 | 240.7 | 11.1 | 229.6 | 0.0301 | 0.0009 | 0.218 | 0.009 | 396 | 16 |
| | | | | 343.2 | 287.3 | 11.1 | 276.2 | 0.0338 | 0.0010 | 0.246 | 0.010 | 423 | 17 |
| | | | | 343.1 | 340.2 | 11.1 | 329.1 | 0.0375 | 0.0010 | 0.275 | 0.010 | 452 | 17 |
| | | | | 343.1 | 389.9 | 11.1 | 378.8 | 0.0408 | 0.0010 | 0.300 | 0.011 | 477 | 18 |
| | | | | 343.2 | 427.0 | 11.1 | 415.9 | 0.0434 | 0.0011 | 0.319 | 0.011 | 491 | 18 |
| | | | | 343.1 | 457.5 | 11.1 | 446.4 | 0.0451 | 0.0011 | 0.333 | 0.012 | 506 | 19 |
| | | | | 343.2 | 484.1 | 11.1 | 473.0 | 0.0466 | 0.0011 | 0.344 | 0.013 | 518 | 19 |
| | | | | 343.1 | 517.1 | 11.1 | 506.0 | 0.0484 | 0.0011 | 0.358 | 0.013 | 533 | 20 |
| 0.300 | 0.001 | 0.400 | 0.001 | 313.1 | 6.5 | 5.5 | 1.0 | 0.0034 | 0.0003 | 0.034 | 0.003 | 11 | 10 |
| | | | | 313.1 | 10.3 | 5.5 | 4.8 | 0.0095 | 0.0004 | 0.097 | 0.004 | 18 | 4 |
| | | | | 313.2 | 15.0 | 5.5 | 9.5 | 0.0146 | 0.0004 | 0.151 | 0.005 | 23 | 2 |
| | | | | 313.1 | 26.2 | 5.5 | 20.7 | 0.0243 | 0.0004 | 0.254 | 0.006 | 30 | 2 |
| | | | | 313.1 | 36.2 | 5.5 | 30.7 | 0.0306 | 0.0004 | 0.321 | 0.007 | 36 | 1 |
| | | | | 313.2 | 46.5 | 5.5 | 40.9 | 0.0356 | 0.0005 | 0.376 | 0.008 | 41 | 1 |
| | | | | 313.1 | 54.8 | 5.5 | 49.3 | 0.0391 | 0.0005 | 0.414 | 0.009 | 45 | 1 |
| | | | | 313.1 | 67.5 | 5.5 | 62.0 | 0.0436 | 0.0005 | 0.464 | 0.009 | 50 | 1 |
| | | | | 313.1 | 86.4 | 5.5 | 80.8 | 0.0489 | 0.0005 | 0.523 | 0.010 | 58 | 1 |
| | | | | 313.1 | 114.2 | 5.5 | 108.6 | 0.0547 | 0.0005 | 0.589 | 0.011 | 69 | 1 |
| | | | | 313.1 | 148.4 | 5.5 | 142.8 | 0.0599 | 0.0005 | 0.648 | 0.011 | 82 | 2 |
| | | | | 313.2 | 189.3 | 5.5 | 183.8 | 0.0644 | 0.0006 | 0.701 | 0.012 | 98 | 2 |
| | | | | 313.1 | 219.8 | 5.5 | 214.3 | 0.0671 | 0.0006 | 0.731 | 0.012 | 110 | 2 |
| | | | | 313.1 | 273.7 | 5.5 | 268.2 | 0.0707 | 0.0006 | 0.774 | 0.013 | 130 | 2 |
| | | | | 313.1 | 325.8 | 5.5 | 320.2 | 0.0733 | 0.0007 | 0.805 | 0.013 | 149 | 3 |
| | | | | 313.2 | 381.3 | 5.5 | 375.7 | 0.0756 | 0.0007 | 0.832 | 0.014 | 169 | 3 |
| | | | | 313.2 | 427.5 | 5.5 | 421.9 | 0.0771 | 0.0007 | 0.850 | 0.014 | 186 | 3 |
| | | | | 313.2 | 477.7 | 5.5 | 472.1 | 0.0785 | 0.0007 | 0.867 | 0.014 | 204 | 4 |
| | | | | 313.2 | 513.3 | 5.5 | 507.7 | 0.0794 | 0.0007 | 0.878 | 0.015 | 217 | 4 |
| | | | | 343.1 | 29.2 | 20.3 | 8.9 | 0.0048 | 0.0003 | 0.049 | 0.004 | 70 | 9 |
| | | | | 343.1 | 55.4 | 20.3 | 35.0 | 0.0111 | 0.0004 | 0.114 | 0.005 | 117 | 6 |
| | | | | 343.1 | 91.4 | 20.3 | 71.1 | 0.0173 | 0.0005 | 0.179 | 0.006 | 152 | 6 |
| | | | | 343.1 | 137.5 | 20.3 | 117.2 | 0.0233 | 0.0005 | 0.243 | 0.007 | 184 | 6 |
| | | | | 343.1 | 173.5 | 20.3 | 153.2 | 0.0272 | 0.0006 | 0.285 | 0.008 | 206 | 6 |
| | | | | 343.2 | 199.8 | 20.3 | 179.5 | 0.0298 | 0.0006 | 0.312 | 0.009 | 220 | 7 |
| | | | | 343.2 | 248.2 | 20.3 | 227.9 | 0.0339 | 0.0006 | 0.357 | 0.010 | 244 | 7 |
| | | | | 343.2 | 287.4 | 20.3 | 267.1 | 0.0368 | 0.0006 | 0.388 | 0.011 | 263 | 7 |
| | | | | 343.1 | 339.7 | 20.3 | 319.4 | 0.0402 | 0.0006 | 0.426 | 0.011 | 287 | 8 |
| | | | | 343.2 | 397.8 | 20.3 | 377.5 | 0.0435 | 0.0006 | 0.462 | 0.012 | 312 | 8 |
| | | | | 343.2 | 447.1 | 20.3 | 426.8 | 0.0459 | 0.0007 | 0.489 | 0.013 | 333 | 9 |
| | | | | 343.1 | 490.3 | 20.3 | 470.0 | 0.0480 | 0.0007 | 0.513 | 0.013 | 350 | 9 |
| | | | | 343.1 | 512.0 | 20.3 | 491.7 | 0.0488 | 0.0007 | 0.523 | 0.014 | 360 | 10 |
| 0.300 | 0.002 | 0.200 | 0.002 | 313.2 | 8.2 | 6.8 | 1.4 | 0.0061 | 0.0002 | 0.082 | 0.003 | 6 | 4 |
| | | | | 313.1 | 11.7 | 6.8 | 4.9 | 0.0128 | 0.0003 | 0.173 | 0.005 | 11 | 2 |
| | | | | 313.2 | 17.2 | 6.8 | 10.4 | 0.0197 | 0.0003 | 0.267 | 0.006 | 15 | 1 |
| | | | | 313.1 | 29.4 | 6.8 | 22.6 | 0.0293 | 0.0003 | 0.402 | 0.007 | 21 | 1 |
| | | | | 313.1 | 54.6 | 6.8 | 47.8 | 0.0399 | 0.0003 | 0.553 | 0.008 | 33 | 1 |
| | | | | 313.1 | 97.5 | 6.8 | 90.7 | 0.0490 | 0.0004 | 0.685 | 0.009 | 50 | 1 |
| | | | | 313.1 | 155.9 | 6.8 | 149.1 | 0.0550 | 0.0005 | 0.775 | 0.010 | 73 | 1 |
| | | | | 313.1 | 220.3 | 6.8 | 213.5 | 0.0587 | 0.0005 | 0.830 | 0.011 | 98 | 2 |
| | | | | 313.2 | 292.1 | 6.8 | 285.3 | 0.0613 | 0.0006 | 0.870 | 0.011 | 125 | 2 |

**Table A.6** (*continued*)

| $w_1$ | $u(w_1)$ | $w_2$ | $u(w_2)$ | $T$ | $P_{tot}$ | $P_{res}$ | $P_{CO2}$ | $x_{CO2}$ | $u(x_{CO2})$ | $\alpha$ | $u(\alpha)$ | $H$ | $u(H)$ |
|---|---|---|---|---|---|---|---|---|---|---|---|---|---|
| | | | | K | kPa | kPa | kPa | – | | $mol_{CO2}\ mol^{-1}_{MDEA}$ | | kPa $m^3$ $kmol^{-1}$ | |
| | | | | 313.2 | 379.6 | 6.8 | 372.8 | 0.0634 | 0.0006 | 0.901 | 0.012 | 157 | 2 |
| | | | | 313.1 | 440.6 | 6.8 | 433.8 | 0.0645 | 0.0006 | 0.918 | 0.012 | 179 | 3 |
| | | | | 313.1 | 501.8 | 6.8 | 495.0 | 0.0654 | 0.0006 | 0.931 | 0.013 | 202 | 3 |
| | | | | 343.2 | 32.2 | 26.6 | 5.6 | 0.0043 | 0.0002 | 0.058 | 0.003 | 38 | 6 |
| | | | | 343.1 | 45.0 | 26.6 | 18.4 | 0.0091 | 0.0003 | 0.122 | 0.005 | 59 | 4 |
| | | | | 343.2 | 67.8 | 26.6 | 41.2 | 0.0147 | 0.0003 | 0.198 | 0.006 | 80 | 3 |
| | | | | 343.1 | 124.3 | 26.6 | 97.7 | 0.0233 | 0.0004 | 0.318 | 0.007 | 119 | 4 |
| | | | | 343.2 | 154.9 | 26.6 | 128.3 | 0.0270 | 0.0004 | 0.369 | 0.007 | 135 | 3 |
| | | | | 343.2 | 192.0 | 26.6 | 165.4 | 0.0306 | 0.0004 | 0.420 | 0.008 | 152 | 3 |
| | | | | 343.2 | 240.7 | 26.6 | 214.1 | 0.0345 | 0.0004 | 0.476 | 0.009 | 174 | 4 |
| | | | | 343.2 | 290.3 | 26.6 | 263.7 | 0.0378 | 0.0004 | 0.523 | 0.010 | 195 | 4 |
| | | | | 343.2 | 338.3 | 26.6 | 311.7 | 0.0404 | 0.0004 | 0.560 | 0.010 | 216 | 4 |
| | | | | 343.2 | 391.9 | 26.6 | 365.3 | 0.0429 | 0.0004 | 0.596 | 0.011 | 237 | 5 |
| | | | | 343.2 | 446.5 | 26.6 | 419.9 | 0.0450 | 0.0004 | 0.627 | 0.011 | 259 | 5 |
| | | | | 343.1 | 484.5 | 26.6 | 457.9 | 0.0463 | 0.0004 | 0.647 | 0.012 | 274 | 5 |
| | | | | 343.1 | 518.1 | 26.6 | 491.5 | 0.0474 | 0.0004 | 0.662 | 0.012 | 288 | 6 |

[a] Standard uncertainties are reported (level of confidence 0.68). Standard uncertainty for temperature is $u(T)$ = 0.1 K, for total and residual pressure is $u(P_{tot})$ = $u(P_{res})$ = 0.9 kPa and for $CO_2$ pressure is $u(P_{CO2})$ = 1.3 kPa.

**Table A.7**
Measured mole fraction solubility $x_{CO2}$, loading $a$ and Henry's constant $H$ for $CO_2$ in MDEA (1) – $H_2O$ (3) blends as a function of weight fraction $w$ of unloaded solvent and pressure (total pressure $P_{tot}$, residual pressure $P_{res}$ and their difference, $CO_2$ partial pressure $P_{CO2}$) at temperatures of 313 K and 343 K.[a]

| $w_1$ | $u(w_1)$ | $T$ | $P_{tot}$ | $P_{res}$ | $P_{CO2}$ | $x_{CO2}$ | $u(x_{CO2})$ | $\alpha$ | $u(\alpha)$ | $H$ | $u(H)$ |
|---|---|---|---|---|---|---|---|---|---|---|---|
| | | K | kPa | kPa | kPa | | | $mol_{CO2}\ mol^{-1}_{MDEA}$ | | kPa $m^3$ $kmol^{-1}$ | |
| 0.700 | 0.006 | 313.1 | 9.3 | 5.1 | 4.2 | 0.0089 | 0.0003 | 0.034 | 0.004 | 20 | 4 |
| | | 313.2 | 27.4 | 5.1 | 22.3 | 0.0416 | 0.0004 | 0.166 | 0.007 | 22 | 1 |
| | | 313.2 | 51.2 | 5.1 | 46.1 | 0.0674 | 0.0008 | 0.277 | 0.009 | 27 | 1 |
| | | 313.1 | 81.3 | 5.1 | 76.2 | 0.0935 | 0.0014 | 0.396 | 0.012 | 31 | 1 |
| | | 313.1 | 117.0 | 5.1 | 111.9 | 0.1119 | 0.0020 | 0.483 | 0.013 | 38 | 1 |
| | | 313.2 | 162.3 | 5.1 | 157.2 | 0.1283 | 0.0026 | 0.564 | 0.015 | 45 | 1 |
| | | 313.1 | 197.8 | 5.1 | 192.7 | 0.1373 | 0.0030 | 0.610 | 0.016 | 51 | 1 |
| | | 313.1 | 261.8 | 5.1 | 256.7 | 0.1495 | 0.0036 | 0.674 | 0.017 | 62 | 1 |
| | | 313.1 | 307.9 | 5.1 | 302.8 | 0.1558 | 0.0040 | 0.708 | 0.017 | 70 | 1 |
| | | 313.1 | 353.9 | 5.1 | 348.9 | 0.1611 | 0.0042 | 0.736 | 0.018 | 77 | 1 |
| | | 313.1 | 423.3 | 5.1 | 418.2 | 0.1672 | 0.0046 | 0.770 | 0.019 | 88 | 1 |
| | | 313.1 | 477.1 | 5.1 | 472.0 | 0.1710 | 0.0048 | 0.791 | 0.020 | 97 | 1 |
| | | 343.1 | 87.0 | 23.2 | 63.8 | 0.0208 | 0.0003 | 0.081 | 0.001 | 131 | 3 |
| | | 343.1 | 163.7 | 23.2 | 140.5 | 0.0365 | 0.0003 | 0.145 | 0.002 | 161 | 2 |
| | | 343.1 | 239.6 | 23.2 | 216.5 | 0.0491 | 0.0005 | 0.198 | 0.003 | 182 | 2 |
| | | 343.1 | 310.5 | 23.2 | 287.4 | 0.0590 | 0.0006 | 0.241 | 0.003 | 199 | 2 |
| | | 343.1 | 371.3 | 23.2 | 348.1 | 0.0665 | 0.0007 | 0.273 | 0.004 | 212 | 2 |
| | | 343.2 | 425.9 | 23.2 | 402.8 | 0.0721 | 0.0008 | 0.298 | 0.004 | 225 | 3 |
| | | 343.1 | 467.7 | 23.2 | 444.5 | 0.0763 | 0.0009 | 0.317 | 0.005 | 234 | 3 |
| | | 343.2 | 499.6 | 23.2 | 476.4 | 0.0794 | 0.0010 | 0.331 | 0.005 | 240 | 3 |
| 0.900 | 0.006 | 313.1 | 25.0 | 4.2 | 20.8 | 0.0179 | 0.0005 | 0.032 | 0.001 | 83 | 4 |
| | | 313.2 | 65.1 | 4.2 | 60.9 | 0.0437 | 0.0007 | 0.079 | 0.002 | 98 | 3 |
| | | 313.1 | 111.6 | 4.2 | 107.3 | 0.0678 | 0.0010 | 0.126 | 0.003 | 108 | 2 |
| | | 313.1 | 134.5 | 4.2 | 130.2 | 0.0785 | 0.0012 | 0.148 | 0.003 | 112 | 2 |
| | | 313.1 | 178.7 | 4.2 | 174.4 | 0.0956 | 0.0015 | 0.183 | 0.003 | 121 | 2 |
| | | 313.2 | 206.7 | 4.2 | 202.4 | 0.1039 | 0.0018 | 0.201 | 0.004 | 128 | 2 |
| | | 313.1 | 247.0 | 4.2 | 242.8 | 0.1189 | 0.0022 | 0.234 | 0.004 | 132 | 2 |
| | | 313.1 | 277.5 | 4.2 | 273.2 | 0.1253 | 0.0025 | 0.248 | 0.004 | 140 | 2 |
| | | 313.1 | 313.7 | 4.2 | 309.4 | 0.1368 | 0.0029 | 0.275 | 0.005 | 143 | 2 |
| | | 313.2 | 340.4 | 4.2 | 336.2 | 0.1415 | 0.0031 | 0.286 | 0.005 | 150 | 2 |
| | | 313.1 | 377.5 | 4.2 | 373.3 | 0.1500 | 0.0035 | 0.306 | 0.005 | 155 | 2 |
| | | 313.1 | 410.6 | 4.2 | 406.4 | 0.1571 | 0.0038 | 0.323 | 0.005 | 160 | 2 |
| | | 313.2 | 445.0 | 4.2 | 440.8 | 0.1627 | 0.0041 | 0.337 | 0.006 | 166 | 2 |
| | | 313.2 | 474.4 | 4.2 | 470.2 | 0.1674 | 0.0044 | 0.349 | 0.006 | 172 | 3 |
| | | 343.1 | 78.7 | 13.5 | 65.2 | 0.0051 | 0.0005 | 0.009 | 0.001 | 946 | 103 |
| | | 343.2 | 127.0 | 13.5 | 113.6 | 0.0166 | 0.0007 | 0.029 | 0.001 | 505 | 24 |
| | | 343.1 | 150.9 | 13.5 | 137.4 | 0.0195 | 0.0008 | 0.035 | 0.002 | 518 | 25 |
| | | 343.1 | 255.9 | 13.5 | 242.5 | 0.0317 | 0.0009 | 0.057 | 0.002 | 557 | 19 |
| | | 343.1 | 332.2 | 13.5 | 318.8 | 0.0398 | 0.0009 | 0.072 | 0.002 | 578 | 18 |
| | | 343.1 | 404.1 | 13.5 | 390.6 | 0.0471 | 0.0010 | 0.086 | 0.003 | 593 | 17 |
| | | 343.1 | 436.3 | 13.5 | 422.9 | 0.0502 | 0.0010 | 0.092 | 0.003 | 600 | 17 |
| | | 343.1 | 464.5 | 13.5 | 451.0 | 0.0529 | 0.0011 | 0.097 | 0.003 | 606 | 18 |
| | | 343.1 | 488.8 | 13.5 | 475.3 | 0.0551 | 0.0011 | 0.101 | 0.003 | 612 | 18 |

[a] Standard uncertainties are reported (level of confidence 0.68). Standard uncertainty for temperature is $u(T)$ = 0.1 K, for total and residual pressure is $u(P_{tot})$ = $u(P_{res})$ = 0.9 kPa and for $CO_2$ pressure is $u(P_{CO2})$ = 1.3 kPa.

**Table A.8**
Measured mole fraction solubility $x_{CO2}$, loading a and Henry's constant $H$ for $CO_2$ in MDEA (1) – TEG (4) blends as a function of weight fraction $w$ of unloaded solvent, temperature $T$ and pressure (total pressure $P_{tot}$, residual pressure $P_{res}$ and their difference, $CO_2$ partial pressure $P_{CO2}$).[a]

| $w_1$ | $u(w_1)$ | $T$ | $P_{tot}$ | $P_{res}$ | $P_{CO2}$ | $x_{CO2}$ | $u(x_{CO2})$ | $\alpha$ | $u(\alpha)$ | $H$ | $u(H)$ |
|---|---|---|---|---|---|---|---|---|---|---|---|
| | | K | kPa | kPa | kPa | | | $mol_{CO2}$ $mol^{-1}_{MDEA}$ | | kPa $m^3$ $kmol^{-1}$ | |
| 0.000 | 0.000 | 303.1 | 192.5 | 2.3 | 190.3 | 0.0143 | 0.0010 | – | – | 1761 | 136 |
| | | 313.1 | 212.2 | 2.3 | 209.9 | 0.0134 | 0.0011 | – | – | 2095 | 174 |
| | | 323.1 | 231.3 | 2.4 | 228.9 | 0.0126 | 0.0011 | – | – | 2454 | 219 |
| | | 333.1 | 249.6 | 2.6 | 247.1 | 0.0119 | 0.0011 | – | – | 2829 | 269 |
| | | 343.2 | 267.3 | 2.7 | 264.6 | 0.0113 | 0.0011 | – | – | 3216 | 324 |
| | | 353.2 | 284.3 | 3.0 | 281.3 | 0.0108 | 0.0011 | – | – | 3606 | 382 |
| | | 363.1 | 300.7 | 3.3 | 297.3 | 0.0103 | 0.0011 | – | – | 3997 | 443 |
| | | 373.2 | 316.7 | 3.7 | 313.0 | 0.0100 | 0.0011 | – | – | 4389 | 506 |
| | | 383.2 | 332.2 | 4.3 | 327.8 | 0.0097 | 0.0011 | – | – | 4767 | 568 |
| | | 393.1 | 347.5 | 5.0 | 342.5 | 0.0095 | 0.0011 | – | – | 5148 | 632 |
| 0.300 | 0.003 | 303.2 | 57.3 | 2.4 | 54.9 | 0.0256 | 0.0010 | 0.075 | 0.003 | 267 | 13 |
| | | 313.1 | 95.0 | 2.5 | 92.5 | 0.0228 | 0.0010 | 0.067 | 0.003 | 510 | 26 |
| | | 323.1 | 139.8 | 2.5 | 137.2 | 0.0198 | 0.0010 | 0.057 | 0.003 | 883 | 50 |
| | | 333.1 | 183.8 | 2.5 | 181.3 | 0.0169 | 0.0010 | 0.049 | 0.003 | 1377 | 92 |
| | | 343.2 | 222.6 | 2.5 | 220.1 | 0.0146 | 0.0010 | 0.042 | 0.003 | 1951 | 151 |
| | | 353.2 | 255.1 | 2.6 | 252.5 | 0.0129 | 0.0010 | 0.037 | 0.003 | 2557 | 226 |
| | | 363.1 | 282.0 | 2.8 | 282.0 | 0.0115 | 0.0011 | 0.033 | 0.003 | 3231 | 323 |
| | | 373.2 | 304.9 | 3.1 | 301.8 | 0.0109 | 0.0011 | 0.031 | 0.003 | 3702 | 395 |
| | | 383.2 | 325.2 | 3.8 | 321.4 | 0.0102 | 0.0011 | 0.029 | 0.003 | 4216 | 480 |
| | | 393.2 | 343.7 | 4.6 | 339.1 | 0.0098 | 0.0011 | 0.028 | 0.003 | 4692 | 561 |
| 0.500 | 0.003 | 303.1 | 44.7 | 2.3 | 42.4 | 0.0279 | 0.0011 | 0.051 | 0.002 | 183 | 10 |
| | | 313.2 | 77.7 | 2.5 | 75.2 | 0.0253 | 0.0011 | 0.047 | 0.002 | 362 | 20 |
| | | 323.2 | 119.5 | 2.6 | 116.9 | 0.0221 | 0.0011 | 0.041 | 0.002 | 649 | 40 |
| | | 333.2 | 165.1 | 2.8 | 162.2 | 0.0189 | 0.0011 | 0.034 | 0.002 | 1068 | 75 |
| | | 343.2 | 207.2 | 3.2 | 204.1 | 0.0161 | 0.0012 | 0.029 | 0.002 | 1595 | 131 |
| | | 353.2 | 243.3 | 3.5 | 239.8 | 0.0139 | 0.0012 | 0.025 | 0.002 | 2186 | 207 |
| | | 363.2 | 273.4 | 4.4 | 273.4 | 0.0121 | 0.0012 | 0.022 | 0.002 | 2909 | 317 |
| | | 373.2 | 298.8 | 5.3 | 293.5 | 0.0113 | 0.0012 | 0.021 | 0.002 | 3371 | 395 |
| | | 383.1 | 320.7 | 6.5 | 314.3 | 0.0105 | 0.0013 | 0.019 | 0.002 | 3910 | 494 |
| | | 393.1 | 339.6 | 8.3 | 331.3 | 0.0101 | 0.0013 | 0.018 | 0.002 | 4354 | 578 |
| | | 313.1 | 57.4 | 1.6 | 55.7 | 0.0186 | 0.0011 | 0.034 | 0.002 | 367 | 26 |
| | | 313.1 | 104.3 | 1.6 | 102.7 | 0.0329 | 0.0015 | 0.061 | 0.003 | 376 | 22 |
| | | 313.1 | 158.2 | 1.6 | 156.5 | 0.0485 | 0.0014 | 0.091 | 0.004 | 383 | 17 |
| | | 313.2 | 213.3 | 1.6 | 211.7 | 0.0634 | 0.0013 | 0.121 | 0.004 | 390 | 15 |
| | | 313.1 | 263.8 | 1.6 | 262.2 | 0.0759 | 0.0013 | 0.147 | 0.004 | 398 | 14 |
| | | 313.2 | 303.9 | 1.6 | 302.3 | 0.0855 | 0.0013 | 0.168 | 0.005 | 403 | 14 |
| | | 313.2 | 344.1 | 1.6 | 342.5 | 0.0944 | 0.0013 | 0.187 | 0.005 | 410 | 13 |
| | | 313.1 | 375.4 | 1.6 | 373.7 | 0.1010 | 0.0014 | 0.202 | 0.005 | 415 | 13 |
| | | 313.1 | 406.5 | 1.6 | 404.9 | 0.1072 | 0.0014 | 0.215 | 0.005 | 421 | 13 |
| | | 313.2 | 431.9 | 1.6 | 430.3 | 0.1120 | 0.0015 | 0.226 | 0.006 | 426 | 13 |
| | | 313.2 | 473.3 | 1.6 | 471.6 | 0.1196 | 0.0015 | 0.244 | 0.006 | 433 | 14 |
| | | 313.1 | 505.1 | 1.6 | 503.5 | 0.1250 | 0.0016 | 0.256 | 0.006 | 440 | 14 |
| | | 313.1 | 528.3 | 1.6 | 526.7 | 0.1289 | 0.0017 | 0.265 | 0.006 | 444 | 14 |

[a] Standard uncertainties are reported (level of confidence 0.68). Standard uncertainty for temperature is $u(T)$ = 0.1 K, for total and residual pressure is $u(P_{tot})$ = $u(P_{res})$ = 0.9 kPa and for $CO_2$ pressure is $u(P_{CO2})$ = 1.3 kPa.

## Appendix B

The parameters for the so-called "soft model" used to describe the VLE data in the aqueous systems studied in this work are presented in Table B.1. Reference is made to equations Eqs. (4)–(7). The parameters are given with their significant numbers.

**Table B.1**
Model parameters (Eq. (4)).

| Systems | Parameters | | | | | | | |
|---|---|---|---|---|---|---|---|---|
| | A | B | $k_{1,a}$ | $k_{1,b}$ | $k_{2,a}$ | $k_{2,b}$ | $k_{3,a}$ | $k_{3,b}$ |
| 30 wt% MDEA – 60 wt% MEG – 10 wt% $H_2O$ | 1.487 | 10.16 | −17.924 | −96.8894 | −10 | 1.77 | 29 | 3.55 |
| 30 wt% MDEA – 40 wt% MEG – 30 wt% $H_2O$ | 1.496 | 10.24 | −19.004 | −104.0863 | −10 | 1.56 | −199 | 3.91 |
| 30 wt% MDEA – 20 wt% MEG – 50 wt% $H_2O$ | 1.480 | 10.12 | −19.686 | −108.8514 | −10 | 1.27 | 55 | 2.86 |
| 70 wt% MDEA – 30 wt% $H_2O$ | 1.241 | 10.03 | −20.083 | −109.9550 | −10 | 1.39 | 55 | 3.45 |
| 90 wt% MDEA – 10 wt% $H_2O$ | −0.296 | 10.03 | −18.919 | −108.7841 | −10 | −1.04 | 55 | 0.52 |

## Appendix C. Supplementary data

Supplementary data to this article can be found online at https://doi.org/10.1016/j.jct.2020.106176.

## References


[1] M. Stewart, K. Arnold, Part 1 - Gas Sweetening, Gulf Professional Publishing, 2011, pp. 1–140.
[2] O. Økland, S. Davies, R.M. Ramberg, H. Rognø, Steps to the Subsea Factory. in OTC-24307-MS (Offshore Technology Conference, 2013). doi: 10.4043/24307-MS.
[3] GATEkeeper. H2S scavenging: Using Triazine, 2014.
[4] M.G. Lioliou, J. Sandrød, M. Stipanicev, Ø. Birketveit, Qualification and field performance of subsea H2S scavenger injection, 2017.
[5] A.J.L. Hutchinson, Process for treating gases, 1939.
[6] E.R. McCartney, Gas purification and dehydration process, 1948.
[7] W.F. Chapin, Purification and dehydration of gases, 1950.
[8] E.R. McCartney, Extraction of acidic impurities and moisture from gases, 1951.
[9] A.L. Kohl, R.B. Nielsen, Chapter 2 - Alkanolamines for Hydrogen Sulfide and Carbon Dioxide Removal, in: Gas Purification, Gulf Professional Publishing, 1997, pp. 40–186.
[10] B.B. Woertz, Experiments with solvent-amine-water for removing co2 from gas, Can. J. Chem. Eng. 50 (1972) 425–427.
[11] K. Sridharan, M.M. Sharma, New systems and methods for the measurement of effective interfacial area and mass transfer coefficients in gas—liquid contactors, Chem. Eng. Sci. 31 (1976) 767–774.
[12] C. Alvarez-Fuster, N. Midoux, A. Laurent, J.C. Charpentier, Chemical kinetics of the reaction of CO2 with amines in pseudo m–nth order conditions in polar and viscous organic solutions, Chem. Eng. Sci. 36 (1981) 1513–1518.
[13] M.H. Oyevaar, H.J. Fontein, K.R. Westerterp, Equilibria of carbon dioxide in solutions of diethanolamine in aqueous ethylene glycol at 298 K, J. Chem. Eng. Data 34 (1989) 405–408.
[14] J.-H. Song, S.-B. Park, J.-H. Yoon, H. Lee, K.-H. Lee, Solubility of Carbon Dioxide in Monoethanolamine + Ethylene Glycol + Water and Monoethanolamine + Poly(ethylene glycol) + Water at 333.2 K, J. Chem. Eng. Data 42 (1997) 143–144.
[15] I.L. Leites, Thermodynamics of CO2 solubility in mixtures monoethanolamine with organic solvents and water and commercial experience of energy saving gas purification technology, Energy Convers. Manage. 39 (1998) 1665–1674.
[16] H.-J. Xu, C.-F. Zhang, Z.-S. Zheng, Selective H2S Removal by Nonaqueous Methyldiethanolamine Solutions in an Experimental Apparatus, Ind. Eng. Chem. Res. 41 (2002) 2953–2956.
[17] S.-W. Park, J.-W. Lee, B.-S. Choi, J.-W. Lee, Absorption of carbon dioxide into non-aqueous solutions of N-methyldiethanolamine, Korean J. Chem. Eng. 23 (2006) 806–811.
[18] J. Tan, H. Shao, J. Xu, L. Du, G. Luo, Mixture absorption system of monoethanolamine–triethylene glycol for CO2 capture, Ind. Eng. Chem. Res. 50 (2011) 3966–3976.
[19] D. Eimer, Simultaneous removal of water and hydrogen sulphide from natural gas, NTNU, 1994.
[20] R.R. Wanderley, Y. Yuan, G.T. Rochelle, H.K. Knuutila, CO2 solubility and mass transfer in water-lean solvents, Chem. Eng. Sci. 202 (2019) 403–416.
[21] A. Hartono, O. Juliussen, H.F. Svendsen, Solubility of N2O in Aqueous Solution of Diethylenetriamine, J. Chem. Eng. Data 53 (2008) 2696–2700.
[22] D.-Y. Peng, D.B. Robinson, A new two-constant equation of state, Ind. Eng. Chem. Fund. 15 (1976) 59–64.
[23] J.J. Carroll, J.D. Slupsky, A.E. Mather, The solubility of carbon dioxide in water at low pressure, J. Phys. Chem. Ref. Data 20 (1991) 1201–1209.
[24] A. Penttilä, C. Dell'Era, P. Uusi-Kyyny, V. Alopaeus, The Henry's law constant of N2O and CO2 in aqueous binary and ternary amine solutions (MEA, DEA, DIPA, MDEA, and AMP), Fluid Phase Equilib. 311 (2011) 59–66.
[25] A. Hartono, E.O. Mba, H.F. Svendsen, Physical properties of partially CO2 loaded aqueous monoethanolamine (MEA), J. Chem. Eng. Data 59 (2014) 1808–1816.
[26] E. Skylogianni, R.R. Wanderley, S.S. Austad, H.K. Knuutila, Density and viscosity of the nonaqueous and aqueous mixtures of methyldiethanolamine and monoethylene glycol at temperatures from 283.15 to 353.15 K, J. Chem. Eng. Data 64 (2019) 5415–5431.
[27] C. Perinu, B. Arstad, K.-J. Jens, NMR spectroscopy applied to amine–CO2–H2O systems relevant for post-combustion CO2 capture: A review, Int. J. Greenhouse Gas Control 20 (2014) 230–243.
[28] C. Perinu, B. Arstad, K.-J. Jens, 13C NMR Experiments and Methods used to Investigate Amine-CO2-H2O Systems, Energy Proc. 37 (2013) 7310–7317.
[29] P. Brúder, K.G. Lauritsen, T. Mejdell, H.F. Svendsen, CO2 capture into aqueous solutions of 3-methylaminopropylamine activated dimethyl-monoethanolamine, Chem. Eng. Sci. 75 (2012) 28–37.
[30] A. Hartono et al., Characterization of 2-piperidineethanol and 1-(2-hydroxyethyl)pyrrolidine as strong bicarbonate forming solvents for CO2 capture, Int. J. Greenhouse Gas Control 63 (2017) 260–271.
[31] I.M. Bernhardsen, A.A. Trollebø, C. Perinu, H.K. Knuutila, Vapour-liquid equilibrium study of tertiary amines, single and in blend with 3-(methylamino)propylamine, for post-combustion CO2 capture, J. Chem. Thermodyn. 138 (2019) 211–228.
[32] D.-Q. Zheng, W.-D. Ma, R. Wei, T.-M. Guo, Solubility study of methane, carbon dioxide and nitrogen in ethylene glycol at elevated temperatures and pressures, Fluid Phase Equilib. 155 (1999) 277–286.
[33] A.C. Galvão, A.Z. Francesconi, Solubility of methane and carbon dioxide in ethylene glycol at pressures up to 14 MPa and temperatures ranging from (303 to 423) K, J. Chem. Thermodyn. 42 (2010) 684–688.
[34] F.-Y. Jou, R.D. Deshmukh, F.D. Otto, A.E. Mather, Vapour-liquid equilibria of H2S and CO2 and ethylene glycol at elevated pressures, Chem. Eng. Commun. 87 (1990) 223–231.
[35] M. Wise, A. Chapoy, Phase Behaviour of CO2 in Monoethylene Glycol between 263.15–343.15 K and 0.2–40.3 MPa: An Experimental and Modelling Approach, J. Chem. Eng. Data 62 (2017) 4154–4159.
[36] J.M. Campbell, Amine-based processes. in Gas Conditioning and Processing vol. 4, 1998.
[37] K.P. Shen, M.H. Li, Solubility of carbon dioxide in aqueous mixtures of monoethanolamine with methyldiethanolamine, J. Chem. Eng. Data 37 (1992) 96–100.
[38] C. Perinu, I.M. Bernhardsen, D.D.D. Pinto, H.K. Knuutila, K.-J. Jens, NMR Speciation of Aqueous MAPA, Tertiary Amines, and Their Blends in the Presence of CO2: Influence of pKa and Reaction Mechanisms, Ind. Eng. Chem. Res. 57 (2018) 1337–1349.
[39] M. Nitta, K. Hayashi, Y. Furukawa, H. Sato, Y. Yamanaka, 13C-NMR study of acid dissociation constant (pKa) effects on the CO2 absorption and regeneration of aqueous tertiary alkanolamine–piperazine blends, Energy Procedia 63 (2014) 1863–1868.
[40] R. Behrens et al., Monoalkylcarbonate Formation in Methyldiethanolamine–H2O–CO2, Ind. Eng. Chem. Res. 56 (2017) 9006–9015.
[41] C. Perinu, B. Arstad, A.M. Bouzga, J.A. Svendsen, K.J. Jens, NMR-Based Carbamate Decomposition Constants of Linear Primary Alkanolamines for CO2 Capture, Ind. Eng. Chem. Res. 53 (2014) 14571–14578.
[42] D. Eimer, Gas treating: Absorption Theory and Practice, John Wiley & Sons Inc., 2014.
[43] F. Barzagli, S. Lai, F. Mani, Novel non-aqueous amine solvents for reversible CO2 capture, Energy Procedia 63 (2014) 1795–1804.
[44] D.I. Sagdeev, M.G. Fomina, G.Kh. Mukhamedzyanov, I.M. Abdulagatov, Experimental study of the density and viscosity of polyethylene glycols and their mixtures at temperatures from 293K to 473K and at atmospheric pressure, J. Chem. Thermodyn. 43 (2011) 1824–1843.
[45] W.Y. Tawfik, A.S. Teja, The densities of polyethylene glycols, Chem. Eng. Sci. 44 (1989) 921–923.
[46] M.F.V. Pereira, H.M.N.T. Avelino, F.J.P. Caetano, J.M.N.A. Fareleira, Viscosity of liquid diethylene, triethylene and tetraethylene glycols at moderately high pressures using a vibrating wire instrument, Fluid Phase Equilib. 480 (2019) 87–97.
[47] E.A. Crespo et al., New measurements and modelling of high pressure thermodynamic properties of glycols, Fluid Phase Equilib. 436 (2017) 113–123.
[48] C.-Y. Tsai, A.N. Soriano, M.-H. Li, Vapour pressures, densities, and viscosities of the aqueous solutions containing (triethylene glycol or propylene glycol) and (LiCl or LiBr), J. Chem. Thermodyn. 41 (2009) 623–631.
[49] N.V. Sastry, R.R. Thakor, M.C. Patel, Thermophysical Properties for Diethylene Glycol + Nitrobenzene and Triethylene Glycol + (Chloro-, Bromo-, Nitro-) Benzene Systems at Different Temperatures, Int. J. Thermophys. 29 (2008) 610–618.
[50] A. Valtz, M. Teodorescu, I. Wichterle, D. Richon, Liquid densities and excess molar volumes for water + diethylene glycolamine, and water, methanol, ethanol, 1-propanol + triethylene glycol binary systems at atmospheric pressure and temperatures in the range of 283.15–363.15 K, Fluid Phase Equilib. 215 (2004) 129–142.
[51] W.V. Steele, R.D. Chirico, S.E. Knipmeyer, A. Nguyen, Measurements of Vapour Pressure, Heat Capacity, and Density along the Saturation Line for ε-Caprolactam, Pyrazine, 1,2-Propanediol, Triethylene Glycol, Phenyl Acetylene, and Diphenyl Acetylene, J. Chem. Eng. Data 47 (2002) 689–699.
[52] A. Kumagai, H. Mochida, S. Takahashi, Liquid viscosities and densities of HFC-134a+glycol mixtures, Int. J. Thermophys. 14 (1993) 45–53.
[53] F.-Y. Jou, R.D. Deshmukh, F.D. Otto, A.E. Mather, Vapourliquid equilibria for acid gases and lower alkanes in triethylene glycol, Fluid Phase Equilib. 36 (1987) 121–140.
[54] M. Wise, A. Chapoy, Carbon dioxide solubility in Triethylene Glycol and aqueous solutions, Fluid Phase Equilib. 419 (2016) 39–49.

## Supporting Information

# Carbon Dioxide Solubility in Mixtures of Methyldiethanolamine with Monoethylene Glycol, Monoethylene Glycol – Water, Water and Triethylene Glycol

*Eirini Skylogianni [1], Cristina Perinu[1,2], Blanca Y. Cervantes Gameros[1], Hanna K. Knuutila[1*]*

[1] Department of Chemical Engineering, Norwegian University of Science and Technology (NTNU), NO-7491 Trondheim, Norway

[2] Department of Process, Energy and Environmental Technology, University of Southeast Norway, NO-3603 Kongsberg, Norway

* hanna.knuutila@ntnu.no

The file includes:

A. Complementary data plots

B. Density data

C. Karl-Fischer titration results

D. NMR spectra

E. Uncertainty analysis

## A. Complementary data plots

MDEA-MEG mixtures

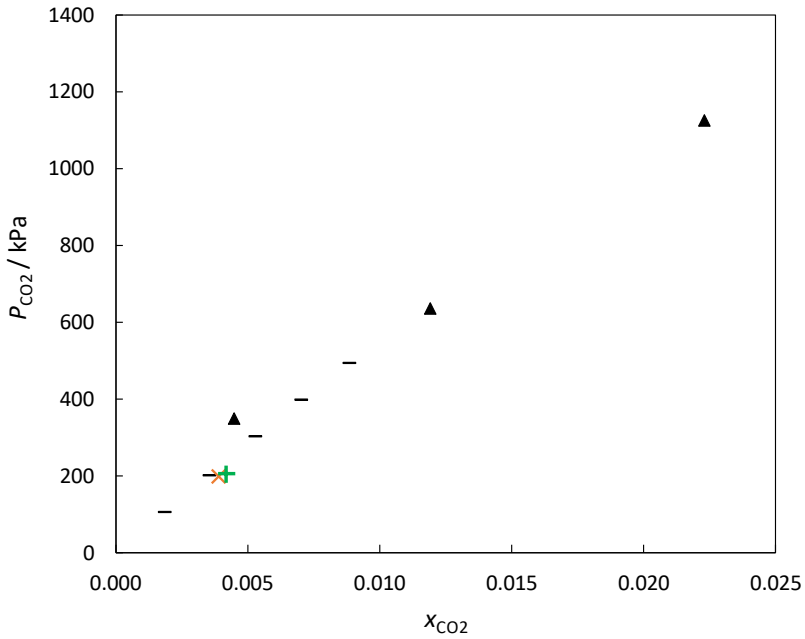


**Figure S. 1**: Carbon dioxide solubility in MEG expressed in mole fraction ($x_{CO2}$) as a function of pressure at 303.15 K. (▲) Galvao and Franscesconi (2010)[1], (—) Serpa et al. (2013)[2], (×) This work (A), (+) This work (B).

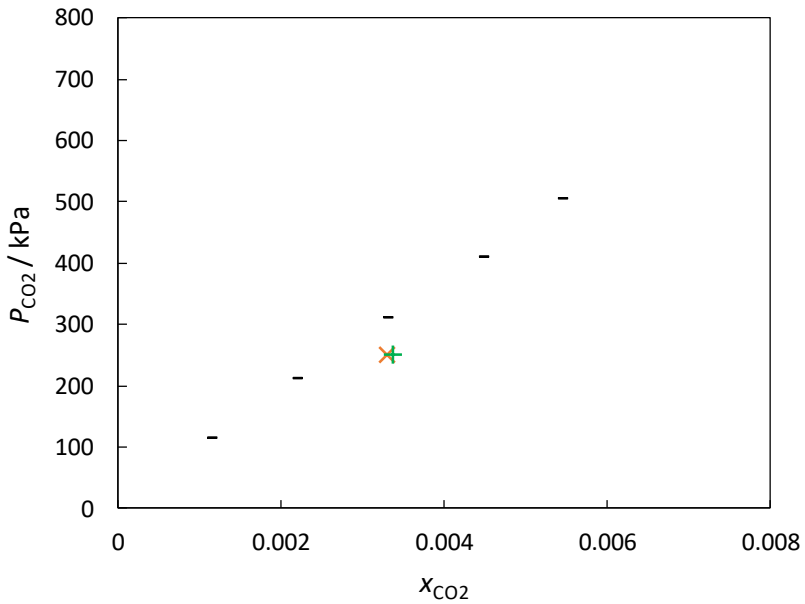


**Figure S. 2**: Carbon dioxide solubility in MEG expressed in mole fraction ($x_{CO2}$) as a function of pressure at 333.15 K. (—) Serpa et al. (2013)[2], (×) This work (A), (+) This work (B).

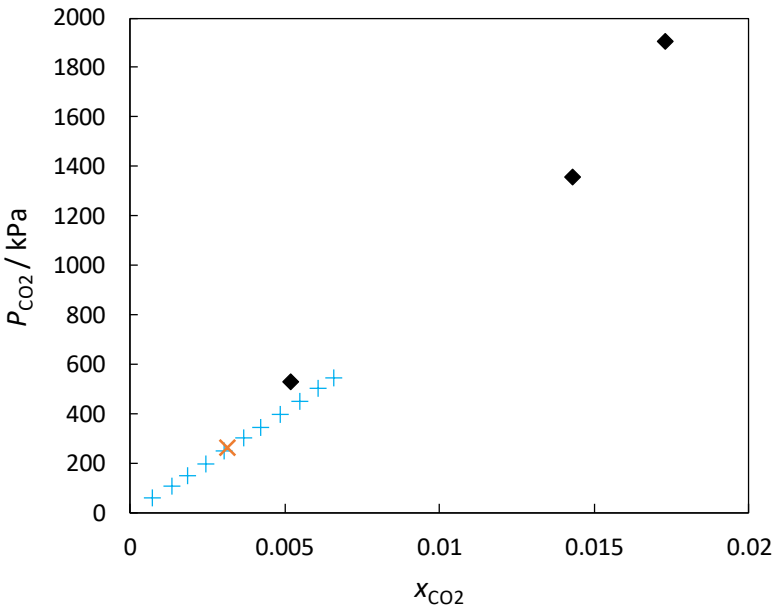


**Figure S. 3**: Carbon dioxide solubility in MEG expressed in mole fraction ($x_{CO2}$) as a function of pressure at 343.15 K. (♦) Wise and Chapoy (2017)[3], (×) This work (A), (+) This work (isothermal experiment).

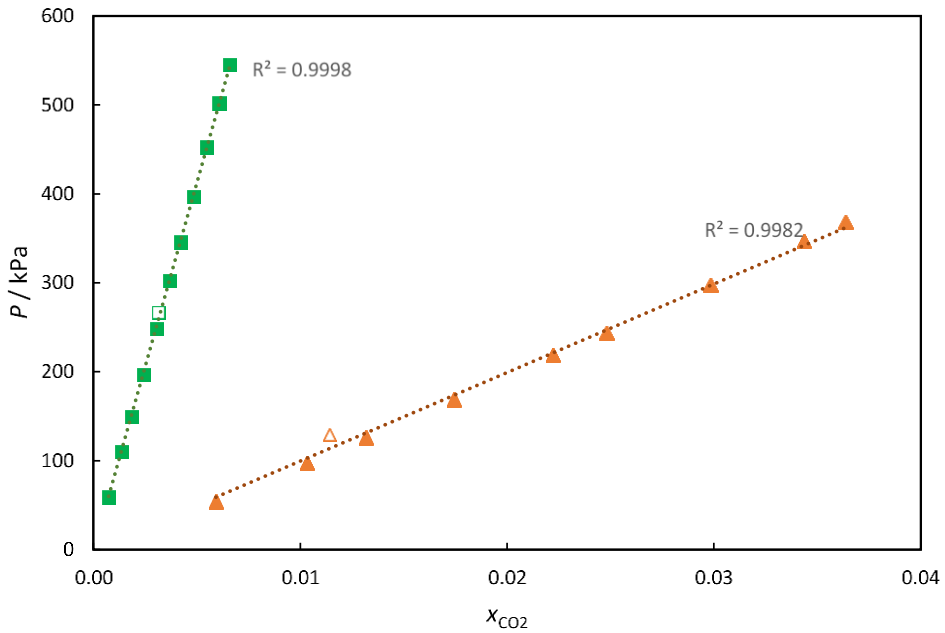


**Figure S. 4**: Partial pressure of $CO_2$ as a function of $CO_2$ solubility expressed in mole fraction ($x_{CO2}$) in pure MEG and pure MDEA at 343 K. Hollow symbols denote previous experiment (data from Table A. 2) and filled symbols denote isothermal experiment (data from Table A. 3); (■) MEG and (▲) MDEA. Dotted lines are linear trendlines; the linearity between $P$ and $x$ is assessed through the coefficient of determination, $R^2$.

MDEA-MEG-$H_2O$ mixtures

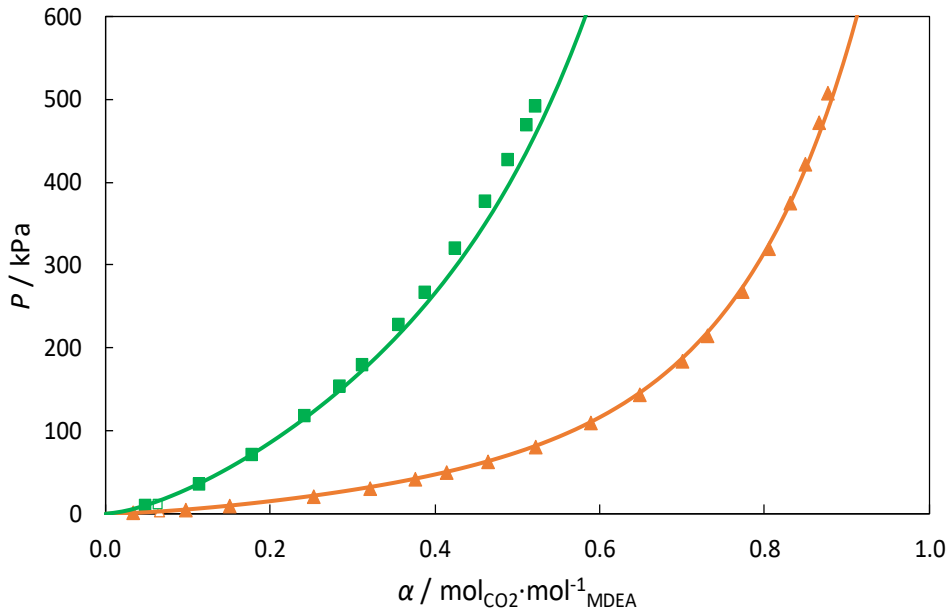


**Figure S. 5**: Partial pressure of $CO_2$ as a function of $CO_2$ loading in a solution of 30 wt% MDEA – 40 wt% MEG – 30 wt% $H_2O$. Hollow symbols denote previous experiment (data from Table A. 5) and filled symbols denote isothermal experiment (data from Table A. 6); (▲) 313.2 K, (■) 343.2 K. The lines represent model estimations.

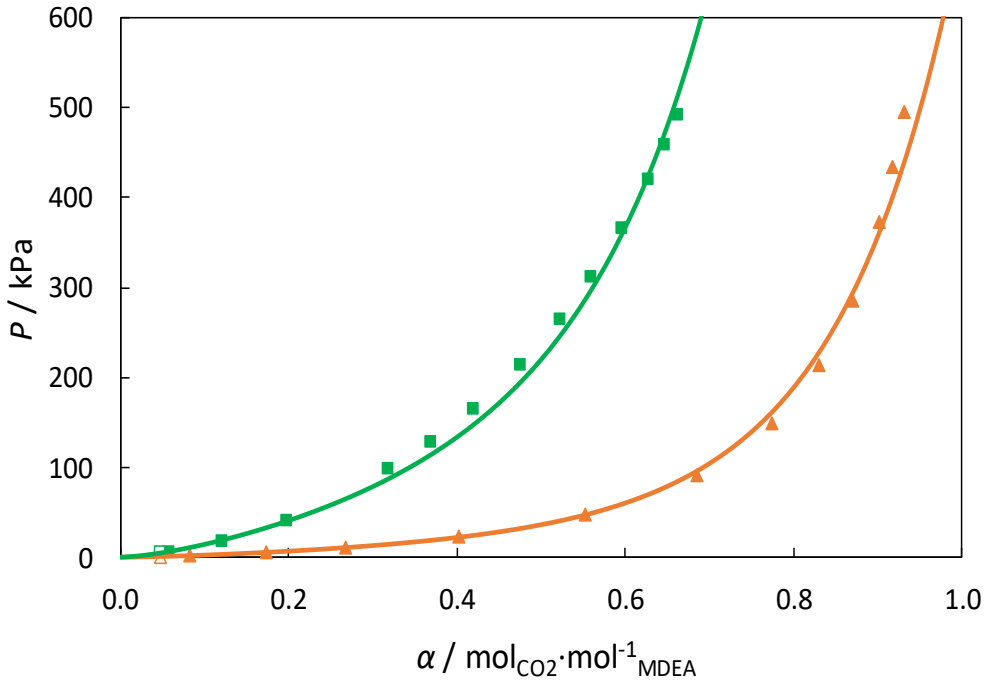


**Figure S. 6**: Partial pressure of $CO_2$ as a function of $CO_2$ loading in a solution of 30 wt% MDEA – 20 wt% MEG – 50 wt% $H_2O$. Hollow symbols denote previous experiment (data from Table A. 5) and filled symbols denote isothermal experiment (data from Table A. 6); (▲) 313.2 K, (■) 343.2 K. The lines represent model estimations.

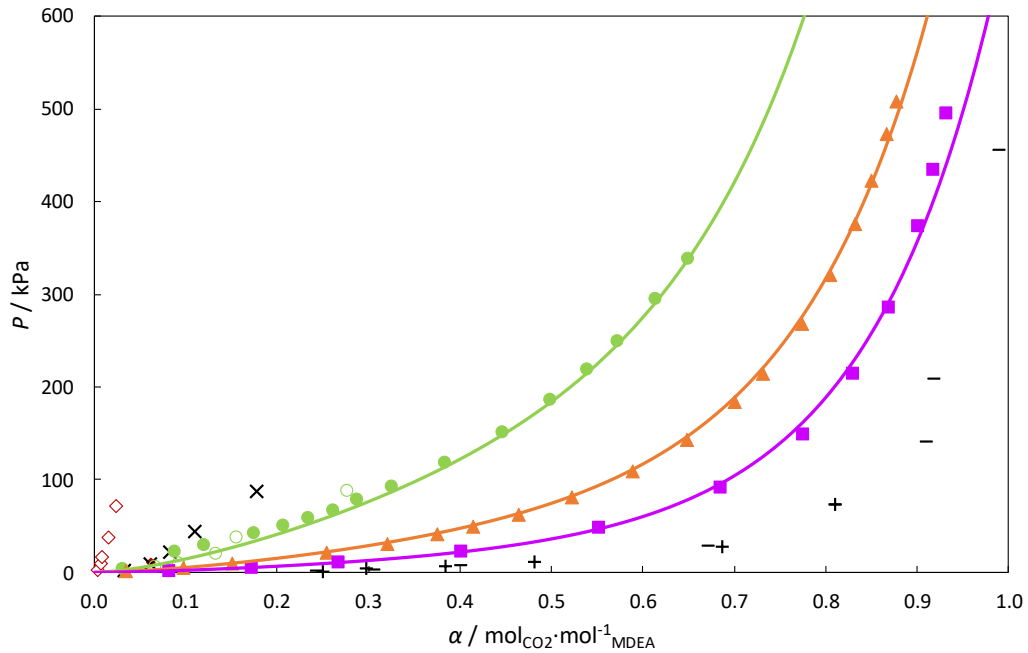


**Figure S. 7**: Partial pressure of $CO_2$ as a function of $CO_2$ loading in MDEA (1) – MEG (2) – $H_2O$ (3) blends at 313 K. 30 wt% MDEA – 70 wt% MEG: (♦) This work and (◊) data from Xu et al.[4], 30 wt% MDEA – 65 wt% MEG – 5 wt% $H_2O$: (×) Xu et al.[4], 30 wt% MDEA – 60 wt% MEG – 10 wt% $H_2O$: (●) This work and (○) Xu et al.[4], 30 wt% MDEA – 40 wt% MEG – 30 wt% $H_2O$: (▲) This work, 30 wt% MDEA – 20 wt% MEG – 50 wt% $H_2O$: (■) This work, 30 wt% MDEA – 70 wt% $H_2O$: (+) Xu et al.[4] and (-) Shen and Li[5]. The lines represent model estimations.

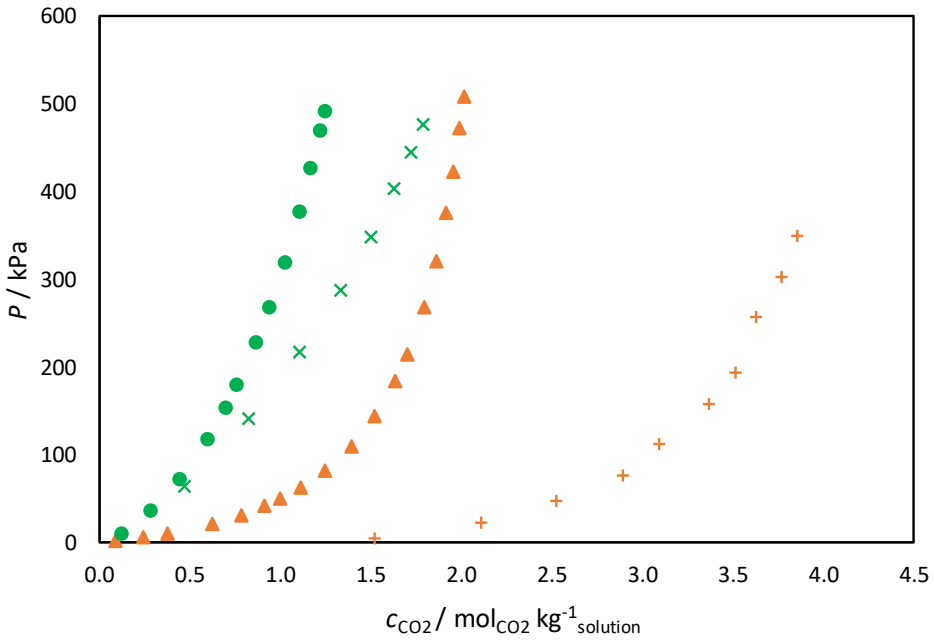


**Figure S. 8**: Partial pressure of $CO_2$ as a function of $CO_2$ liquid phase concentration in 30 wt% MDEA – 40 wt% MEG – 30 wt% $H_2O$ and 70 wt% MDEA – 30 wt% $H_2O$. (▲) denotes data obtained at 313 K with MDEA – MEG – $H_2O$ system, (+) 313 K with MDEA – $H_2O$ system; (●) 343 K with MDEA – MEG – $H_2O$ system and (×) 343 K with MDEA – $H_2O$ system.

MDEA-TEG mixtures

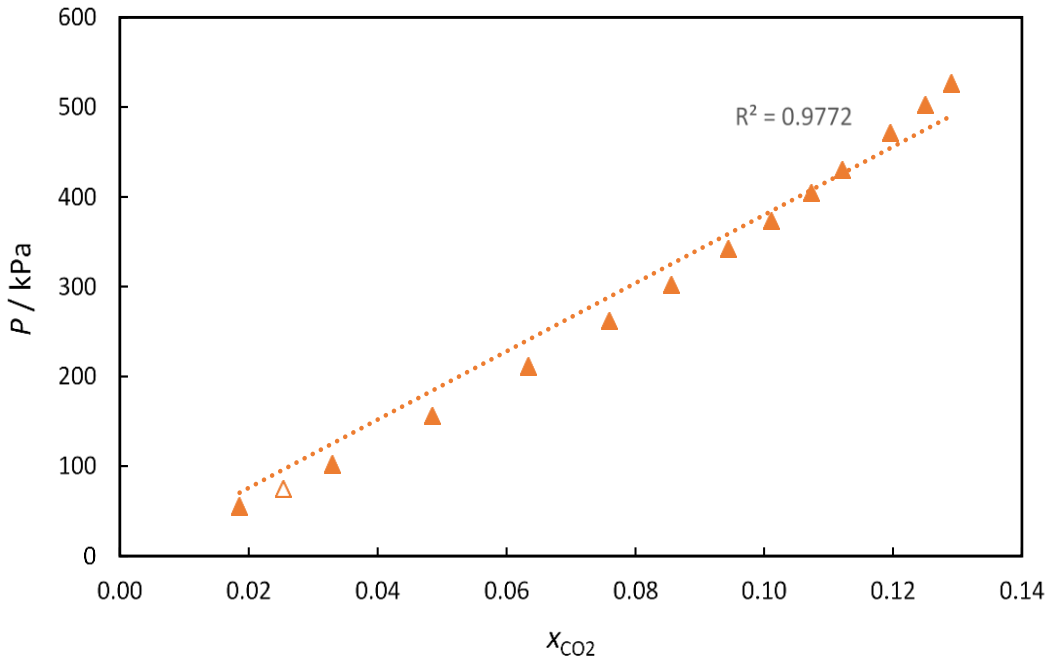


**Figure S. 9***:* Partial pressure of $CO_2$ as a function of $CO_2$ solubility expressed in mole fraction ($x_{CO2}$) in 50 wt% MDEA – 50 wt% TEG at 313 K. Hollow symbol denotes previous experiment and filled symbols denote isothermal experiment (Table A. 8). Dotted line is linear trendline.

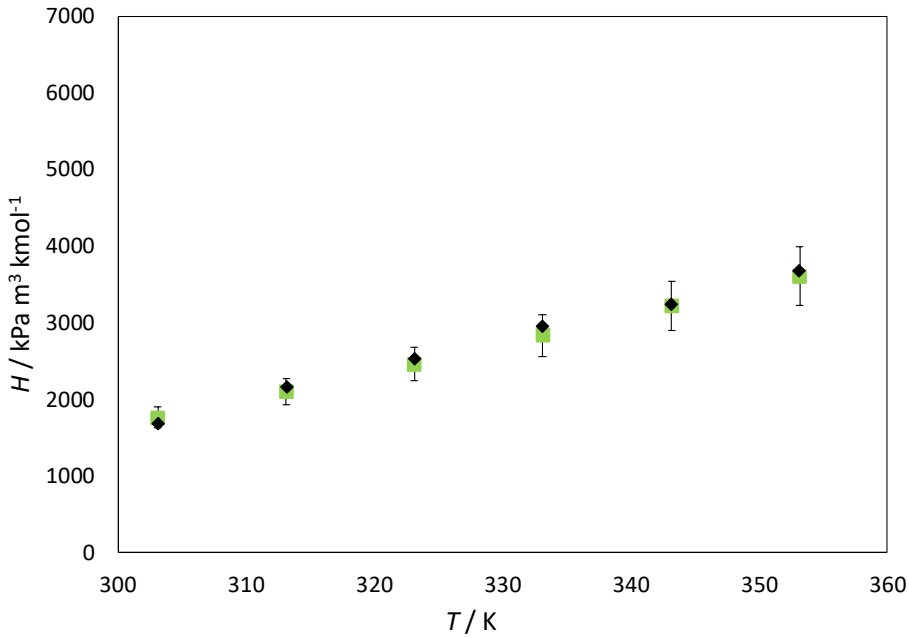


**Figure S. 10***:* Henry's constant as a function of temperature for pure TEG. (♦) Tan et al.[6], (■) This work. Error bars in the measured Henry's constants are included.

## B. Density data

**Table S. 1:** Density $\rho$ in MDEA (1) – MEG (2) – $H_2O$ (3) and MDEA (1) – TEG (4) blends as a function of weight fraction $w$ of unloaded solvent and temperature $T$ at pressure $P$ = 102 kPa for some of the mixtures studied in this work. [a]

| | | | | | | | | $\rho$ (kg m$^{-3}$) | | | | |
|---|---|---|---|---|---|---|---|---|---|---|---|---|
| $w_1$ | $u(w_1)$ | $w_2$ | $u(w_2)$ | $w_3$ | $u(w_3)$ | $w_4$ | $u(w_4)$ | 303.15 K | 313.15 K | 323.15 K | 333.15 K | 343.15 K |
| 0.050 | 0.001 | 0.950 | 0.001 | - | - | - | - | 1103.90* | 1095.40* | 1086.90* | 1078.50* | 1070.00* |
| 0.100 | 0.001 | 0.900 | 0.001 | - | - | - | - | 1106.01 | 1098.98 | 1091.72 | - | - |
| | | | | | | | | 1097.88* | 1090.19* | 1082.34* | 1074.31* | 1066.12* |
| 0.300 | 0.002 | 0.200 | 0.002 | 0.500 | 0.002 | - | - | 1052.98 | 1046.67 | 1040.21 | - | 1025.78 |
| | | | | | | | | 1049.93* | 1044.14* | 1038.23* | 1032.19* | 1025.98* |
| - | - | - | - | - | - | 1.000 | 0.006 | 1115.58 | 1107.82 | 1099.84 | 1091.86 | 1084.28 |
| 0.300 | 0.003 | - | - | - | - | 0.700 | 0.003 | 1089.45 | 1081.63 | 1073.79 | 1066.24 | 1058.14 |
| 0.500 | 0.003 | - | - | - | - | 0.500 | 0.003 | 1072.82 | 1065.08 | 1057.57 | 1050.41 | 1041.68 |
| | | | | | | | | 353.15 K | 363.15 K | 373.15 K | 383.15 K | 393.15 K |
| 0.050 | 0.001 | 0.950 | 0.001 | - | - | - | - | 1061.50* | 1052.90* | 1044.30* | 1035.60* | 1026.80* |
| 0.100 | 0.001 | 0.900 | 0.001 | - | - | - | - | 1069.25 | - | - | - | - |
| | | | | | | | | 1057.77* | 1049.24* | 1040.54* | 1031.67* | 1022.61* |
| 0.300 | 0.002 | 0.200 | 0.002 | 0.500 | 0.002 | - | - | 1018.12 | - | - | - | - |
| | | | | | | | | 1019.61* | 1013.05* | 1006.29* | 999.30* | 992.09* |
| - | - | - | - | - | - | 1.000 | 0.006 | 1076.37 | 1068.73$^{+}$ | 1060.87$^{+}$ | 1053.01$^{+}$ | 1045.15$^{+}$ |
| 0.300 | 0.003 | - | - | - | - | 0.700 | 0.003 | 1050.17 | 1042.42$^{+}$ | 1034.58$^{+}$ | 1026.73$^{+}$ | 1018.89$^{+}$ |
| 0.500 | 0.003 | - | - | - | - | 0.500 | 0.003 | 1033.71 | 1018.98$^{+}$ | 1010.98$^{+}$ | 1002.98$^{+}$ | 994.98$^{+}$ |

[a] Standard uncertainties are reported in composition (level of confidence 0.68). Standard uncertainties not included above are for temperature $u(T)$ = 0.01 K, for pressure $u(P)$ = 3 kPa and for density measurements $u(\rho)$ = 0.09, 0.09, 0.04, 0.03, 0.05 and 0.05 kg m$^{-3}$ at the temperatures 303.15, 313.15, 323.15, 333.15, 343.15 and 353.15 K, respectively.

*: model by Skylogianni et al.[7]

+: extrapolated values

## C. Karl-Fischer titration results

**Table S. 2**: Water content $c_w$ before and after the solubility measurements of $CO_2$ in pure MDEA (1), pure MEG (2), pure TEG (4) and selected mixtures of them, accompanied by the corresponding standard uncertainties (level of confidence 0.68).

| System | | | | | | | *Before* | | *After* | |
|---|---|---|---|---|---|---|---|---|---|---|
| $w_1$ | $u(w_1)$ | $w_2$ | $u(w_2)$ | $w_4$ | $u(w_4)$ | *info* | $c_w$ | $u(c_w)$ | $c_w$ | $u(c_w)$ |
| | | | | | | | ppm | ppm | ppm | ppm |
| - | - | 1.000 | | - | - | *313 K* | 146 | 11 | 1857 | 37 |
| 1.000 | | - | - | - | - | *313 K* | 1155 | 40 | 5012 | 156 |
| 0.050 | 0.001 | 0.950 | 0.001 | - | - | - | 610 | 37 | 1722 | 89 |
| 0.500 | 0.002 | 0.500 | 0.002 | - | - | - | 810 | 13 | 1599 | 43 |
| - | - | - | - | 1.000 | - | *313 K* | 340 | 17 | 1605 | 25 |
| 0.300 | 0.003 | - | - | 0.700 | 0.003 | - | 1048 | 17 | 1165 | 91 |
| 0.300 | 0.003 | - | - | 0.500 | 0.003 | - | 596 | 22 | 3371 | 96 |

## D. NMR spectra

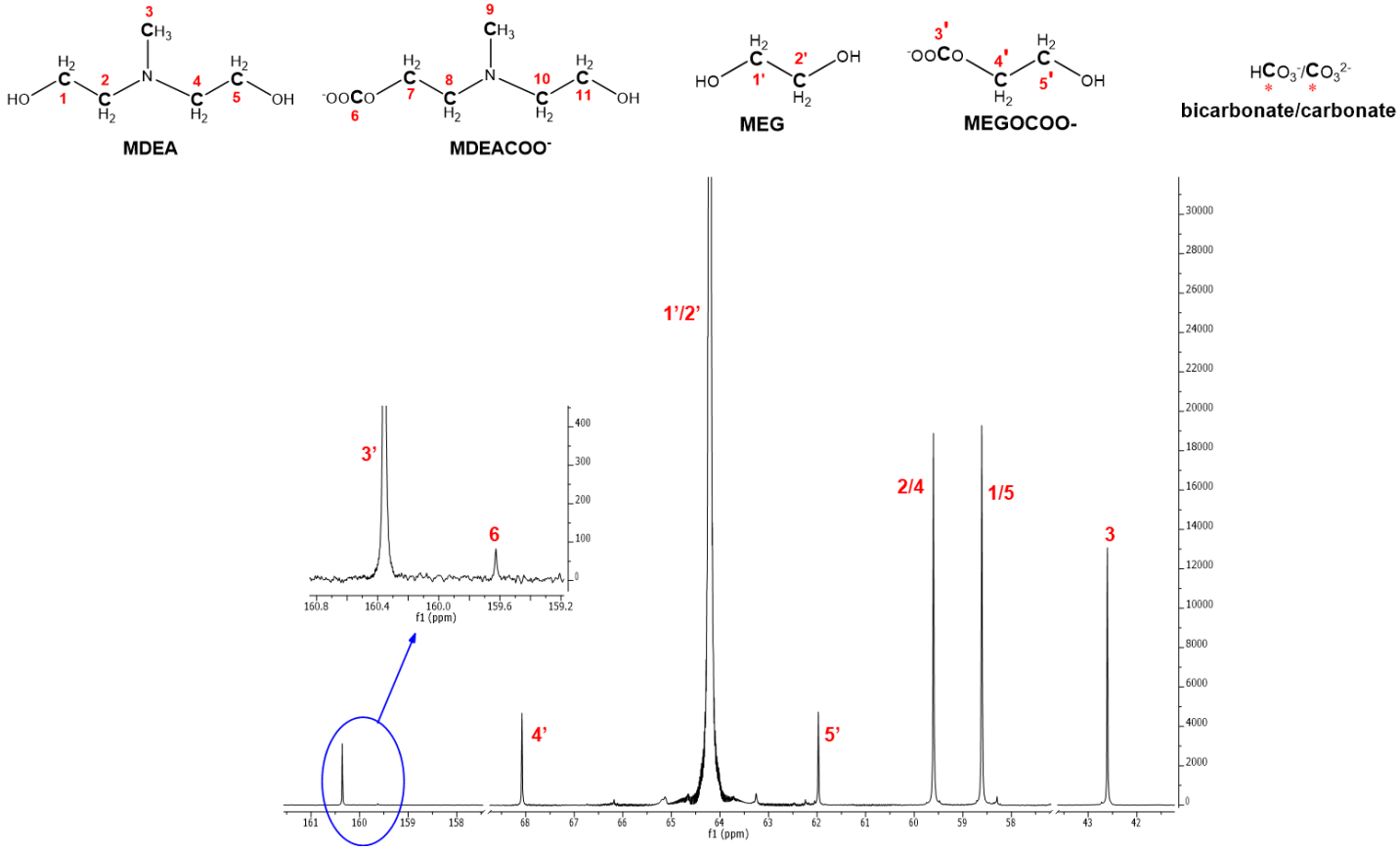


**Figure S. 11**: $^{13}C$ NMR spectrum of 5 wt% MDEA – 95 wt% MEG – $CO_2$.

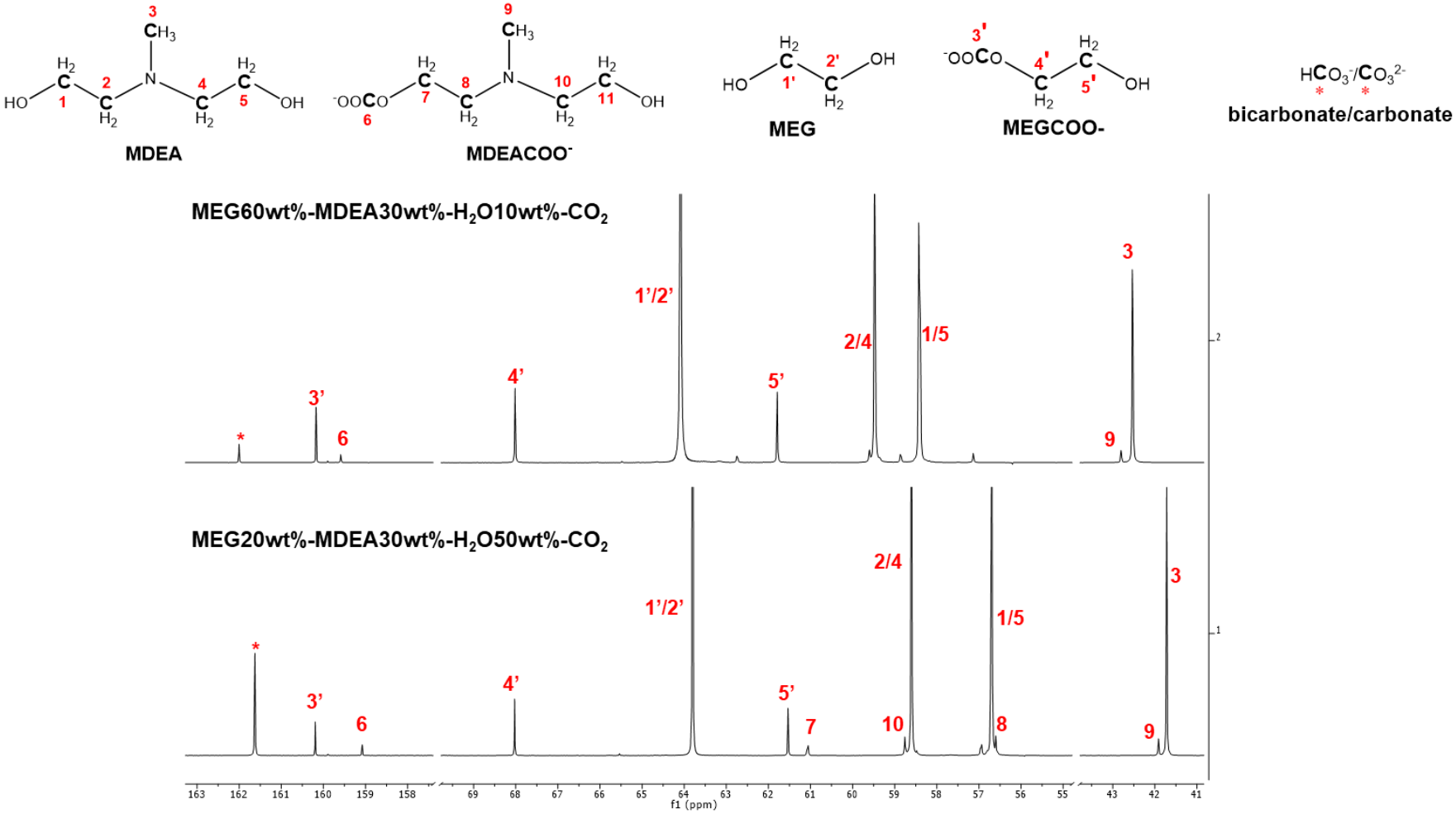


**Figure S. 12**: $^{13}C$ NMR spectrum of $CO_2$ – MDEA – MEG – $H_2O$ systems.

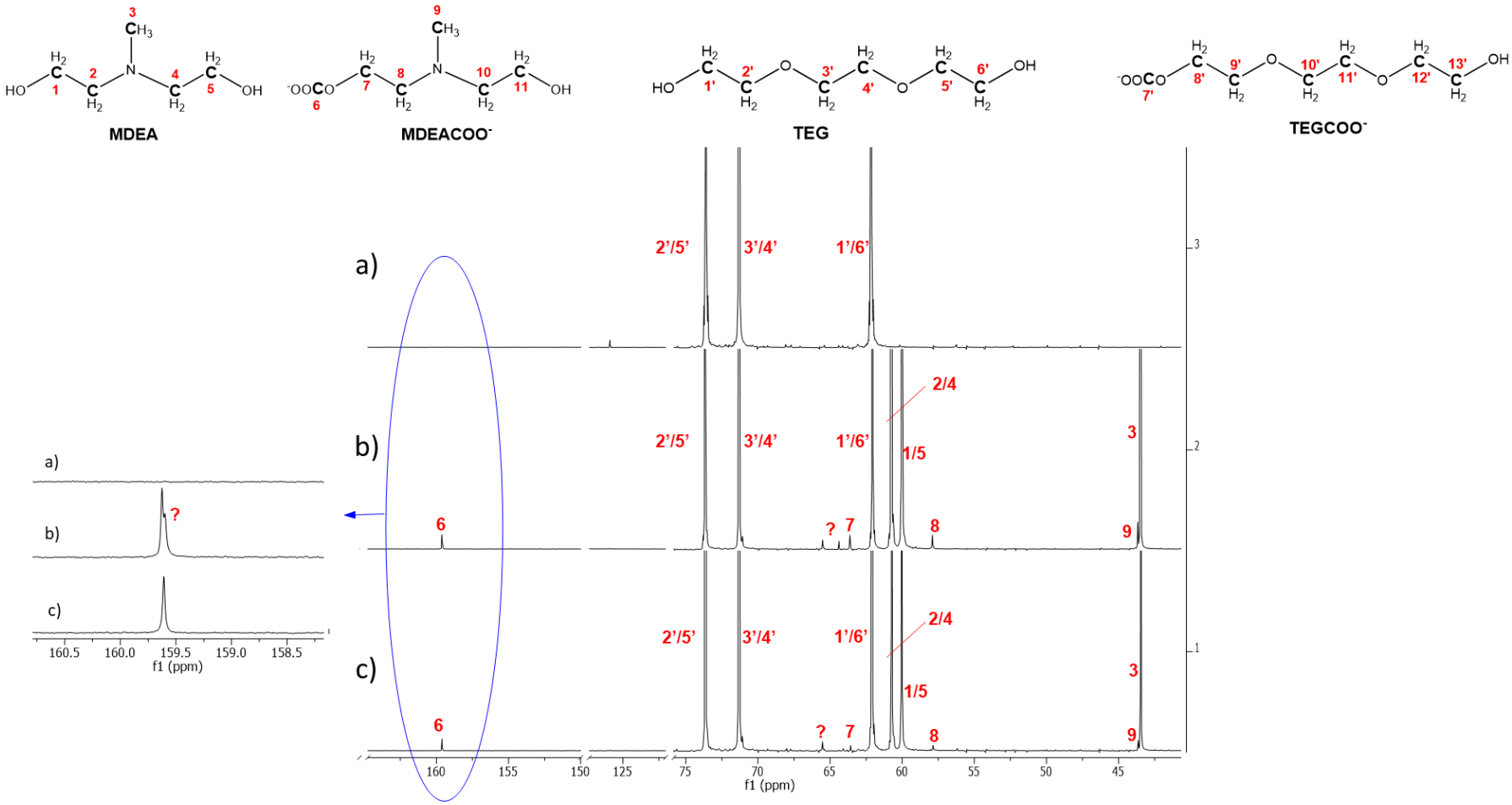


**Figure S. 13**: $^{13}C$ NMR spectrum of a) $CO_2$ – TEG, b) 50 wt% MDEA – 50 wt% TEG – $CO_2$, c) 30 wt% MDEA – 70 wt% TEG – $CO_2$.

## E. Uncertainty Analysis

In this section, the uncertainty calculations are presented. We report the standard uncertainties and combined standard uncertainties when applicable (level of confidence 0.68).

Uncertainty of the solution composition in wt.%, *w*

The weight fraction of a binary mixture, here MDEA (1) and MEG/TEG/$H_2O$ (2), is given by:

$$w_1 = \frac{m_1}{m_1 + m_2} \quad (S.1)$$

where m: mass. The standard uncertainty of the composition of each component is equal to each other in binary mixtures. Using the Law of propagation of uncertainty, the uncertainty in weight fractions is defined as:

$$u^2(w_1) = \left(\frac{\partial w_1}{\partial m_1}\right)^2_{m_2} u^2(m_1) + \left(\frac{\partial w_1}{\partial m_2}\right)^2_{m_1} u^2(m_2) \quad (S.2),$$

leading to:

$$u(w) = u(w_1) = u(w_2) = \frac{u(m)}{(m_1 + m_2)^2}\sqrt{m_1^2 + m_2^2} \quad (S.3)$$

where $u(m)$ is the uncertainty of the mass.

For a ternary system, the uncertainty of the weight fractions is found by:

$$u(w_1) = \frac{u(m)}{(m_1 + m_2 + m_3)^2}\sqrt{2\,m_1^2 + (m_2 + m_3)^2} \quad (S.4)$$

$$u(w_2) = \frac{u(m)}{(m_1 + m_2 + m_3)^2}\sqrt{2\,m_2^2 + (m_1 + m_3)^2} \quad (S.5)$$

$$u(w_3) = \frac{u(m)}{(m_1 + m_2 + m_3)^2}\sqrt{2\,m_3^2 + (m_1 + m_2)^2} \quad (S.6)$$

The uncertainty of the mass includes both the accuracy of the scale, $u_{scale}(m) = 1 \cdot 10^{-6}$ kg, and the chemicals' purity, according to:

$$u(m) = \sqrt{u^2_{scale}(m) + u^2_{purity,i}(m)} \quad (S.7)$$

$u_{\text{purity}}$ (m) is calculated for each component, and it is equal to a $/\sqrt{3}$ assuming uniform distribution is followed. The numerator, a, is the maximum deviation from the measured value, i.e. purity%·mass. The purity of water is considered 100%.

**Table S. 3**: Composition in Weight Fraction *w* and Standard Uncertainties for the binaries {MDEA (1) + MEG (2)}, {MDEA (1) + $H_2O$ (3)} and {MDEA (1) + TEG (4)}.

| $w_1$ | $u(w_1) = u(w_2)$ | $u(w_1) = u(w_2)$ | $u(w_1) = u(w_2)$ |
|---|---|---|---|
| | MDEA-MEG | MDEA-$H_2O$ | MDEA-TEG |

| | | | |
|---|---|---|---|
| 0.000 | 0.000 | 0.000 | 0.000 |
| 0.050 | 0.001 | - | - |
| 0.100 | 0.001 | - | - |
| 0.300 | 0.001 | - | 0.003 |
| 0.500 | 0.002 | - | 0.003 |
| 0.700 | 0.003 | 0.006 | - |
| 0.900 | 0.005 | 0.006 | - |
| 1.000 | 0.006 | 0.006 | 0.006 |

**Table S. 4:** Composition in Weight Fraction *w* and Standard Uncertainties for {MDEA (1) + MEG (2) + Water (3)}

| $w_1$ | $w_2$ | $w_3$ | $u(w_1)$ | $u(w_2)$ | $u(w_3)$ |
|---|---|---|---|---|---|
| 0.300 | 0.200 | 0.500 | 0.002 | 0.002 | 0.002 |
| 0.300 | 0.400 | 0.300 | 0.001 | 0.001 | 0.001 |
| 0.300 | 0.599 | 0.101 | 0.001 | 0.001 | 0.001 |

Uncertainty of the partial pressure of $CO_2$, $P_{CO_2}$

The partial pressure of carbon dioxide was calculated according to Eq. (S.8) and the derived uncertainty is shown in Eq. (S.9).

$$P_{CO_2} = P_{tot} - P_{res} \quad (S.8)$$

$$u_c^2(P_{CO_2}) = \left(\frac{\partial P_{CO_2}}{P_{tot}}\right)^2_{P_{res}} u^2(P_{tot}) + \left(\frac{\partial P_{CO_2}}{\partial P_{res}}\right)^2_{P_{tot}} u^2(P_{red}) \quad = 2 \cdot u^2(P) \quad (S.9)$$

where $u(P) = u(P_{tot}) = u(P_{res})$ is the pressure transducer's uncertainty (0.15% Full Scale, i.e. 0.9 kPa. The resulted uncertainty is $u(P) = 1.3$ kPa.

Uncertainty of $CO_2$ loading, a

By definition:

$$\alpha = \frac{n_{abs}}{n_{MDEA}} \qquad (S.10)$$

$$u(\alpha)^2 = \frac{1}{n_{MDEA}^2}(u(n_{abs})^2 + a^2 u(n_{MDEA})^2) \qquad (S.11)$$

where $n_{abs}$ are the $CO_2$ moles absorbed in the liquid phase and $n_{MDEA}$ the amine moles of the solution inside the reactor. It is assumed that no amine vaporization takes place which is a valid assumption due to the low vapor pressure of the MDEA.

The uncertainty $u(n_{abs})$ as well as $u(n_{MDEA})$ are needed.

Uncertainty of the number of moles of amine in the reactor, $n_{MDEA}$

The solution is prepared gravimetrically and is charged into a flask, through which it is introduced in the reactor. By weighing the flask before ($m_{tot,flask}$) and after introducing the solution to the reactor ($m_{tot,residue}$), the total mass introduced is known, $m_{intr}$.

Taking into account the molecular weight of the amine and the amount of amine introduced into the reactor, $m_{intr}w_{MDEA}$, the number of mols of the amine in the reactor can be known, $n_{MDEA}$.

$$n_{MDEA} = \frac{m_{MDEA}}{Mr_{MDEA}} = \frac{m_{intr}\, w_{MDEA}}{Mr_{MDEA}} = \frac{(m_{tot,flask} - m_{tot,residue})\, w_{MDEA}}{Mr_{MDEA}} \quad (S.12)$$

$$u(n_{MDEA})^2 = 2\left(\frac{w_{MDEA}}{Mr_{MDEA}}\right)^2 u_c(m_{intr})^2 + \left(\frac{m_{intr}}{Mr_{MDEA}}\right)^2 u(w_{MDEA})^2 \quad (S.13)$$

where $u_c(m_{intr}) = 2 \cdot u(m)$ because $m = m_{tot,flask} - m_{tot,residue}$ and $u(m_{tot,flask}) = u(m_{tot,residue}) = u(m)$ as calculated earlier.

Uncertainty of the number of moles of $CO_2$ absorbed, $n_{abs}$

The number of moles of $CO_2$ introduced in the reactor by the $CO_2$ cylinder is calculated by $n_{ci} - n_{ca}$, where *ci* stands for cylinder initial and *ca* for cylinder after. The amount of gas absorbed by the solution, $n_{abs}$, is the difference between the amount introduced in the reactor minus the amount of $CO_2$ that exists in the gas phase in equilibrium with the solution, $n_{gas}$.

Based on PVT data, the number of moles in each case was calculated, using Peng-Robinson Equation of State. In the derivations below, the compressibility factor is not shown, because its effect in the calculated uncertainties was evaluated and found negligible.

$$n_{abs} = (n_{ci} - n_{cf}) - n_{gas} \quad (S.14)$$

$$n_{abs} = \frac{p_{ci}V_c}{RT_{ci}} - \frac{p_{ca}V_c}{RT_{ca}} - \frac{p_{gas}V_{gas}}{RT_{gas}} = \frac{p_{ci}V_c}{RT_{ci}} - \frac{p_{ca}V_c}{RT_{ca}} - \frac{p_{gas,tot}(V_r - V_{liq})}{RT_{gas}} + \frac{p_s(V_r - V_{liq})}{RT_{gas}} \quad (S.15)$$

$$u(n_{abs})^2 = \left[\left(\frac{V_c}{RT_{ci}}\right)^2 + \left(\frac{V_c}{RT_{ca}}\right)^2 + 2\left(\frac{V_{gas}}{RT_{gas}}\right)^2\right] u(p)^2 + \left[\left(\frac{p_{ci}}{RT_{ci}}\right)^2 + \left(\frac{p_{ca}}{RT_{ca}}\right)^2\right] u(V_c)^2 + \left[\left(\frac{p_{gas,tot}}{RT_{gas}}\right)^2 + \left(\frac{p_s}{RT_{gas}}\right)^2\right] u(V_{gas})^2 + \left[\left(\frac{p_{ci}V_c}{RT_{ci}^2}\right)^2 + \left(\frac{p_{ca}V_c}{RT_{ca}^2}\right)^2 + \left(\frac{p_{gas,tot}V_{gas}}{RT_{gas}^2}\right)^2 + \left(\frac{p_sV_{gas}}{RT_{gas}^2}\right)^2\right] u(T)^2 \quad (S.16),$$

where *r* denotes reactor, *liq* denotes the liquid phase (solvent) and $p_s$ denotes the vapor pressure of the solvent.

Uncertainty of the molar fraction of $CO_2$ in liquid phase, $x_{CO_2}$

By definition:

$$x_{CO_2} = \frac{n_{abs}}{n_{tot}} = \frac{n_{abs}}{n_{sol+}\, n_{abs}} \qquad (S.17)$$

$$u\left(x_{CO_2}\right)^2 = \left(-\frac{n_{abs}^2}{(n_{tot}+n_{abs})^2}\right)^2 u(n_{sol})^2 + \left(\frac{n_{sol}+n_{abs}-n_{abs}n_{sol}}{(n_{sol}+n_{abs})^2}\right)^2 u(n_{abs})^2 \qquad (S.18)$$

The only unknown is the $u(n_{sol})$.

For its calculation, we consider the following equations:

- Binary solutions, MDEA (1) and MEG/TEG/$H_2O$ (2):

$$n_{sol} = \frac{m_{intr}w_1}{Mr_1} + \frac{m_{intr}w_2}{Mr_2} \qquad (S.19)$$

$$u(n_{sol})^2 = \left(\frac{w_1}{Mr_1}+\frac{w_2}{Mr_2}\right)^2 u(m_{intr})^2 + \left(\frac{m_{intr}}{Mr_1}\right)^2 u(w_1)^2 + \left(\frac{m_{intr}}{Mr_2}\right)^2 u(w_2)^2 \quad (S.20)$$

- Ternary solutions, MDEA (1), MEG (2) and $H_2O$ (3):

$$n_{sol} = \frac{m_{intr}w_1}{Mr_1} + \frac{m_{intr}w_2}{Mr_2} + \frac{m_{intr}w_3}{Mr_3} \qquad (S.21)$$

$$u(n_{sol})^2 = \left(\frac{w_1}{Mr_1}+\frac{w_2}{Mr_2}+\frac{w_3}{Mr_3}\right)^2 u(m_{intr})^2 + \left(\frac{m_{intr}}{Mr_1}\right)^2 u(w_1)^2 + \left(\frac{m_{intr}}{Mr_2}\right)^2 u(w_2)^2 + \left(\frac{m_{intr}}{Mr_3}\right)^2 u(w_3)^2 \qquad (S.22)$$

Uncertainty of Henry's constant, $H$

Henry's constant in this work is expressed in kPa·m$^3$·kmol$^{-1}$ and it is calculated as:

$$H = \frac{P_{CO_2}}{c} = \frac{P_{CO_2}\, V_{solv}}{n_{abs}} \qquad (S.23)$$

Its uncertainty can be calculated by:

$$u(H)^2 = \left(\frac{V_{solv}}{n_{abs}}\right)^2 u(P)^2 + \left(\frac{P_{CO_2}}{n_{abs}}\right)^2 u(V_{solv})^2 + \left(-\frac{P_{CO_2}V_{solv}}{n_{abs}^2}\right)^2 u(n_{abs})^2 \qquad (S.24)$$

where $V_{solv}$ is the volume of the solvent inside the reactor.

Because $V_{solv} = m_{intr}/\rho_{solv}$ ,

$$u(V_{solv})^2 = \left(\frac{1}{\rho_{solv}}\right)^2 u(m_{intr})^2 + \left(-\frac{m_{intr}}{\rho_{solv}^2}\right)^2 u(\rho_{solv})^2 \qquad (S.25).$$

Uncertainty of density, $\rho$

The uncertainty in density was calculated according to the analysis previously reported in the publication of Skylogianni et al. [7]

Uncertainty in water content, $c_w$

The standard uncertainty in the water content was calculated by taking into account both the repeatability of the measurement, $u_{rep}(c_w)$, and the uncertainty deriving from the accuracy of the instrument, $u_{cal}(c_w)$, as defined by measuring water content standards.

$$u(c_w) = \sqrt{u_{rep}^2(c_w) + u_{cal}^2(c_w)} \quad (S.26)$$

The repeatability is calculated by the standard deviation of the means. The uncertainty of the calibration is calculated by the equation below, where $u_{\text{cal,rep}}(c_w)$ is the repeatability of the measurement of the standards, and $u_{\text{cal,ref}}(c_w)$ is the uncertainty of the measurement, assuming Uniform Distribution (Type B).

$$u_{cal}(c_w) = \sqrt{u_{cal,rep}^2(c_w) + u_{cal,ref}^2(c_w)} \quad (S.27)$$

The main contributor to the uncertainty is the repeatability of the measurement, $u_{rep}(c_w)$, resulting in significant uncertainties, as can be seen in Table S. 2.

## REFERENCES


1. Galvão, A. C. & Francesconi, A. Z. Solubility of methane and carbon dioxide in ethylene glycol at pressures up to 14 MPa and temperatures ranging from (303 to 423) K. *The Journal of Chemical Thermodynamics* **42**, 684–688 (2010).
2. Serpa, F. *et al.* Solubility and Thermodynamic Properties of Carbon Dioxide in MEG/Water Mixtures. in (2013).
3. Wise, M. & Chapoy, A. Phase Behavior of CO2 in Monoethylene Glycol between 263.15–343.15 K and 0.2–40.3 MPa: An Experimental and Modeling Approach. *J. Chem. Eng. Data* **62**, 4154–4159 (2017).
4. Xu, H.-J., Zhang, C.-F. & Zheng, Z.-S. Selective H2S Removal by Nonaqueous Methyldiethanolamine Solutions in an Experimental Apparatus. *Ind. Eng. Chem. Res.* **41**, 2953–2956 (2002).
5. Shen, K. P. & Li, M. H. Solubility of carbon dioxide in aqueous mixtures of monoethanolamine with methyldiethanolamine. *J. Chem. Eng. Data* **37**, 96–100 (1992).
6. Tan, J., Shao, H., Xu, J., Du, L. & Luo, G. Mixture Absorption System of Monoethanolamine−Triethylene Glycol for CO2 Capture. *Ind. Eng. Chem. Res.* **50**, 3966–3976 (2011).
7. Skylogianni, E., Wanderley, R. R., Austad, S. S. & Knuutila, H. K. Density and Viscosity of the Nonaqueous and Aqueous Mixtures of Methyldiethanolamine and Monoethylene Glycol at Temperatures from 283.15 to 353.15 K. *J. Chem. Eng. Data* **64**, 5415–5431 (2019).